THE LOW PRESSURE OXIDATION OF COPPER SINGLE CRYSTALS

By
Don Frederick Mitchell

October 1965

Technical Report
to
The Office of Naval Research
Contract NOnr 474(11)

Principal Investigator:
Kenneth R. Lawless, Professor
Department of Materials Science

Research Laboratories for the Engineering Sciences

University of Virginia

Charlottesville

Report No. MS-3531-102-66U
March 1966

THE LOW PRESSURE OXIDATION OF COPPER SINGLE CRYSTALS*

By

Don Frederick Mitchell

October 1965

Technical Report

to

The Office of Naval Research

Contract NOnr 474(11)

Principal Investigator:

Kenneth R. Lawless, Professor

Department of Materials Science

* Thesis submitted to the Graduate School of the University of Virginia in partial fulfillment of the requirements for the degree of Doctor of Philosophy

Division of Materials Science

RESEARCH LABORATORIES FOR THE ENGINEERING SCIENCES

SCHOOL OF ENGINEERING AND APPLIED SCIENCE

UNIVERSITY OF VIRGINIA

CHARLOTTESVILLE, VIRGINIA

Report No. MS-3531-102-66U

March 1966

Copy No. 2

ACKNOWLEDGEMENTS

The writer wishes to thank Dr. Kenneth R. Lawless for his encouragement and many discussions throughout this work.

I am also deeply grateful to the late Dr. Allan T. Gwathmey under whose guidance this work was started.

The assistance of Mr. A. W. Norvelle in the initial preparation of samples is gratefully acknowledged.

I would also like to thank my fellow students for their assistance.

The writer acknowledges the support of this work by the Paint Research Institute and by the Office of Naval Research.

Don Frederick Mitchell

University of Virginia
Charlottesville, Virginia
September, 1965

TABLE OF CONTENTS

I. INTRODUCTION

The critical investigation of the mechanism of oxidation of metallic surfaces is warranted by the rapidity of the destruction by oxidation of man-made metal structures. Although these investigations have been carried out for many years, oxidation theory is still in a rather unsatisfactory state, with only a few theories, applicable to very specific conditions, which seem to be valid. These theories have assumed that a continuous, homogeneous oxide film was formed on the surface initially, and that the rate of further oxidation was governed by the ability of the reactants, including electrons, to travel through this layer of reaction product. These theories were thus concerned with the forces which influence diffusion through metal oxides. In 1951, Bardolle and Bénard (1) showed that the reaction product did not always form as a continuous surface layer, but under suitable conditions formed as discrete islands, which they called germs, on the surface of the metal. This phenomenon has now been observed to occur on several metals (Ag, Cd, Sn, Fe, Cu, Cu-Ni, Mg) under a wide range of temperature, pressure, and oxidizing species.

It was with the knowledge of the wide occurrence of the phenomenon of nucleation of surface oxides that this work was undertaken. The objective of this research was

to determine the mechanism of the low pressure thermal oxidation of copper, from an investigation of 1) the oxide and metal topography, 2) the structural relationships of oxide and metal, 3) the kinetics of the nucleation and growth of the islands of reaction product (nuclei). The system, copper plus oxygen, was chosen for study for two main reasons. One was that it had recently been shown that nucleation of oxide occurred on copper over a wide range of easily obtainable conditions (2, 3). The second reason was that copper had previously been used for oxidation studies in this laboratory and techniques had been developed for the preparation and handling of large single crystal samples.

II. HISTORICAL

In 1951, Bardolle and Bénard (1) demonstrated the process of oxide nucleation on metal surfaces for the first time. In this study, oriented oxide nuclei were obtained on iron surfaces at temperatures of 850° C and oxygen pressures on the order of 10^{-3} torr. It was shown also that crystal face played an important role in both the oxide morphology and the number of nuclei of oxide formed per unit area.

In the same laboratory, in 1955, Grönlund (4) showed that similar results could be obtained on copper. Oxide nuclei were observed to form at temperatures from 300° C to 950° C in oxygen pressures from 10^{-3} torr to 1 torr. From his observations, Grönlund (2) divided the process of oxidation into three stages: 1) induction; 2) nucleation; 3) growth. The first stage, induction, referred to the time between first contact of the metal with oxygen and the first appearance of oxide nuclei on the surface, as observed with the optical microscope. At the end of this induction period many nuclei appeared on the surface simultaneously, representing the second stage in the process, nucleation. The number of these nuclei per unit area of surface remained constant with time as the nuclei grew laterally over the surface with little thickening, until the surface was covered, after

which the oxide began to thicken. This lateral growth represented the third stage of the process. Figures 1a, 1b, 1c show some of the important characteristics which were observed by Grönlund. These include:

1. The number of oxide nuclei/cm^2 was a function of crystal face.
2. The number of oxide nuclei/cm^2 was greater the lower the temperature.
3. The number of oxide nuclei/cm^2 was less the lower the pressure.
4. The duration of the induction period was greater the lower the pressure.

Figure 1d shows the model which Grönlund used to explain his observations. In this model the first step in the oxidation process was the formation of a "primary oxide" film over the surface. Oxide nuclei which have preferred epitaxial relationships with the metal substrate grow out of this film. It was suggested that these "secondary" nuclei grow by surface diffusion of the "primary oxide" to the periphery of the preferentially oriented oxide nuclei. No attempt was made in this model to define the diffusion species exactly; however, it was indicated that both the oxygen and the copper atoms diffused over the surface to the nuclei. The nature of the "primary oxide" was not described by Grönlund;

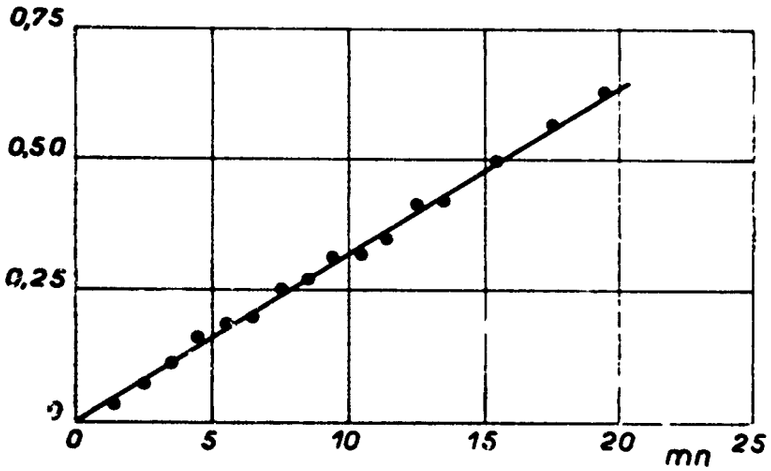

Fig. 22. - Fraction de la surface du cuivre recouverte de germes en fonction du temps

(a)

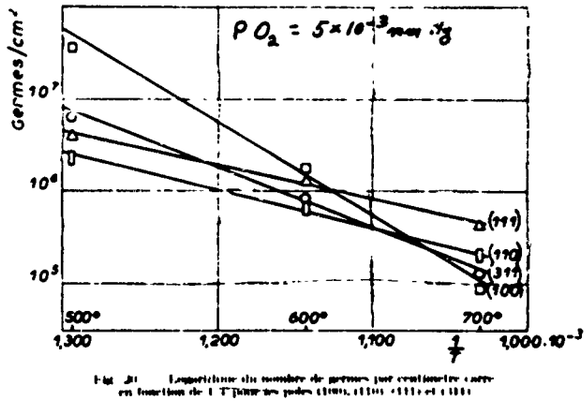

(b)

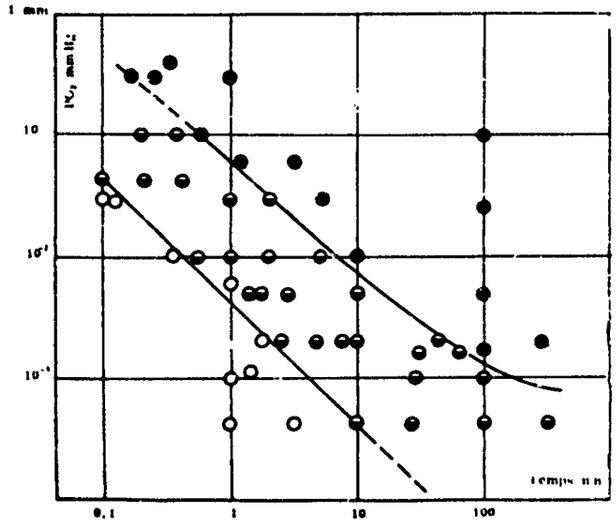

Figure 4 - Conditions de formation des germes d'oxyde Cu_2O à la surface du cuivre à 550°C (Grenier[4])

(c)

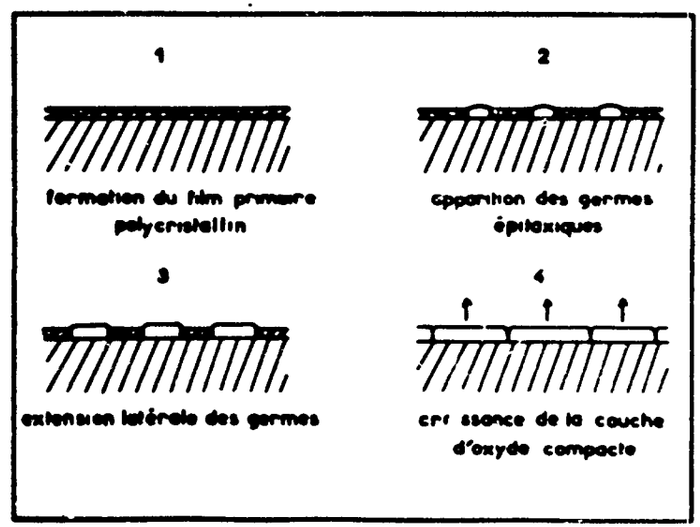

(d)

FIGURE 1

(a),(b),(c): EXPERIMENTAL RESULTS ON LOW PRESSURE OXIDATION OF COPPER BY GRÖNLUND. (2)

(d): THE MODEL USED BY BERNARD (5) TO EXPLAIN THE RESULTS OF GRÖNLUND. (REPRINTED BY PERMISSION OF J. BERNARD)

however, Bénard (5) described it as a polycrystalline disoriented oxide film.

Grönlund's model postulated the concept of a radius of influence associated with each nuclei. Within this radius new nuclei did not form because diffusion of the "primary oxide" to the existing nuclei reduced the probability of formation of additional nuclei.

With the use of the approximation that the radius of influence is proportional to the diffusion constant for surface diffusion of the "primary oxide", the activation energy was determined for diffusion on the major crystallographic faces. These values which represent the slope of an Arrhenius plot of the logarithm of the density of nuclei versus the reciprocal of the absolute temperature are

(111)	(100)	(110)	(311)
8 kcal	23 kcal	10 kcal	15 kcal

In the work of Menzel (6), an activation energy value of 13.2 kcal for the surface diffusion of copper in the presence of a low ($\sim 10^{-4}$ torr) oxygen pressure was obtained. This value was determined for an orientation in the vicinity of the (110) face by annealing of facets and is in agreement with Grönlund's value for surface diffusion during oxidation on the (110) face listed in the above paragraph. This agreement would

support the contention of Rhead (7) that the controlling process in determining the density of nuclei is the surface diffusion rate of copper.

In 1957, Harris, Ball, and Gwathmey (5) reported the occurrence of large nuclei within a thin film of oxide when copper was oxidized at 150° C and 1 atm. The conditions are quite different from the above experiments but seem to indicate that the nucleation process may be important even at atmospheric pressure.

In this regard, Ronnquist (8) studied the kinetics of the initial stages of the oxidation of copper in the 170° - 500° C range at pressures from 10^{-3} atm to 1 atm. Under these conditions considerable cupric oxide was formed along with cuprous oxide. However, according to the author, nuclei were produced and the kinetics were found to obey a $Q^n = kt$ law in which Q is the quantity of oxide formed and n is a function of temperature which varied from .6 at 470° C to 2.5 at 170° C.

G. Van Der Schrick (9) studied the kinetics of the oxidation of copper by microbalance techniques under conditions of nucleation and continuous film formation on polycrystalline samples. Although most of this work was for continuous films formed at high oxygen pressures, a linear oxidation rate law was observed for the first few μg O_2/cm^2 (1 μ g O_2/cm^2 = 150 Å Cu_2O) coverage under nucleating conditions. G. Van Der Schrick (9) also

showed from the discrepancy between gravimetric data on the uptake of oxygen by a sample and the electrometric reduction of oxide on the surface that solution of oxygen into the metal was significant under conditions for nucleation, and thus, concluded that this was the explanation for the induction period. This work was confirmed by C. Van Der Schrick (10).

A discontinuous oxide was observed on single crystal copper surfaces as early as 1954, by Menzel (11). In this work small single crystal copper hemispheres were grown by assymetric cooling of a molten copper drop on a tungsten ribbon. These samples were then oxidized in the same system without the need of first exposing the copper surface to a foreign atmosphere. The growth and form of the oxide nuclei which grew on these "untouched" surfaces were observed continuously by an optical microscope. The results of these studies were in agreement with the observations of Grönlund. More recent work by Menzel and Niederauer (12) showed that the number of nuclei was not a function of the dislocation density of the copper substrate. In the same work, it was demonstrated that the shape and density of the nuclei were sensitive functions of contaminants.

Low energy electron diffraction has been used to study an earlier stage of the oxidation process than was possible with the techniques of Bénard and Menzel.

This technique has been used by Lee (13), and Simmons (14) to examine the initial stages of the oxidation of copper. Both groups have observed an adsorption structure, one layer thick, on the (100) face before the formation of a true oxide phase. This structure has a cell which is based on the underlying copper lattice of dimensions

$$1 \times Cu\,[100] \text{ by } 2 \times Cu\,[100] .$$

This structure was found to be quite resistant to further oxidation at room temperature.

A more complete picture of the early stages of the oxidation of nickel has been obtained by Farnsworth and Madden (15). From combined low energy electron diffraction and photo-electric work-function measurements, they postulated that on a clean nickel surface, oxygen is initially adsorbed as O_2, in which state it diffuses to lattice defect sites where dissociation occurs. After sufficient oxygen atoms have accumulated on the surface by this process, a place exchange occurs. In this exchange, oxygen atoms occupy some nickel sites and some of the nickel atoms are moved to the surface in a simple periodic manner. With continued addition of oxygen to this structure, it develops into a true nickel oxide.

The excellent work by Orr (16) on the kinetics of nucleation of oxide on magnesium should be mentioned. He found that when oxygen was admitted to a clean

magnesium surface at liquid nitrogen temperature, the oxidation rate first increased and then decreased with time. This phenomenon was explained by a process of nucleation of oxide islands, the edges of which were much more reactive than either the metal surface in between oxide islands or the tops of the oxide islands. It was shown that, at liquid nitrogen temperatures where surface diffusion rates are insignificantly small, if oxidation was to occur, the incoming oxygen molecule was required to hit the surface at the edge of the oxide islands, react and form oxide at that site.

Others who have observed oxide nucleation and growth on systems other than the copper oxygen system are Gulbransen, Mc Millan and Andrew (17) on iron; Martius (18) on nickel; Menzel and Menzel-Kopp (19) on silver; Boggs, Trozzo and Pellissier (20) on tin; Bouillon, Bouillon-Nyssen and Stevens (21) on copper-nickel alloys; Bouillon and Jardinier (22,23) on cadmium; and Oudar (24, 25) on sulfurization of copper. Sufficient kinetic data has not been obtained for any of these systems to extablish a model for oxide nucleation and growth.

III. EXPERIMENTAL

A. Oxidation Apparatus

Two different vacuum reactor systems were used in this research. These will be designated as system A, which was used for the studies on spheres and thin films, and system B, which was used for the studies on copper slices. System A was designed to give samples for investigation by electron diffraction and microscopy, while system B was designed to give oxidation rate data.

1. System A

System A is shown in the photograph in Fig. 2a. The pumping system consisted of a 50 liter/sec, three stage, oil diffusion pump (A) backed by a rotary mechanical pump. The diffusion pump used "Octoil-S" in the early part of this work. Later, however, this oil was replaced by "Convalex-10". There was no noticeable change in the oxidation results using the two different oils; however, "Convalex-10" gave less backstreaming and was thus preferred over "Octoil-S". The diffusion pump was trapped with zeolite (B) which was baked out at 400° C periodically. The pressure above the trap was measured by an inverted Bayard-Alpert type ionization gauge (C) and a Consolidated Electrodynamics Corp. residual gas mass spectrometer, type 21-613. A Veeco, 5/8 inch stainless steel valve (D) with teflon seat separated

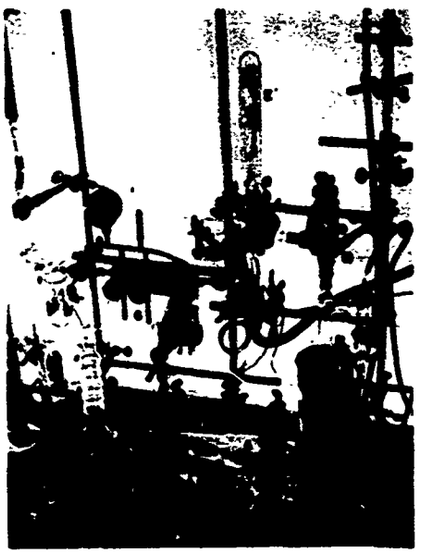

(a)

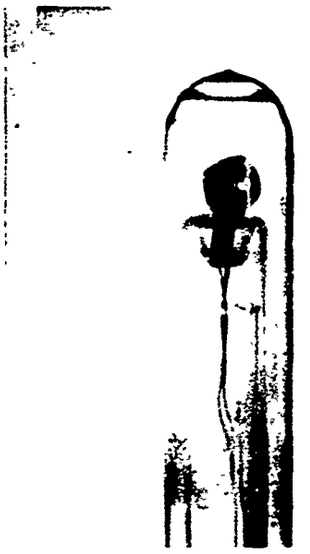

(b)

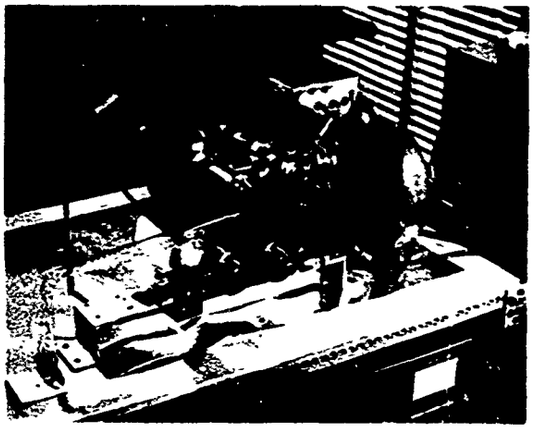

(c)

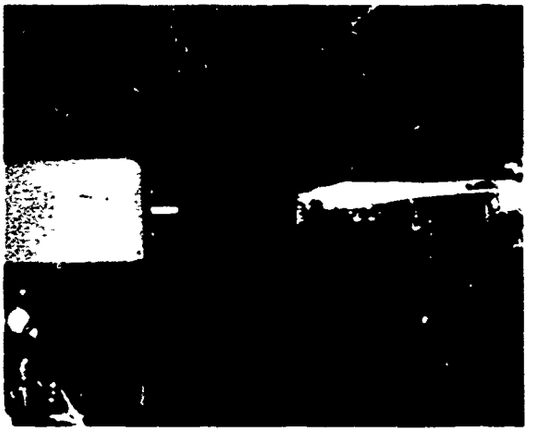

(d)

FIGURE 2

(a), (b) SYSTEM A AND ITS REACTION VESSEL RESPECTIVELY
(c),(d) SYSTEM B AND ITS REACTION VESSEL SHOWING
POSITION OF PYHOMETER

the reaction section (E) of the system from the diffusion pump. All of the reaction vessel (Fig. 2b) which was heated by a surrounding resistance furnace was made of vycor glass. The reaction vessel furnace was operated by a Minneapolis-Honeywell, 0-1000° C, Pyr-O-Vane controller. The thermocouple for the controller was placed at the top of the inside tube of the reaction vessel. As a check, a thermocouple was placed inside a hole drilled in one spherical crystal and the reaction vessel top was modified so that the thermocouple leads could be gotten out of the vacuum system and to a potentiometer. The two thermocouples gave the same value within the ability of the controller to regulate ± 5° C. The remainder of the system was composed of small Hoke stainless steel valves (G) for gas handling and an ultra-high vacuum leak valve (F) (Granville-Phillips), for controlling the oxygen pressure. A Pirani gauge was placed as near as possible to the reaction chamber. The system was regularly pumped to 2×10^{-8} torr at the ionization gauge; however, with the mass spectrometer operating, pressures were generally an order of magnitude higher. The pumping speed at the sample was calculated from pressure drop data to be .73 liters/sec at the crystal and about 3 liters/sec at the ionization gauge location. After characterizing the gases in this system, the mass spectrometer was permanently installed on system B. An

analysis of the residual gases in system A is given in the section on experimental procedures (III-C-i).

2. System B

System B, shown in Fig. 2c, was used primarily to obtain kinetic data. It was of the bakeable ultra-high vacuum design. During bake-out at 250° C, the system was pumped through a Granville-Phillips type "C", ultra-high vacuum valve by an oil diffusion pump backed by a mechanical pump. After bake-out, the system was valved off from the diffusion pump and pumping continued by an 8 liter/sec VacIon sputter ion pump, through a Varian 1½ inch bakeable ultra-high vacuum valve. Hydrogen was admitted through a Granville-Phillips type "C" valve and oxygen through a Granville-Phillips leak valve. The system was also equipped with a Pirani tube for accurate pressure measurements. This Pirani circuit is described below. The system regularly pumped down to less than 10^{-9} torr after bake-out as determined by the ion pump current.

The sample was heated to the desired temperature either by a 1 KW (Lepel) induction heater or by a resistance furnace. The temperature of the sample was determined by an infra-red pyrometer (Infrared Industries, TD-6) when using the induction heater. The pyrometer was coupled to the induction heater so that the sample temperature was automatically controlled to ± 2° C. To

determine the sample temperature accurately, the emissivity of the sample and the effect of the pyrex flat through which the pyrometer saw the sample had to be known. Since the emissivity for copper was very low, the experimental arrangement shown in Fig. 2d was used. The silver coating on the top outside of the reactor chamber increased the apparent emissivity through multiple reflections between the sample and the silver mirror. By placing a thermocouple in a dummy copper sample and calibrating the pyrometer against the thermocouple, an effective emissivity of .11 was found for this geometry. When using the resistance furnace, the temperature of the sample was determined by a thermocouple placed outside the vacuum wall opposite the sample. This thermocouple was connected to a Minneapolis-Honeywell Pyr-O-Vane controller which maintained the desired temperature.

For recording pressure changes in system B, a specially designed electronic circuit was built to operate a standard glass incased Pirani tube (National Research Corporation). The power supply, regulated by a zener diode, delivered 2.1 V DC to a wheatstone bridge network. One arm of the bridge contained the Pirani tube and another arm contained a variable resistor for balancing the bridge. All resistors in the circuit had minimum temperature coefficients. A high impedence,

1 mv full scale maximum sensitivity (Sargent) strip chart recorder was used to indicate the bridge imbalance.

Calibration of the Pirani circuit was made against two different Mc Leod gauges and a sensitivity of $3.7_3 \approx .1$ volt/torr for oxygen was obtained with the Pirani tube envelope at room temperature. Using the strip chart recorder having 200 divisions per 1 mv, this gave a maximum sensitivity of 1.34×10^{-6} torr/div. There was some drift in the circuit zero which was traced to temperature fluctuations of the Pirani tube envelope. The Pirani tube envelope could be immersed in an ice water bath. This had two desirable effects: first, it reduced the zero drift; and second, it increased the sensitivity. However, since it also increased the response time of the instrument, for this work, the tube envelope was kept at room temperature.

B. Sample Preparation

Three different types of single crystal samples were used in this work: spheres, slices, and thin films, all made from American Smelting and Refining Co. 99.999% copper. The single crystal spheres were turned on a lathe from 3/4 inch single crystal rods to a sphere 5/8 inch in diameter, generally with two flat areas 3/8 inch in diameter of a particular crystallographic orientation, and with a stem 1/2 inch long and 1/4 inch in diameter. These samples were etched in a 50% nitric acid, 5% hydrochloric acid solution to remove the cold worked surface layer. The orientation of the flat areas on the spheres were then examined by Laue back reflection x-ray diffraction. Any faces found to be off of the desired orientation by more than two degrees were corrected by additional machining and repetition of the etching procedure. (26)

Single crystal slices, 3/16 inch thick and 5/8 inch in diameter, were likewise cut from the 3/4 inch, 99.999% rods, and a small hole was drilled off center in the samples. These samples were then glued to the head of an acid polishing wheel of Young's design (27) and the surface was polished down 1/16 inch. The glue was then dissolved and the slice remounted, and 1/16 inch was removed from the other side. This gave a slice, 1/16 inch thick which showed no evidence of deformation in

the back reflection Laue X-ray diffraction photographs.

The thin film samples were prepared by evaporation of copper from a tungsten basket onto a freshly cleaved (100) rocksalt substrate heated to 330° C in a Varian 400 liter/sec vacuum evaporator at a pressure of less than 10^{-7} torr. This gave continuous (100) oriented films, 500 Å to 1000 Å thick. (Fig. 3a, 3b) The majority of these samples were oxidized while on the salt substrate with no additional preparation given them. A few films were removed from the rocksalt by floating onto distilled water. These films were then mounted on copper electron microscope grids for oxidation.

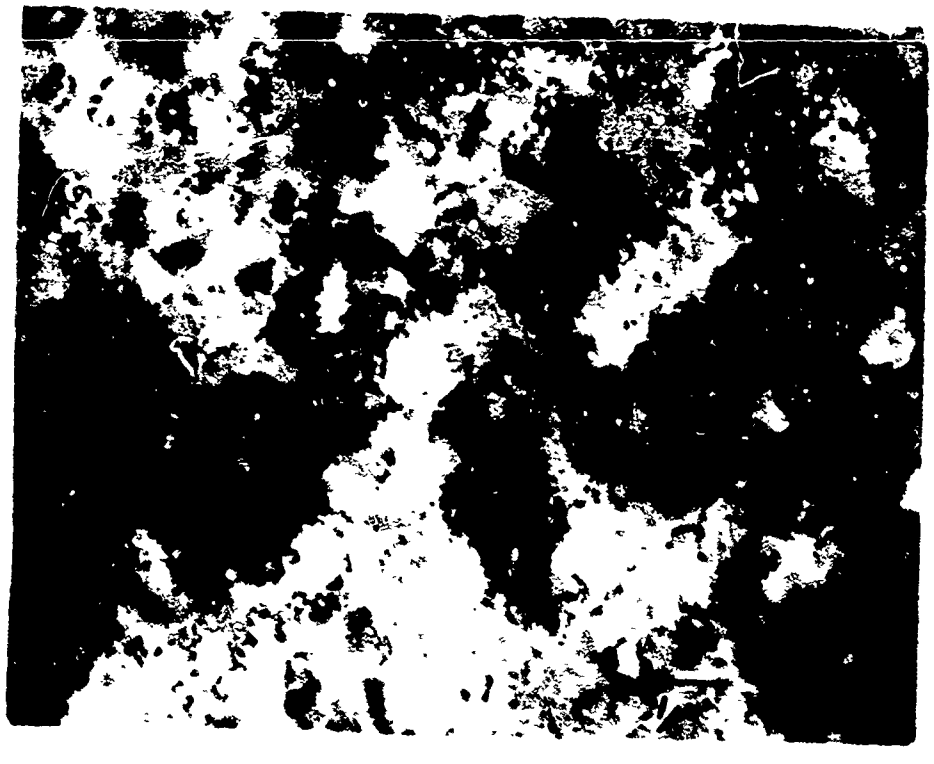

(a)

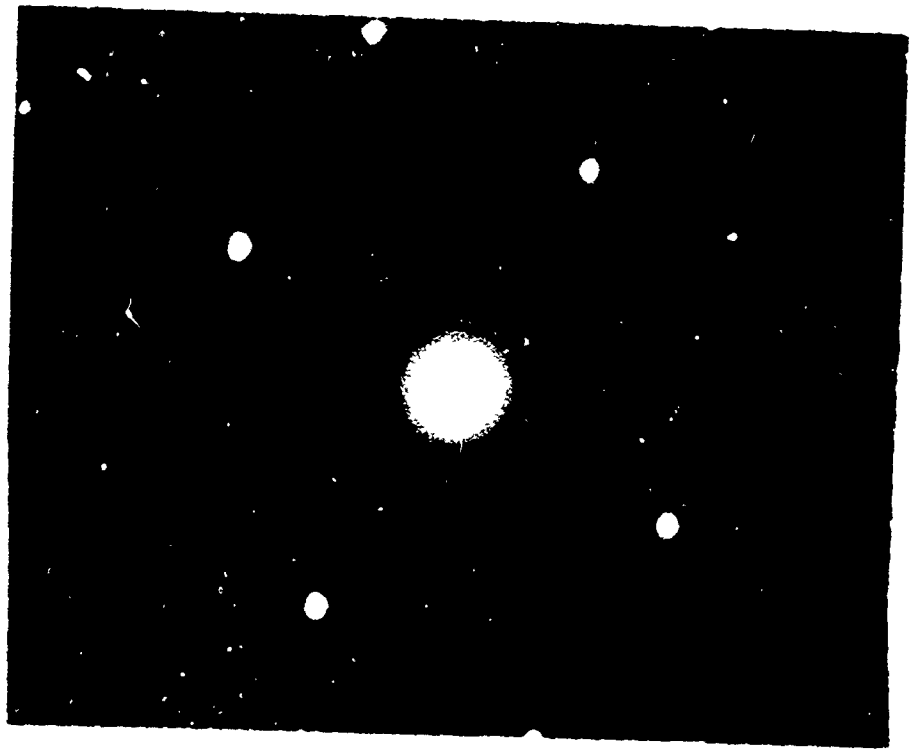

(b)

FIGURE 3

(100) COPPER THIN FILM AS GROWN

(a) Transmission electron micrograph

(b) Transmission electron diffraction pattern

C. Experimental Procedure

1. System A

Single crystal spheres for oxidation in system A were originally prepared and polished as described in the preceding section. Prior to an oxidation, a sphere was polished using 1/0 through 4/0 metallographic emery paper followed by a final mechanical polish with 1 μ alumina on a wet felt polishing cloth. This mechanical polishing treatment, which gave the surface a mirror finish, was followed by an electropolish in a 65% orthophosphoric acid bath after the method of Jacquet (28). The polishing conditions were modified somewhat in that the bath was heated to approximately 50° C and stirred by a magnetic stirrer as vigorously as possible without drawing air bubbles into the polishing solution at the vortex. These modifications allowed the bath to operate at higher voltages ($\sim$ 8 V DC) and current densities ($\sim$ .1 amp/cm^2) than could have otherwise been obtained without producing gas on the sample surface. These modifications permitted a considerable reduction in the time necessary to remove a specific amount of copper from the sample without affecting the quality of the polish. After electro-polishing, the sample was washed in 10% orthophosphoric acid for 30 seconds and then in high purity distilled water for 5 minutes or 18 megohm demineralized water for 10 minutes. The sample was then

blown dry in a stream of dry nitrogen and placed in the vacuum reactor system.

Often it was not necessary to do any additional mechanical polishing between experiments. In these cases, after examination in one experiment, the sample was electropolished for 5 minutes in the phosphoric acid bath, washed, and dried as described above.

After drying, the crystal was placed in the reaction vessel which was then evacuated to 10^{-5} torr or better, flushed with hydrogen (Matheson Co., Ultra High Purity grade 99.999%) and refilled to one atmosphere with hydrogen. Then, with a flow of hydrogen of approximately 20 cc per minute, the crystal was heated to 500° C if the planned oxidation was to be carried out at a temperature of 500° C or lower. However, if the oxidation were to be carried out at a higher temperature than 500° C, the crystal was heated to that higher temperature in flowing hydrogen. The crystal was usually annealed for one hour in the hydrogen flow, although in some experiments the time was as short as ten minutes and in others as long as 24 hours. This variance appeared to have no effect on the results obtained. If the oxidation were to be carried out at less than 500° C, the crystal was cooled in flowing hydrogen to the oxidizing temperature. After a 15 minute wait to permit thermal equilibrium to be obtained, the system was pumped out and the crystal annealed in

a vacuum of 10^{-6} torr or less in the case of low temperature oxidations. It was observed in this system that with crystals above 500° C, it took progressively longer times to obtain the same pressure during annealing for progressively higher temperatures. The time of vacuum annealing, which was varied from 1/2 hour to 24 hours, was not observed to affect the results obtained in system A. A sample mass spectrograph analysis of the gas composition during outgas is listed below:

N_2 + CO	35%	A	.5%
H_2O	35%	CO_2	.1%
H_2	20%	hydrocarbons	.05%
O_2	10%		

After the vacuum annealing period, oxygen was leaked into the reaction vessel while continuing to pump the vessel. In this way, a constant flow of pure oxygen could be maintained.

In the earlier experiments, tank oxygen purified through a silver leak was admitted to the reaction vessel through the leak valve. In later experiments, oxygen from Matheson Co. reagent grade 1 liter glass flasks was used in place of the silver leak purified oxygen. The oxygen from these two sources was of at least 99.9% purity; however, desorption from the system walls resulted in considerably less pure oxygen in the

reaction vessel. A typical mass spectrograph analysis of the oxidizing atmosphere was found to be:

O_2	97.5%	CO_2	.2%
H_2O	1.3%	A	.02%
N_2 + CO	1.0%	others	< .005%

To stop a reaction, the oxygen supply was cut off and the furnace removed from around the reaction vessel. In some experiments the crystal was allowed to cool in vacuum. In other experiments, as soon as the oxygen was pumped out, the valve to the pump was closed and Matheson research grade helium was admitted to a pressure of 2 - 5 torr. A blast of cool air was then directed through the hollow center tube of the reactor. The helium was admitted to the reaction vessel to improve the thermal-contact between the reactor walls and the crystal, and the blast of air helped carry the heat away from the reactor walls. This procedure yielded a cooling rate of approximately 100° C per minute at 400° C compared to a rate of 7° C per minute in vacuum.

After cooling, the system could be filled, if desired, with dry nitrogen to atmospheric pressure and the crystal removed for examination by electron diffraction. (See section on surface examination.)

2. System B

Single crystal slices prepared as described in

Section B above were electropolished, washed, dried, and polished in the same manner as the spheres. They were then placed on a pyrex frame which was positioned in the end of the reaction vessel below the silver mirror. The reaction vessel was bolted to the system which was then evacuated via the oil diffusion pump and baked at 250° C for four hours by lowering a large hood, which contained electric heaters, over the entire system. After baking, the hood was raised, the ion pump started, and the system closed off from the diffusion pump. When the system had cooled to room temperature and reached a pressure of less than 5×10^{-9} torr, the sample was heated by the induction heater and given a hydrogen anneal and outgas treatment. The hydrogen anneal and heat treatment before oxidation were found to affect the results and several different procedures were used in an attempt to determine the cause. (See Sec. IV-A.) After the annealing treatment, the sample was allowed to cool to room temperature. The ion pump was then closed off from the system and approximately 10^{-3} torr of oxygen admitted to the reaction vessel by opening the leak valve momentarily. This gas was partially adsorbed by the walls of the system, causing the pressure in the system to decrease. The process of this adsorption could be followed and recorded by the Pirani circuit and strip chart recorder. If necessary, additional samples of oxygen were admitted to maintain

the pressure at the desired value.

After approximately 1 hour, the system walls apparently became saturated with oxygen and ceased to adsorb gas. The system was then evacuated. It was found that pumping alone would not remove this gas from the walls, since when gas was readmitted, no further adsorption occurred. If the system were rebaked, however, the walls would again adsorb gas. This saturation of the walls was necessary so that when the oxidation of the copper sample was started the results would not be complicated by the adsorption of gas by the system walls.

After the system had equilibrated and the excess gas was pumped out with the ion pump, the sample was reheated to 600° C and then cooled to the temperature of the oxidation. The ion pump was again closed off from the system and the oxidation started by admitting a quantity of oxygen via the leak valve to bring the pressure to the desired value as indicated by the Pirani circuit recorder. When the pressure had dropped to approximately 50% of its original value because of oxygen take-up by the sample, more oxygen was admitted via the leak valve to bring the pressure back to its original value. A typical pressure vs. time plot, as taken from the recorder, is shown in Fig. 4. This process was continued for the duration of the experiment. Occasionally, all of the gas was pumped from the system by

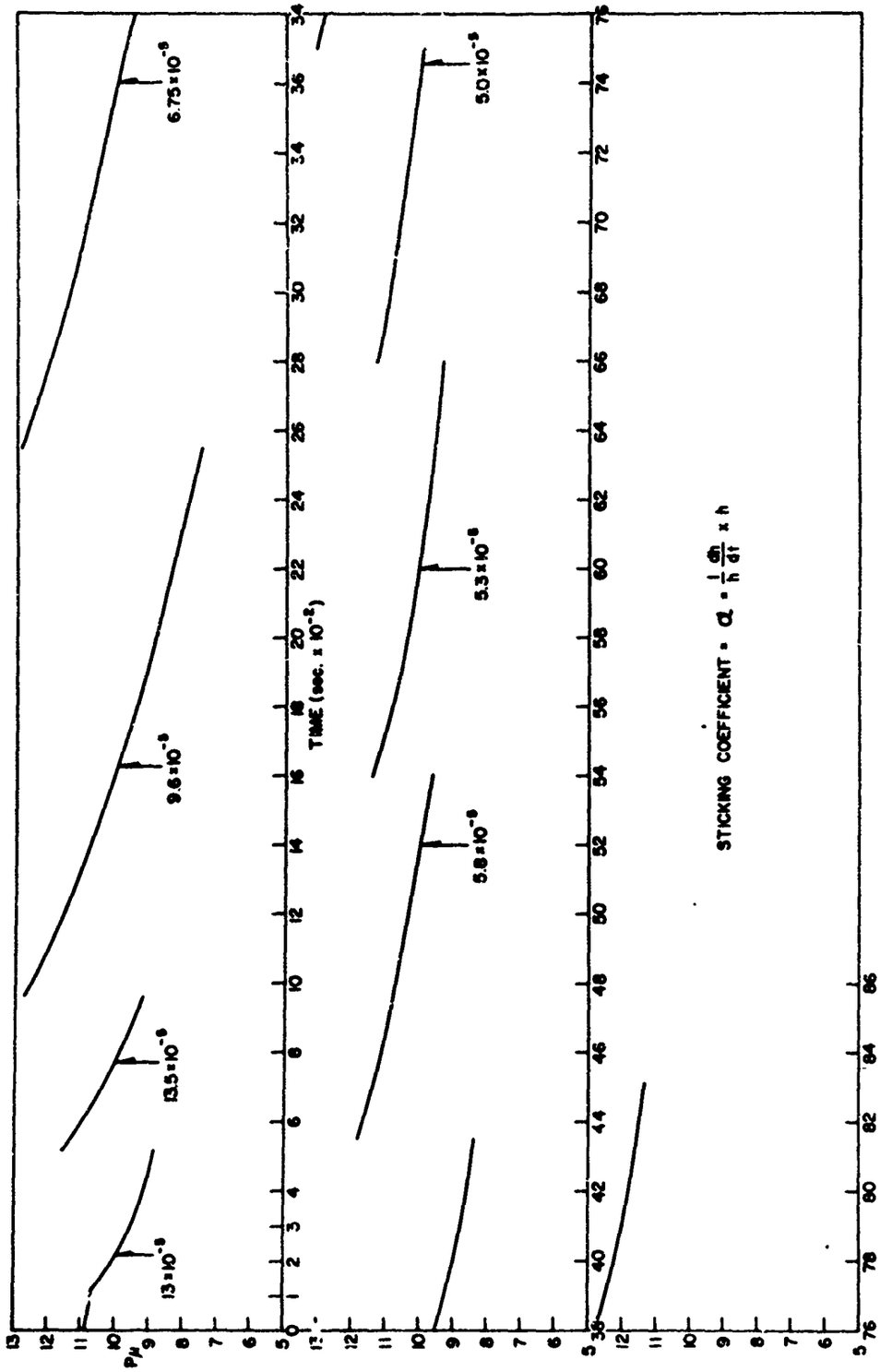

FIGURE 4

A RECORD OF THE PRESSURE IN SYSTEM B VERSUS TIME DURING AN OXIDATION. VALUES OF THE STICKING COEFFICIENT ARE INDICATED AT DIFFERENT POINTS ON THE CURVES.

momentarily opening the valve to the ion pump. This action was taken to remove any impurity gases which could have accumulated in the reaction vessel. Oxygen was immediately reintroduced to the reaction vessel on closure of the ion pump valve. Since the oxidation rate remained at its previous value when oxygen was again readmitted to the system, it was concluded that no large amounts of impurity gases had collected and that the momentary (30 sec) stopping of the oxidation did not change the final results.

The strip chart recorder made a permanent record of the system pressure during the entire experiment and from this record the oxidation kinetics could be obtained. After the sample had oxidized a desired amount, the oxygen remaining was pumped out and the sample allowed to cool in vacuum.

In some experiments, the sample temperature was suddenly changed over a temperature range of ± 50° C. It required only one or two seconds to increase the sample temperature 50° C, but generally about a minute to cool the sample the same amount. This technique was used for obtaining oxidation rate measurements as a function of temperature. It had the advantage that the measurements were obtained from the same sample in the same surface condition. However, there appeared to be a slight hysteresis effect in the oxidation rate when the temperature was changed by larger amounts and the technique

was used primarily as a check on data accumulated from more than one experiment.

D. Surface Examination

1. Electron Diffraction

The first examination of the surface after an oxidized sample had cooled was usually made by glancing angle high energy (100 KV) electron diffraction. When the conditions of oxidation were such as to give little or possibly no true oxide on the sample, the sample was transferred in a nitrogen atmosphere from the reaction vessel to the diffraction apparatus. When it was known that the oxidation had produced considerable oxide on the sample surface, the sample was transferred in air. In either case, the time necessary to transfer a cooled sample from one apparatus to the other was less than 1 minute. Diffraction patterns were photographed in major crystallographic directions at various angles of tilt. From this information, the epitaxial relationships of the oxide to the metal could be obtained. Also, examination by electron diffraction served as a sensitive check for contamination. If a contaminant was present on the surface in sufficient quantity, it could be identified from its diffraction pattern. Usually sufficient contaminant was not present to produce a diffraction pattern. However, the presence of a contaminant could still be detected because it would cause unusual epitaxy in the oxide which could be observed.

2. Optical Microscope

After electron diffraction examination, the crystals

were examined optically with a Bausch and Lomb Balphot Metallograph. When nuclei or other features were large enough to resolve clearly, optical photographs were taken of the surface. Often, however, the surface was too smooth to focus upon and higher resolution microscopy was necessary.

3. Electron Microscopy

In order to obtain higher resolution photographs of the surface features than were possible with optical microscopy, a platinum shadowed carbon replica technique was used to obtain suitable samples for examination in the electron microscope. Three different replication techniques were used in this work. In the earlier experiments, platinum was preshadowed from a 40 mil tungsten filament onto the copper specimen at a 20° incident angle. This was followed by the evaporation of carbon onto the sample at a high incident angle. This replica was then removed from the copper by a 10% ammonium persulfate, 2% ammonium hydroxide solution which slowly dissolved the underlying copper oxide and copper. Because of the slowness of the ammonium persulfate stripping solution, a second technique was developed which used a 2% potassium cyanide solution for removing the replica. However, the cyanide solution attacked the platinum shadowing material and the resolution of the replica was not good. To remedy this difficulty,

the platinum was shadowed onto the sample after some of the carbon had been deposited and then the rest of the carbon was applied. In the final stages of this work, a third technique was used in which the platinum was deposited simultaneously with carbon from commercially prepared platinum impregnated carbon pellets. This was followed by an additional layer of carbon deposited at a high angle as in the two earlier methods. These changes were made in the replication technique as a matter of convenience and to save time. All three of the techniques appeared to give identical resolutions.

The electron microscope used for these studies was an RCA EMU-3B with double condenser. A 50 KV electron beam was used for all replica work; however, the oxidized copper thin films were examined directly using 100 KV electrons.

4. Electrometric Reduction

A large percentage of the samples upon which kinetic measurements had been made were, after cooling, electrometrically reduced by a method first developed by Evans and Miley (29) and improved by Allen (30). This was done as a check on the amount of oxygen taken up by the sample and in an attempt to measure any solution of oxygen into the sample which might have occurred. A de-oxygenated solution of .1 N KCl in distilled water was used as the electrolyte and a current density of .1 milliamperes

per square centimeter was used to reduce the oxide. A reference electrode was connected to a Keithley electrometer and the output from the electrometer fed into a strip chart recorder which thus plotted the reduction curve.

5. Interferometer

A Zeiss interferometer was used to obtain the profile of the surface across an oxide nucleus. A difference of elevation of two adjoining surfaces of as little as 300 Å could be detected with this instrument by measuring the displacement of interference fringes on the surface. This surface profile was used to complement the data obtained from shadow measurements on replicas in the electron microscope.

6. Isolation of Oxide Nuclei from Copper Substrate

A method of isolating the copper oxide nuclei from the copper substrate without apparent attack on the nuclei, which was developed by Beck and Pryor (31), was used in this work on several occasions. It was used to isolate the surface oxide from the copper metal for direct observation in the electron microscope. The system required absolutely anhydrous conditions and the "stripping" was thus performed in a closed system. Methanol was used as the solvent and ammonium acetate as the complexing agent which dissolved the underlying

copper without attacking the oxide. If, however, any water was present, the oxide was also dissolved. Before "stripping" the nuclei from the surface of the sample, a carbon film was evaporated onto the sample to support the nuclei after they were removed from the metal. This also had the advantage that it gave a faint replica of the nuclei before they were placed in the solution. Thus, if any attack on the nuclei had occurred during stripping which changed the size of the nuclei, it could be detected when the stripped samples were examined in the electron microscope.

IV. RESULTS

A. History of Sample

The previous history of the copper samples to be oxidized was found to be an important variable in this work. This appeared to be due primarily to the solubility of various gases in copper. In system A, the high ultimate pressure, as compared to system B, coupled with the hot reaction vessel walls made detection of gas solution in the sample impossible. However, in system B, with an ultimate pressure of less than 10^{-9} torr and the capability of rapid heating of only the sample, the evolution of dissolved gases was readily observable.

Copper samples that had been previously oxidized at a high temperature were re-electropolished and replaced in system B for the next experiment. These samples, when heated to 600° C in a vacuum of less than 10^{-8} torr, evolved no measurable amount of gas. If such a sample was then annealed at 600° C in a few torr of hydrogen for a few minutes and the reactor again pumped-out, large quantities of water vapor were evolved from the sample along with hydrogen gas. The quantity of water vapor was so large that its adsorption on the system walls prevented the previous low pressure from being obtained until after the entire system had been rebaked. After baking, a repeat of the hydrogen anneal and outgassing

gave only hydrogen and little or no detectable water vapor. The rapid pumping of hydrogen by the ion pump permitted pressures of 10^{-9} torr to be obtained as soon as the sample was allowed to cool without rebaking the system. At 600° C the dissolution rate of hydrogen from a saturated sample was quite rapid, being initially about 10^{-4} $\mu g/cm^2 sec$. It required about 1/2 hour of outgassing at 600° C to reduce the dissolution rate of the dissolved hydrogen to 4×10^{-7} $\mu g/cm^2 sec$. The dissolution rate was found to change by about a factor of two for a 25° C temperature change. However, temperatures greater than 600° C were not normally used for outgassing because of the evaporation of the sample. For kinetic work in system B, the samples were outgassed to this extent but samples in system A could never be outgassed to such a low value.

B. Induction Period

The period of time after oxygen was admitted to a clean outgassed copper surface, and before an oxide phase was detectible by glancing angle electron diffraction, is referred to as the induction period. This induction period was found to be a function of temperature, pressure, and crystal face. Figure 5 shows the effect of temperature on the duration of the induction period for the (111) face in System A. For a given temperature, it was found that the induction period was inversely proportional to the oxygen pressure in the range of 10^{-3} to 2×10^{-2} torr. In the initial experiments in system A, it was found that, at pressures below approximately 10^{-4} torr, an oxide phase did not occur on the surface regardless of the length of time of the "oxidation". In System B, it was found, however, that nucleation occurred at pressures below 10^{-6} torr. This was taken as an indication that the residual gases of system A reduced the oxide as fast as it formed at oxygen pressures of less than 10^{-4} torr.

The induction period was found to be shorter for the high index planes regardless of the conditions of temperature and pressure. Figure 6 shows a sphere oxidized at 800° C at 10^{-3} torr which is nucleated on the higher index planes but not yet nucleated on the <111> and <100> poles. The order of appearance of nuclei on the major crystallographic planes from the earliest to the last was (311); (110); (111); (100).

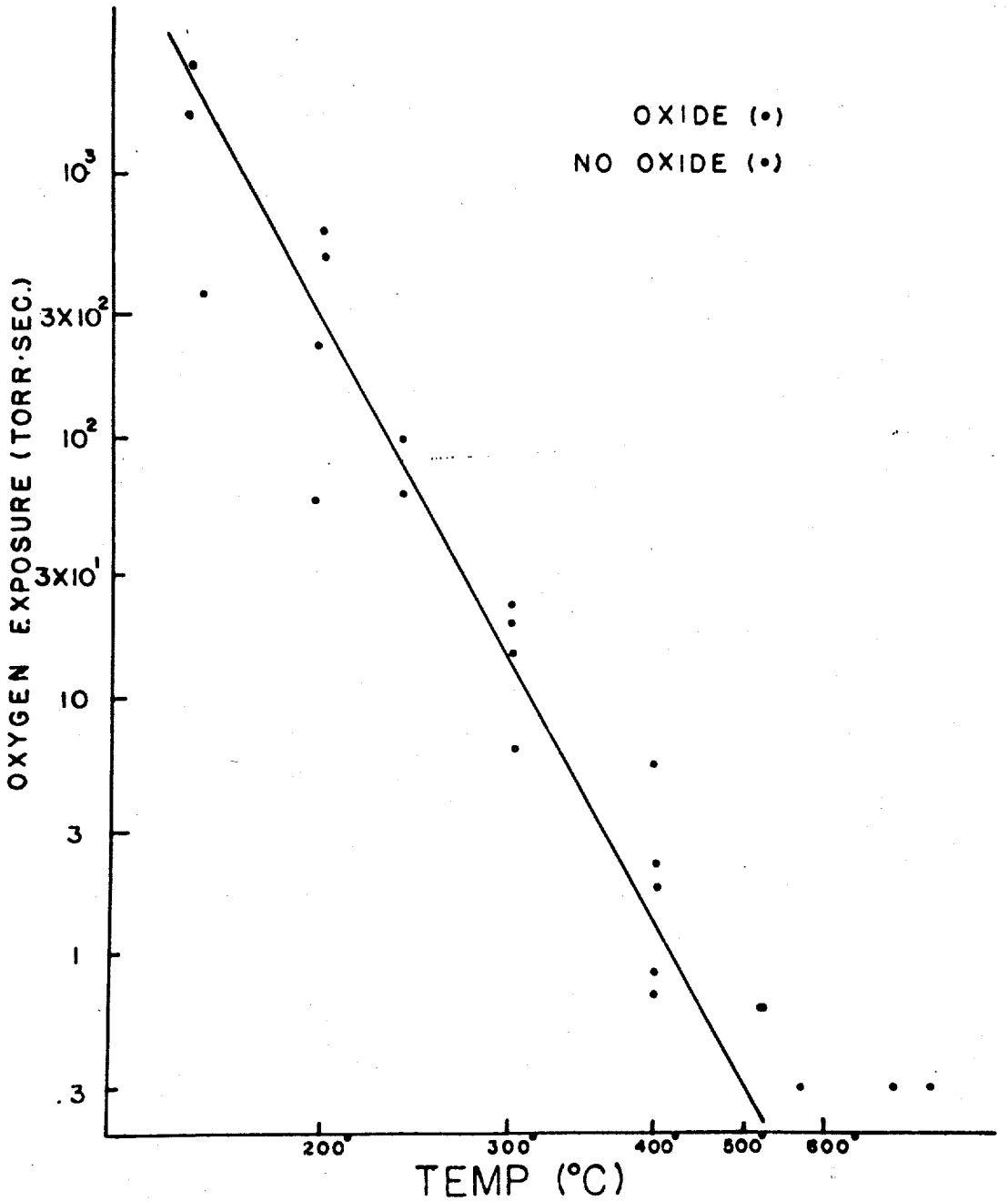

FIGURE 5

DURATION OF THE INDUCTION PERIOD IN TORR · SEC
AS A FUNCTION OF TEMPERATURE FOR THE (111) FACE.

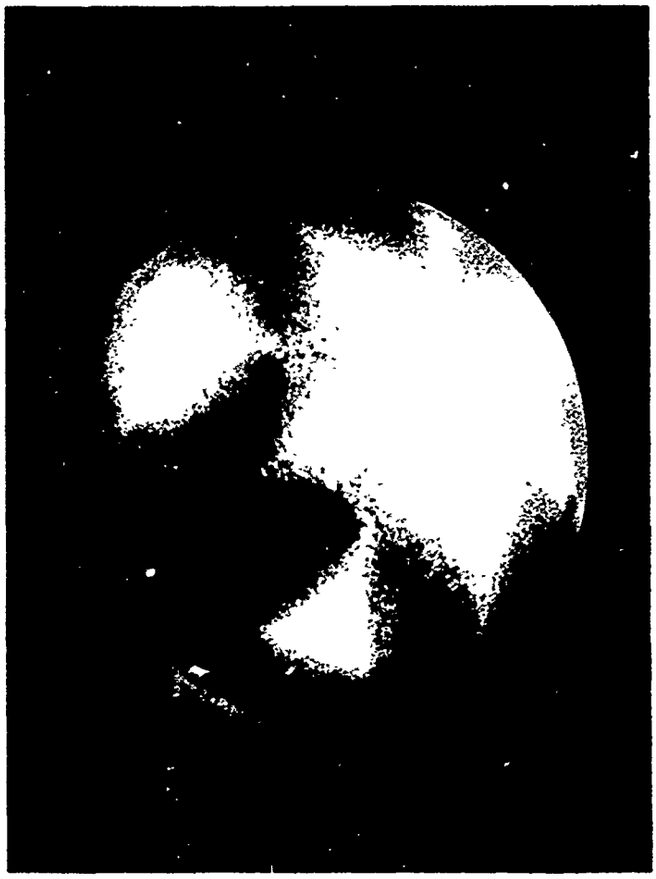

FIGURE 6

OPTICAL MICROGRAPH OF A 5/8 INCH SPHERE SHOWING
VARIATION OF INDUCTION PERIOD WITH ORIENTATION

C. Morphology and Epitaxy

The lateral shape (morphology) and orientation (epitaxy) of the oxide nuclei on a crystal face is governed by the surface and interfacial energies involved and the mechanism of growth. The configuration which is obtained is the lowest energy configuration compatible with the method of growth. Because of the symmetry relationships of the substrate and the oxide, more than one orientation is often obtained, all of which are equivalent from the interfacial energy viewpoint. At this time, information about the factors determining interfacial energies is insufficient to allow a comparison of experimental results with theory. For this reason, this work is limited to reporting the morphology and epitaxy observed.

1. (111) Face

On a clean (111) face oxidized above 250° C, two equivalent orientations of oxide nuclei were formed, a parallel orientation and an anti-parallel orientation in which the $[1\bar{1}0]$ metal axis was parallel to the $[\bar{1}10]$ oxide axis. Both of these orientations appeared as triangular nuclei on the surface. This is apparent in Fig. 7. The two orientations were distinguishable from each other, however, in that one appeared rotated 30° on the surface with respect to the other orientation. Another morphological feature was that nuclei of one of

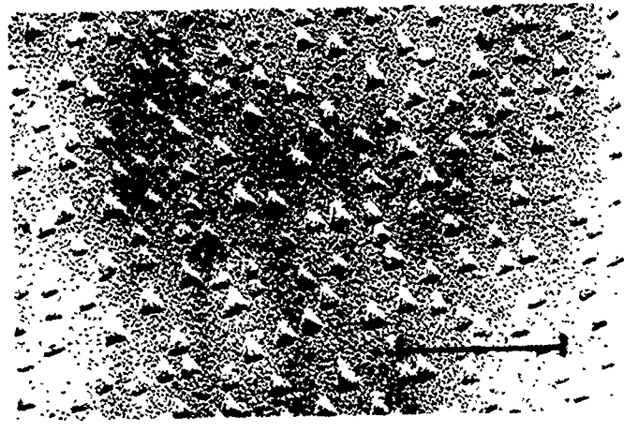

T = 150°C - 65 HR

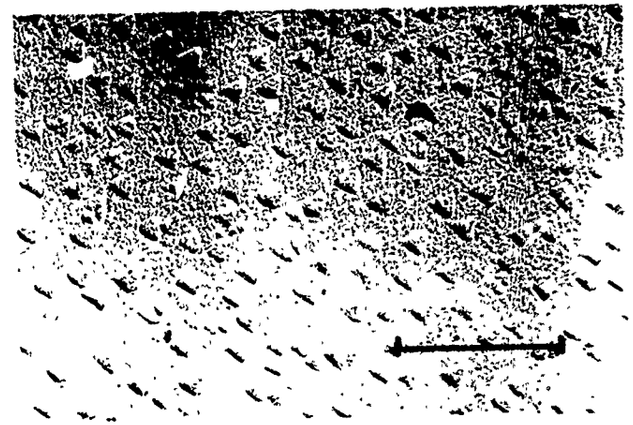

T = 200°C - 15 HR

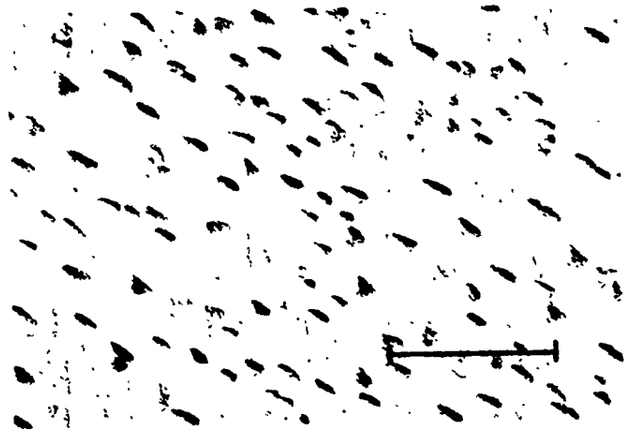

T = 300°C - 40 MIN

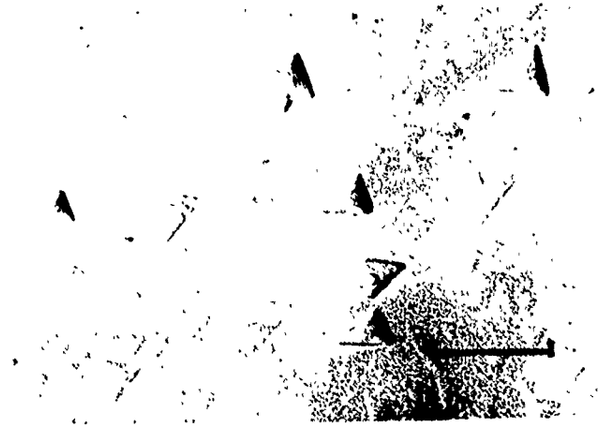

T = 400°C - 5 MIN

FIGURE 7

OXIDATION OF (111) FACE OF CU $P = 10\mu O_2$ - EFFECT OF TEMP.

the orientations grew much higher than the other and that nuclei with this orientation grew at the expense of the other. The taller nuclei were found from electron diffraction to show the parallel orientation while the other orientation was anti-parallel. Below 250° C the parallel oxide orientation was not observed.

Although the density of nuclei decreased and their size increased with increasing temperature, the nuclei retained their general features (Fig. 7). With time, however, the nuclei with a parallel orientation, which started growth as regular triangles, tended to become quite dendritic in character (Fig. 8) apparently because of multiple twinning of the oxide and the presence of neighboring oxide nuclei.

2. <u>(001) Face</u>

On the (001) face there occurred four equivalent orientations of oxide nuclei with the (111) $Cu_2O \parallel$ (001) Cu. The following axial relationships were determined:

$[1\bar{1}0]$ Cu_2O || $[1\bar{1}0]$ Cu
$[1\bar{1}0]$ Cu_2O || $[\bar{1}10]$ Cu
$[110]$ Cu_2O || $[1\bar{1}0]$ Cu
$[110]$ Cu_2O || $[\bar{1}10]$ Cu

These nuclei grew as right triangles, each triangle having its hypotenuse parallel to a <110> direction in the (001) plane of the metal. Nuclei of this type

0 MIN

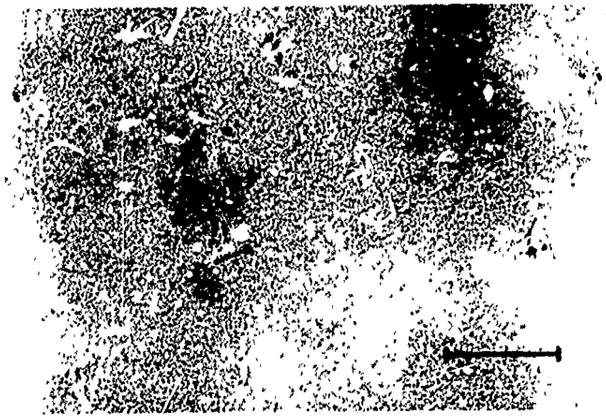

3 MIN

5 MIN

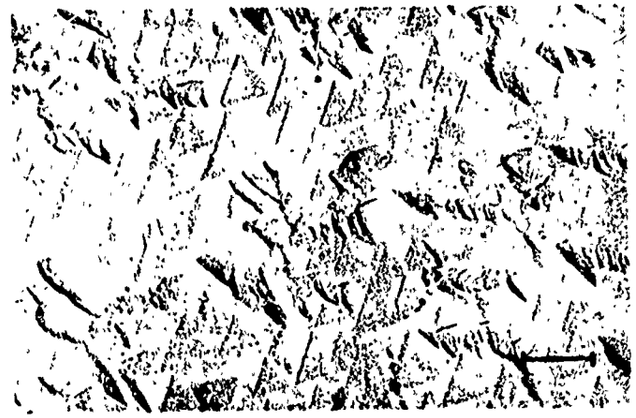

8 MIN

FIGURE 8

EFFECT OF TIME - MICROGRAPHS - (111) CU - T = 400°C P = $10_{\mu}O_2$

shown in Figs. 9a and 9b.

At temperatures above 600° C and pressures of approximately 10^{-2} torr, another shape oxide nucleus was observed along with the low temperature form. These nuclei, as seen in Figs. 10a and 10b, consisted of four rods growing with their long axis in the <710> direction from a common point. However, the rods were not connected at this point but left a low mound about .5μ across between the nuclei instead. The rods were not of equal length, as can be seen in the photographs (Figs. 10a and 10b), due to the fact that the face is slightly off the (001) orientation. The electron diffraction pattern taken in the [100] direction of the metal showed the following epitaxy, (510) Cu_2O || (001) Cu (Fig. 10c). Four equivalent orientations would be expected from symmetry considerations and each is represented by one of the arms of the nuclei.

3. <u>(110) Face</u>

On the (110) face of copper the copper oxide nuclei grew as rods with their long axis parallel to the [100] direction (Fig. 11a). The oxide was in the parallel orientation (110) Cu_2O || (110) Cu and [100] Cu_2O || [100] Cu.

4. <u>(311) Face</u>

On the (311) face, oxide nuclei grew in a dendritic manner as shown in Fig. 11b. On surfaces slightly off

(a)

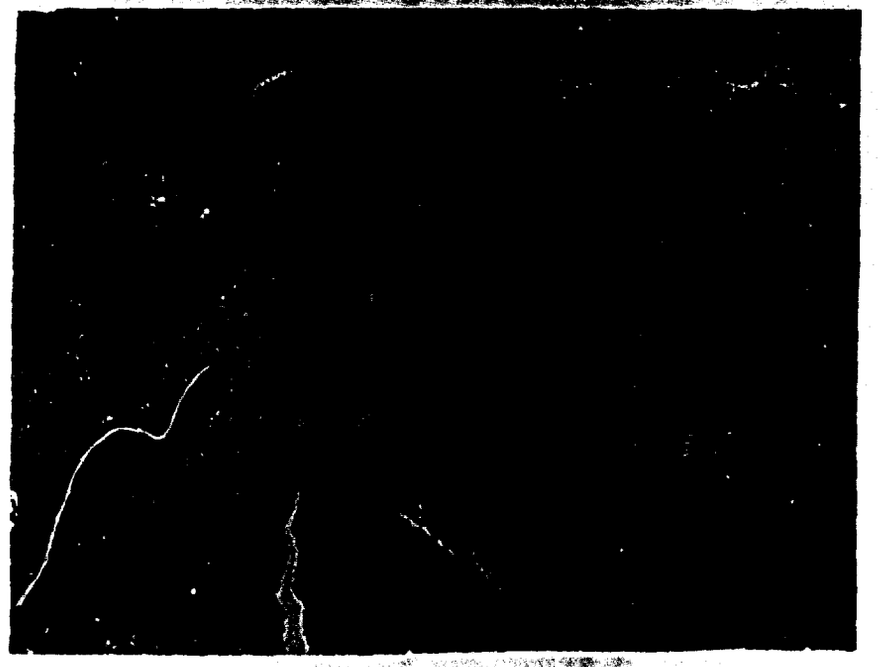

(b)

FIGURE 9

ELECTRON MICROGRAPHS OF OXIDE NUCLEI ON (100) FACE OF COPPER.

(a) 400°C, 10^{-2} torr, 5 minutes

(b) 700°C, 3 X 10^{-4} torr, 10 minutes

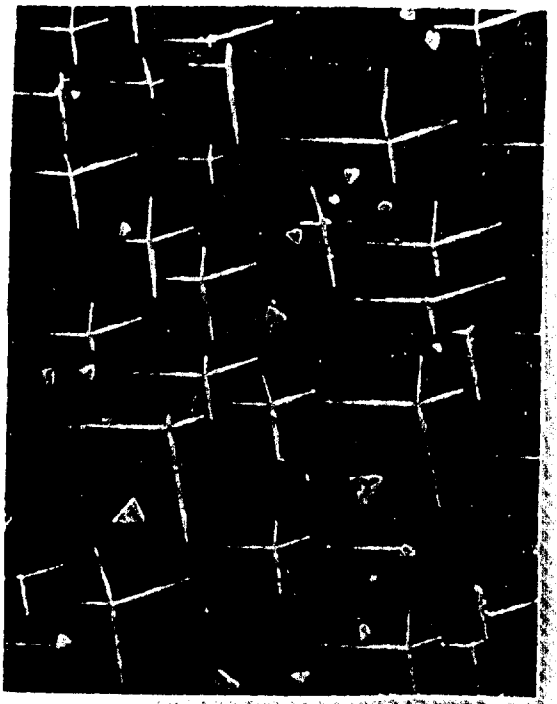

(a) X 500

(b)

(c)

FIGURE 10

OPTICAL MICROGRAPH, ELECTRON MICROGRAPH, AND ELECTRON DIFFRACTION PATTERN OF HIGH TEMPERATURE FORM OF OXIDE NUCLEI ON (100) FACE.

(a) 700°C, 10^{-2} torr, 5 seconds
(b) 700°C, 10^{-2} torr, 1 second
(c) 700°C, 10^{-2} torr, 1 second

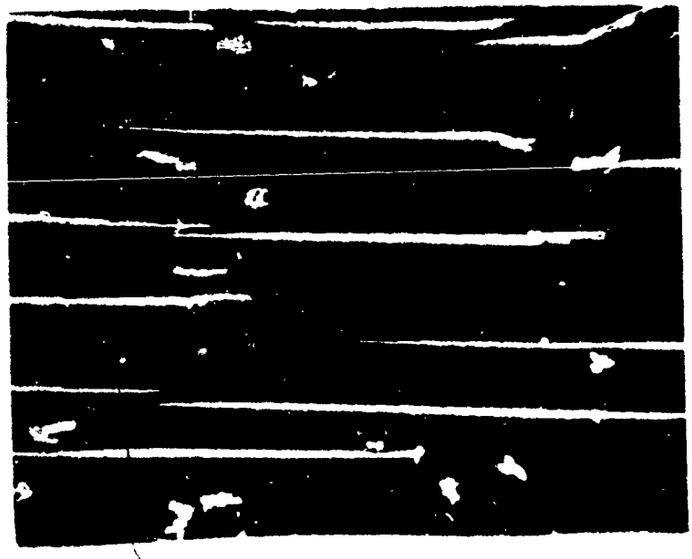

(a) X 100

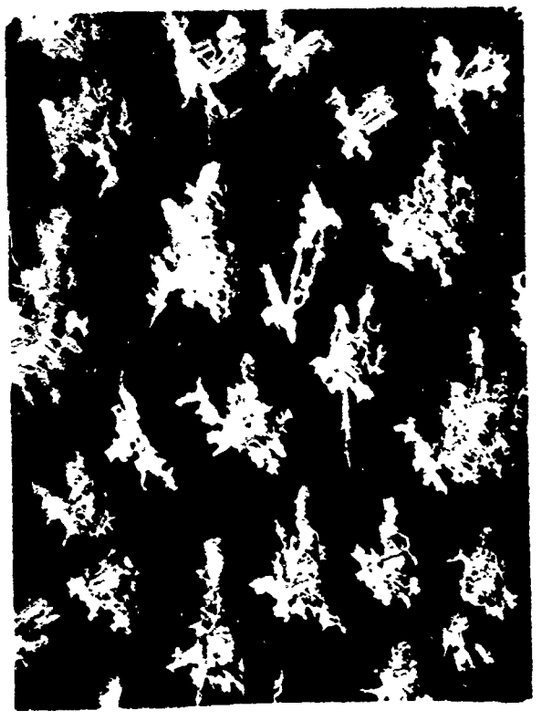

(b) X 800

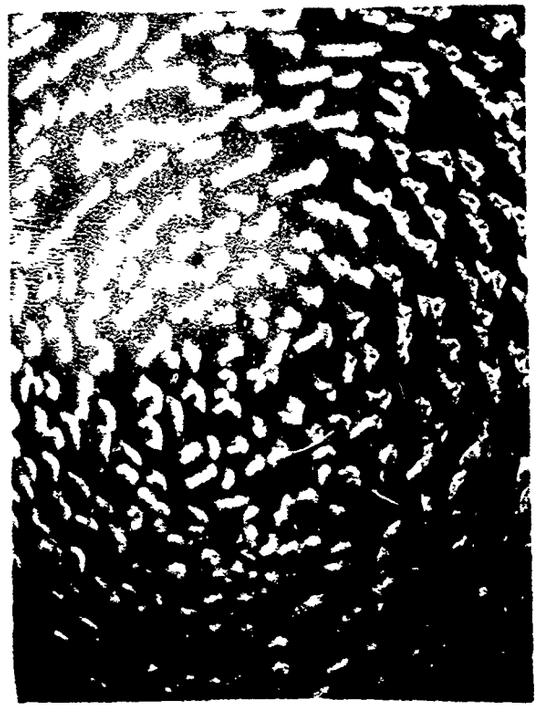

(c) X 300

FIGURE 11

OPTICAL MICROGRAPH OF OXIDE NUCLEI

(a) (110) face, 600°C, 5 X 10^{-5} torr, 20 minutes
(b) (311) face, 500°C, 2 X 10^{-3} torr, 5 minutes
(c) (311) face, 500°C, 10^{-3} torr, 30 minutes

the (311) face the nuclei grew somewhat longer in the direction normal to the [311] pole direction. Thus, when looking down on a spherical surface, one is given the impression of the nuclei arranged in circles about the [311] pole. This is shown in Fig. 11c.

B. Topography

1. Oxide Nuclei

Several methods were available for determining the topographic features (profile) of the oxide nuclei. The simplest and most frequently used method utilized the observation of replicas in the electron microscope. Platinum shadowed carbon replicas of the surface were made in the usual manner, except that the platinum was evaporated in a known crystallographic direction and at a specific, precisely known angle to the surface. This was generally a simple procedure since the majority of the samples that were used in this work were spheres with both a (111) and a (100) plane cut on their surfaces. Since two different interplanar angles were possible for these planes, 54°44' and 125°16', depending on the specific planes cut on the crystal, two different conditions for simultaneously shadowing both faces of each crystal were necessary. If the specific planes were (001) and (111) with an interplanar angle of 54°44', then for a shadowing angle of 20° the shadowing direction had to be approximately a $[3\bar{2}1]$ direction. The projection of the $[3\bar{2}1]$ direction onto both the (001) and (111) faces is approximately 8° from the $[1\bar{1}0]$ direction. If the specific planes were (100) and $(\bar{1}11)$ with an interplanar angle of 125°16', the shadowing direction was approximately a $[23\bar{3}]$ direction. This direction was adjusted so that

the shadowing angle was 27° on each of these faces. The projection of this direction on the (100) face is an <011> direction, and on the (111) face, the projection is now a <211> direction.

A slight modification of the above procedure involved dispersing small (.80μ) polystyrene latex spheres on the surface before making the usual platinum shadowed carbon replica (Fig. 14a). This addition allowed a much more accurate determination of the shadowing angle (by measuring the shadow length of the sphere in the replica) than the previous method where the sample was aligned for shadowing by sighting along a 20° wedge.

In some electron microscopic examinations of the replicas, it was found that the replica had broken and the broken edge had curled over. In a few cases the impressions in the replica from one or more oxide nuclei happened to be right on th rolled over portion of the replica so that a silhouette of the profile of a nucleus could be seen and photographed. Such a profile of two oxide nuclei is shown in Fig. 12b. Observations of this type provided good confirmation of profiles determined more indirectly from the normal replicas.

A Zeiss interferometer with a thallium light (λ = .27μ) source was also used to determine the oxide profiles. By measuring the displacement of the interference fringes (Fig. 14b) along the surface, the altitude of any point

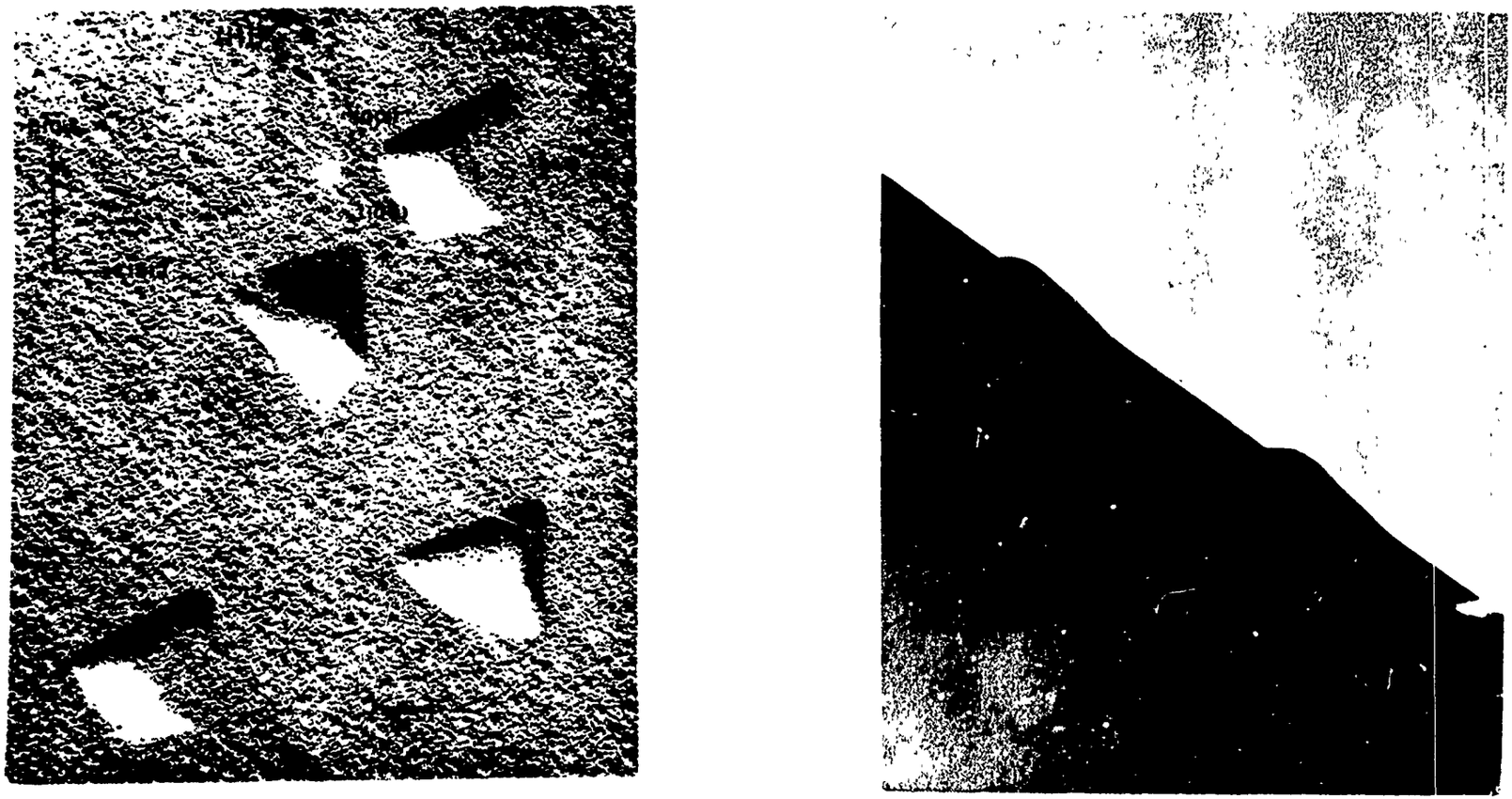

(a) (b)

FIGURE 12

ELECTRON MICROGRAPHS OF OXIDE NUCLEI ON (111) FACE FORMED AT 250°C, 10^{-3}TORR, 20 HOURS.

could be determined. Because of the small lateral magnification available in the light microscope, this technique was limited to studies of large nuclei formed at the higher temperatures.

a. (111) Face

Figures 12a and 12b show an example of typical nuclei observed on the (111) face of copper when the oxidation was carried out at temperatures of 300° C or less. The oxide nuclei were in the form of three sided pyramids, two sides being steeply inclined to the metal surface and the third side making a small angle with the surface. The crystal faces on one of the nuclei are identified in Fig. 12a. The other nuclei are similar except that they appear rotated 120° according to the side of the nuclei on which the high index plane is found. Figure 12b shows a silhouette of the vertical cross section to two of these nuclei. The faintly visible nucleus in the lower left hand corner of the figure can be used to determine the direction of the cross section.

Figure 13a shows the two types of nuclei formed at temperatures above 300° C with the planes of the parallel oriented nucleus labelled. The tops of these nuclei were frequently truncated by approximately (111) planes. The anti-parallel oriented nuclei which are also visible in this micrograph are much too shallow to give any indication of the planes from which they are formed.

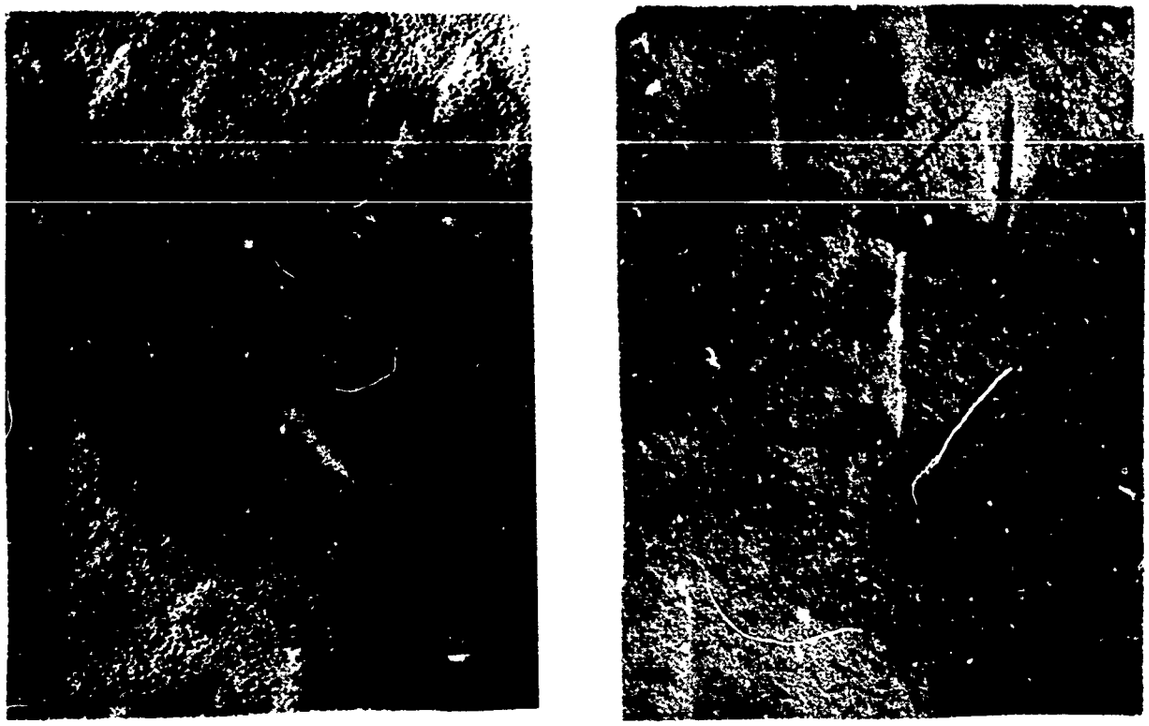

(a) (b)

(c) X 600

FIGURE 13

ELECTRON AND OPTICAL MICROGRAPHS OF OXIDE NUCLEI

(a) 400°C, 10^{-2} torr, 5 minutes

(b) 250°C, 2 X 10^{-3} torr, 12 hours

(c) 800°C, 10^{-3} torr, 15 hours

b. (100) Face

Figure 13b shows a typical micrograph of the nuclei obtained on the (100) surface at all but the higher temperatures and pressures. The indices assigned to the various surfaces of the nuclei can only be considered as approximate since the surfaces are obviously not well defined. The nuclei obtained at high temperatures and pressures as described in Section IV-C (Fig. 10) tended to be bound by (110) surfaces.

2. Metal Surface

The topography of the metal surface in the vicinity of the oxide nuclei was examined by the same techniques that were used to examine the nuclei themselves. For temperatures below 600° C, the metal surface was not detectably modified by the presence of the oxide nuclei. Above this temperature, however, the metal surface was noticeably affected by the presence of the oxide nuclei for distances of as much as 30 microns (Fig. 13c). Figure 14a shows a section of a nucleus on the (110) face which has two latex spheres on it for use in determining the height of the various features while Fig. 14c shows the development of faces extending onto the metal surface from the edge of the same nucleus. Figure 14d shows the tip of the same nucleus. The most striking feature in both Fig. 14c and Fig. 14d is the appearance of long facets, which are apparently (111) planes,

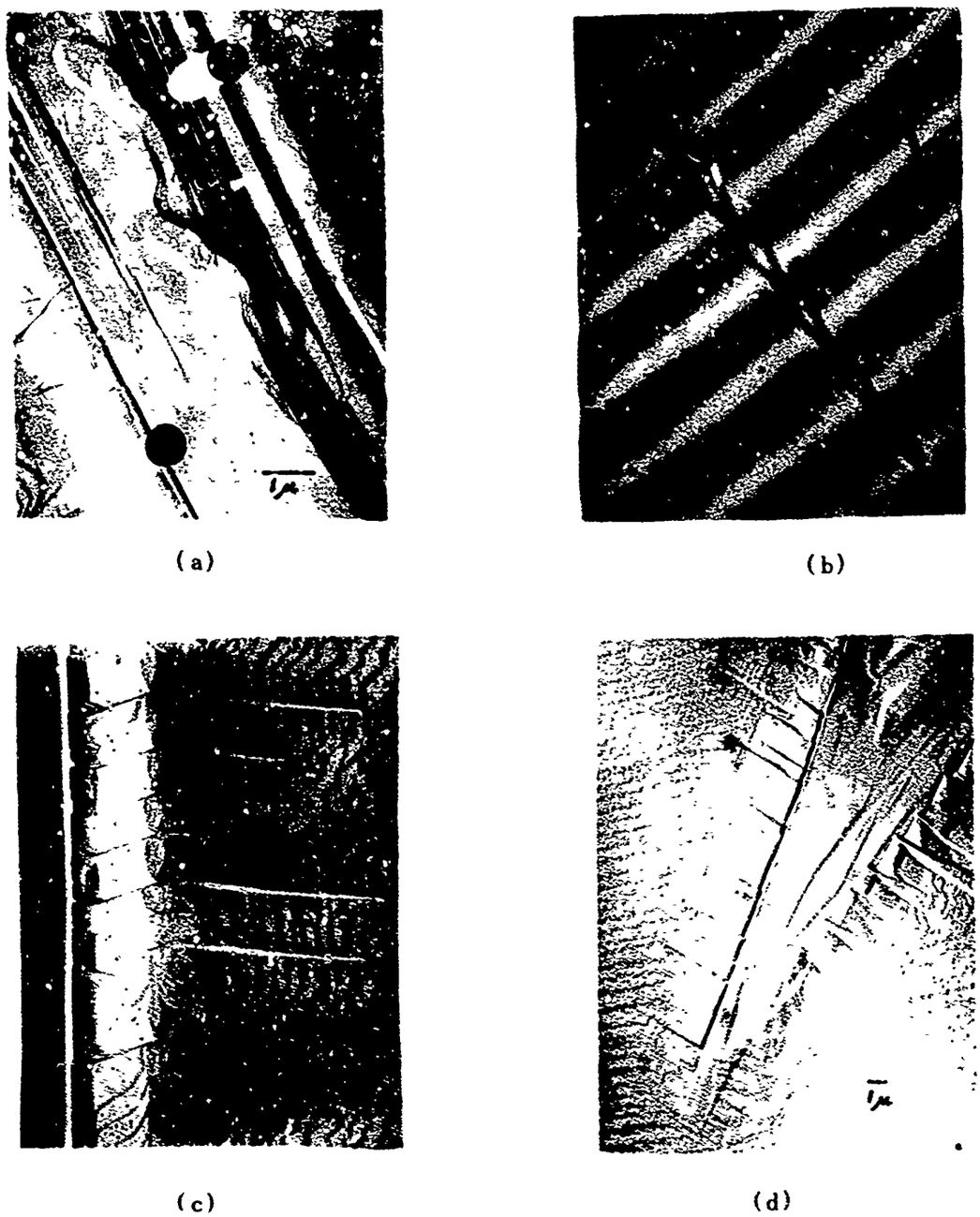

(a) (b)

(c) (d)

FIGURE 14

ELECTRON MICROGRAPHS AND INTERFERENCE MICROGRAPH OF OXIDE NUCLEI

(a) (110) face, 600°C, 5 X 10^{-5} torr, 20 minutes
(b) (110) face, 650°C, 2 X 10^{-5} torr, 1 hour
(c) (110) face, 600°C, 5 X 10^{-5} torr, 20 minutes
(d) (110) face, 600°C, 5 X 10^{-5} torr, 20 minutes

extending in the [1$\bar{1}$0] direction of the copper. This direction is perpendicular to the edge of the oxide nucleus which runs in the [00$\bar{1}$] direction of the metal.

The metal surface beneath the oxide nuclei could be examined by dissolving the oxide nuclei with a short rinse of dilute hydrochloric acid and then replicating the surface. Figure 15 shows an idealized cross section perpendicular to the axis of growth for the nucleus, shown in Fig. 14, which was formed on the (110) face of copper by oxidation at 650° C and 2 x 10^{-5} torr oxygen for one hour. The vertical scale has been expanded ten fold for clarity.

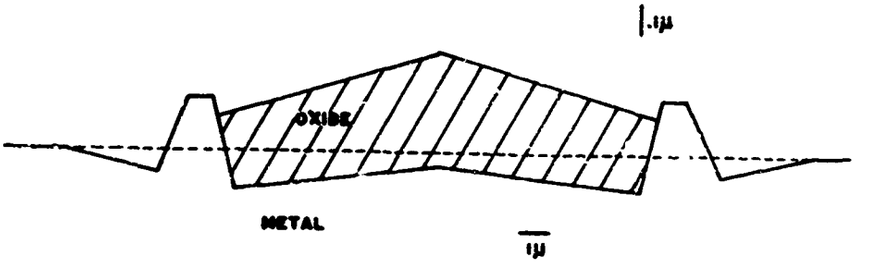

FIGURE 15

IDEALIZED CROSS SECTION OF AN OXIDE NUCLEUS ON THE (1:0) FACE (NOTE DIFFERENCE IN HORIZONAL AND VERTICAL SCALE)

E. Density

The number of oxide nuclei per square centimeter of surface, hereafter referred to as the density of oxide nuclei, was found to be a strong function of temperature and oxygen pressure. The density was also found to be slightly dependent on surface orientation, but independent of time, once the nuclei had obtained a size of approximately 10μ.

Figure 16 shows the temperature dependency of the density of oxide nuclei for the various faces of copper studied for an oxygen pressure of 10^{-2} torr. The straight line fit of this data to an Arrhenius plot indicates that the density of nuclei is determined by a simple activation energy controlled process.

The density of nuclei was found to be directly proportional to the oxygen pressure over the range of 10^{-2} - 10^{-6} torr on the (111) face. This relation is shown in Fig. 17 for the (111) face of copper at 600° C (the reliability of the point obtained at 10^{-6} torr is uncertain). The available data indicate that the same relation is true for the other crystal faces studied over the range of 10^{-2} - 10^{-3} torr for all temperatures.

The density of oxide nuclei was not a simple function of time. When observed by the optical microscope, there appeared no nuclei throughout the induction period. After the appearance of the first nuclei, the density rose

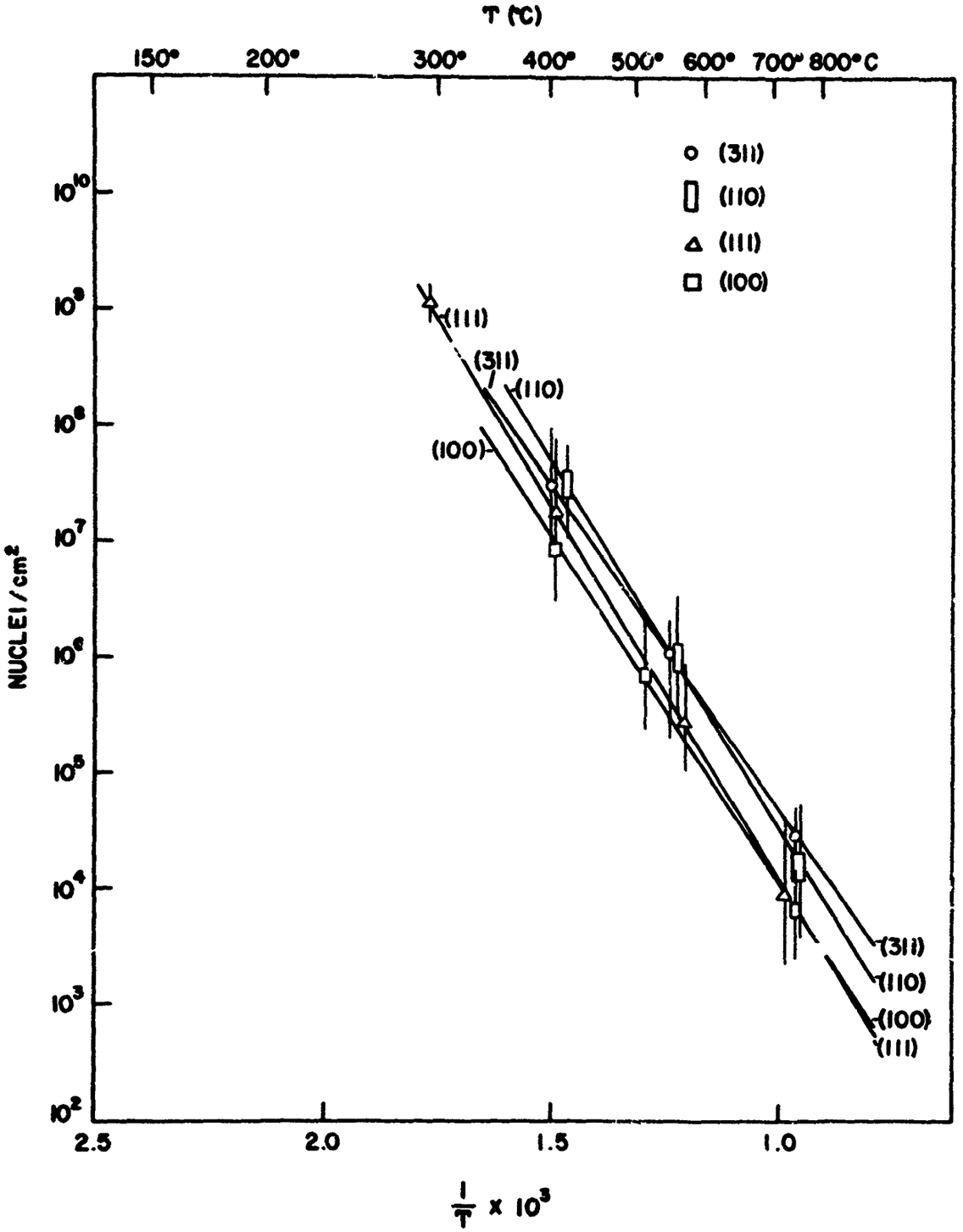

FIGURE 16

DENSITY OF NUCLEI PER SQUARE CENTIMETER AS A FUNCTION OF TEMPERATURE FOR VARIOUS CRYSTAL FACES AT 10^{-2} TORR.

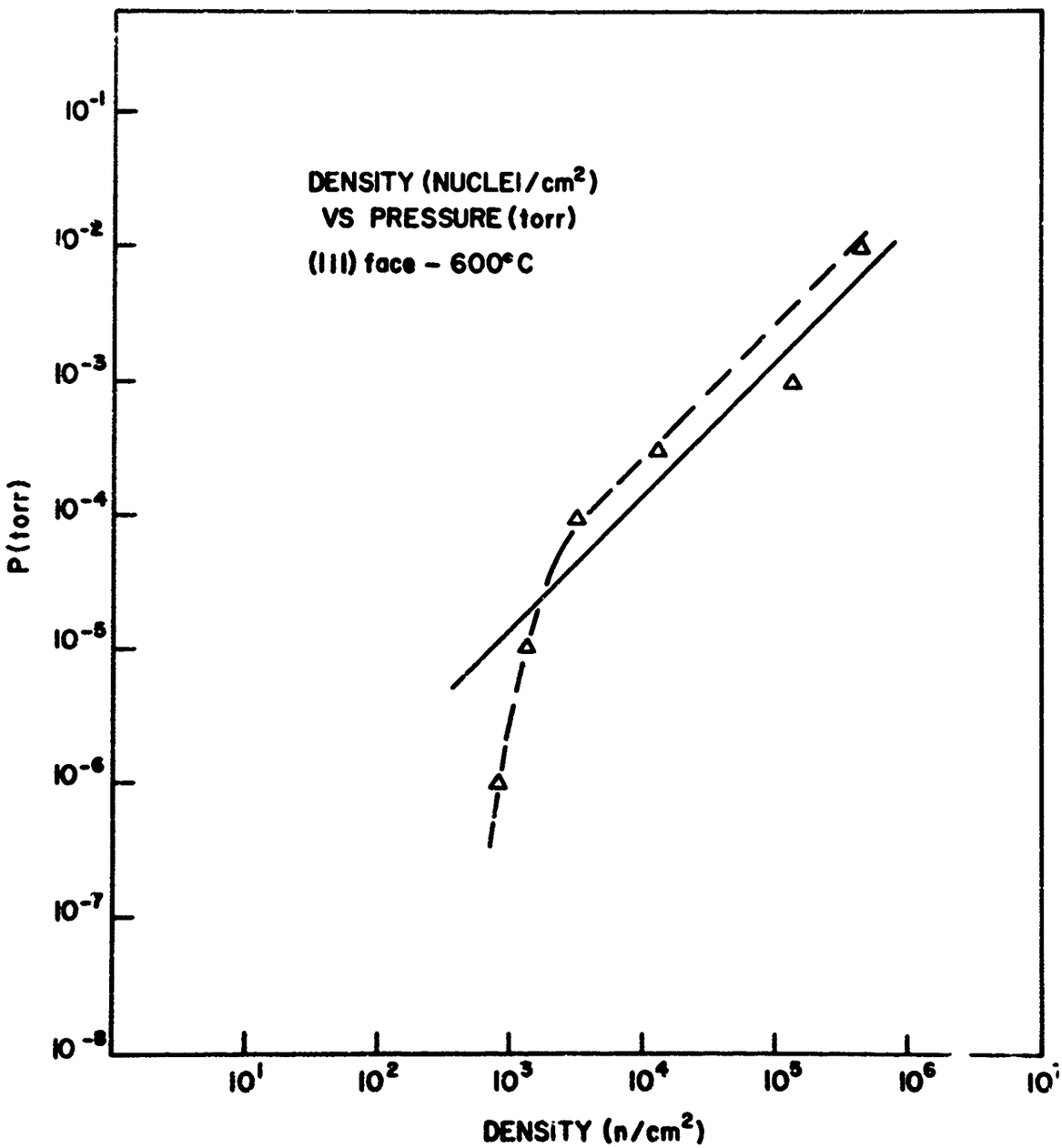

FIGURE 17

DENSITY OF NUCLEI AS A FUNCTION OF OXYGEN PRESSURE
FOR THE (111) FACE AT 600°C.

very rapidly to a maximum value at which level the density remained until the nuclei began growing together. As adjacent nuclei grew together, the density of nuclei decreased. When the surface was examined by replica techniques in the electron microscope, however, it appeared that at an earlier time in the oxidation, before oxide nuclei could have been seen in the optical microscope, there was a greater density of nuclei but that many of these small nuclei disappeared before growing large enough to be seen in the optical microscope. (See Fig. 8)

F. Stripped Nuclei

A few experiments were made on polycrystalline specimens under oxidation conditions which would produce large isolated nuclei. The purpose of these experiments was to remove these nuclei, unattacked, from the copper substrate in an ethanol-ammonia acetate solution so that they might be examined directly by transmission electron microscopy. Figure 18a shows the oxide stripped from an area of a polycrystalline copper sample in which the grains have an orientation near (111). The oxide nuclei in the micrograph show Bragg extinction contours typical of monocrystalline material, and electron diffraction patterns confirmed that these nuclei were single crystals. Higher magnification micrographs showed that the nuclei were free of dislocations except at the boundary where two nuclei had grown together. However, because of the small size of oxide nuclei, dislocations which may have been present in the nuclei as grown on the metal surface could have been removed by climb after the nuclei were removed from the metal. The micrograph also slows clearly that the oxide nuclei are considerably thinner in the center than at their edges. The dark regions in the micrograph correspond to thicker oxide which formed along a grain boundary in the copper. The micrograph also gives no indication of the presence of any oxide in the region between nuclei.

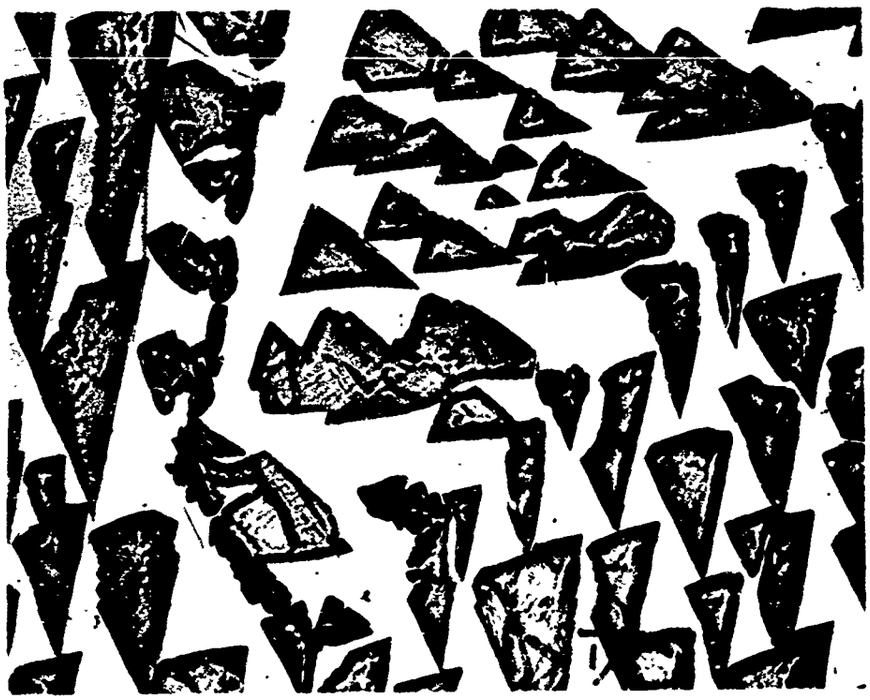

(a)

(b)

FIGURE 18

(a): TRANSMISSION ELECTRON MICROGRAPH OF STRIPPED OXIDE NUCLEI FROM POLYCRYSTALLINE COPPER OXIDIZED AT 400°C, 10^{-2} TORR, FOR 20 MINUTES

(b)· ELECTRON MICROGRAPH OF REPLICA OF THERMALLY FACETED (100) SURFACE, 500°C, 10^{-3} TORR, 30 MINUTES

G. Thermal Faceting

A by-product of the oxidation of copper at pressures below 10^{-3} torr and temperatures above 500° C was the development of facets on the metal surface. Figure 18b shows the facets developed on the (100) face during the induction period. Figure 27c shows a similar development of (111) and (100) type planar facets on a (311) copper surface under similar oxidizing conditions. The development of thermal facets is also noticeable in the majority of the electron micrographs of oxidations carried out at 600° C and above in this work. It is clear that the major facets developed are always of the type $\{111\}$ or $\{100\}$, but the curvature of the edges of these facets shows that some high index planes are also present.

H. Oxide Strain

It was possible in certain experiments to obtain very precise measurements of the lattice parameters of the oxide and of the metal by means of measurements of electron diffraction patterns. From these measurements, the strain of the oxide could be determined. The conditions necessary to obtain a suitable diffraction pattern for such measurements were as follows: 1) temperatures above 500° C, 2) pressures of 10^{-3} torr or less, and 3) oxidation times such that the crystal was at the end of the induction period or very early in the nucleation period. Under these conditions, the surface of the sample was made-up of very shallow steps with extremely smooth surfaces, apparently formed by thermal etching. A typical micrograph of such a surface is shown in Fig. 18b.

The diffraction pattern from the smooth steps was essentially that of a two dimensional grating and consisted of continuous straight lines normal to the shadow edge of the crystal. These lines are obvious in Fig. 19, which shows a diffraction pattern from a (111) face after oxidation under the above conditions. Oxide diffraction lines from a highly oriented cuprous oxide were also present parallel to the diffraction lines from copper. The strong intensity of the diffraction lines from copper indicated that either the oxide was present in patches on the surface with bare metal between, or that the oxide

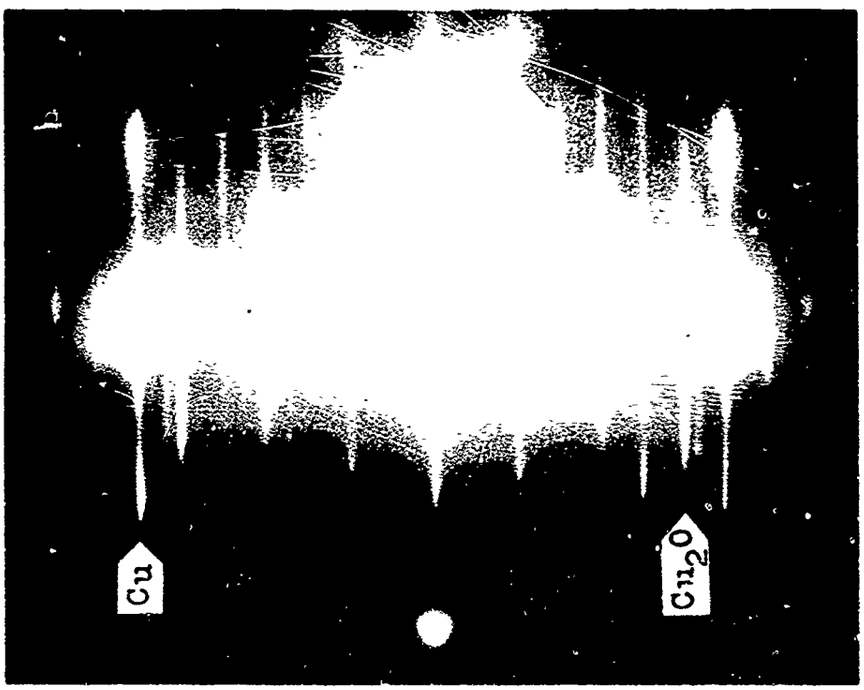

FIGURE 19

GLANCING ANGLE ELECTRON DIFFRACTION PATTERN OF (111) FACE IN $[01\bar{1}]$ DIRECTION. OXIDIZED AT 700°C, 6 X 10^{-3} TORR, 1 MINUTE.

was extremely thin (on the order of 10 Å). The smoothness of the surfaces, as seen in the replicas, suggested that the latter case was more likely.

The diffraction patterns were complicated by multiple diffraction, in which a diffracted beam from either oxide or metal acted as a primary beam and was diffracted again. Most of the features of Fig. 19 can be explained on this basis.

Lattice parameter measurements were made by measuring the distance between the vertical lines and converting these to d_{hkl} values by use of the diffraction camera constant. The precision of the measurements in this case was much higher than that normally obtained from spot measurements in electron diffraction. Measurements were made on diffraction patterns from bulk copper samples which were either 1) annealed and thoroughly outgassed, or 2) saturated with oxygen. These patterns showed only diffraction lines from copper and the lattice parameters for both samples were identically those of bulk copper.

Measurements were then made of the oxide lines in the diffraction patterns from (111) samples oxidized at 500° C to 800° C, using the measurements of the copper diffraction line spacings as an internal standard. The d_{220} and d_{422} values for the oxide were determined from these measurements. This data is shown in Table 1. The bulk values of the oxide parameters are also included.

From this data it is seen that the oxide on the (111) face is compressed laterally in both the $[1\bar{1}0]$ and the $[2\bar{1}\bar{1}]$ directions.

TABLE 1

Compression of Thin Oxide Film on (111) Face

Temp. of Oxidation	Spacing Determined	Measured Value (Å)	Bulk Value	% Compression
500° C	$[42\bar{2}]$ Cu_2O	$.860_5 \pm .002$	.8715	1.3 ± .2
500° C	$[2\bar{2}0]$ Cu_2O	$1.487 \pm .003$	1.510	1.5 ± .2
700° C	$[2\bar{2}0]$ Cu_2O	$1.489 \pm .003$	1.510	1.4 ± .2
800° C	$[42\bar{2}]$ Cu_2O	$.863_0 \pm .001$	.8715	1.1 ± .2
800° C	$\lvert 2\bar{2}0 \rvert$ Cu_2O	$1.493 \pm .004$	1.510	1.1 ± .2

Also present in some of the diffraction patterns was a set of lines with a very small spacing between them. These are apparent in Fig. 19, and will be considered in the next section.

I. Unusual Diffraction Results

1. Adsorption Structures

In some experiments in which the oxygen exposure was either slightly more or slightly less than that required to produce the first scattered oxide nuclei, electron diffraction patterns showed extra streaks which indicated periodic lattice spacings which were based on the copper substrate lattice.

a. (100) Face

Figure 20a shows a (100)[011] pattern and Fig. 20b a (100)[001] pattern from a copper surface after exposure to oxygen at 500° C and a pressure of 5×10^{-4} torr for 10 hours. Figure 20a shows only the streaks expected from a normal smooth copper surface with several additional weak oxide lines. On the other hand, Fig. 20b, from the same surface but with the electron beam in a different direction, shows three extra diffraction lines between each pair of normal lines. These patterns indicate that there exists on the surface a periodic structure with the dimensions of $\underline{a} \times 2\underline{a}$, where $\underline{a}$ is the normal [100] spacing of the face centered copper cell. The relationship of these two diffraction patterns to the LEED pattern observed by Simmons (14) for an oxygen adsorption structure on (100) copper is shown in the reciprocal lattice drawing of Fig. 21a.

Figure 20c shows a (100)[011] pattern from a copper

(a)

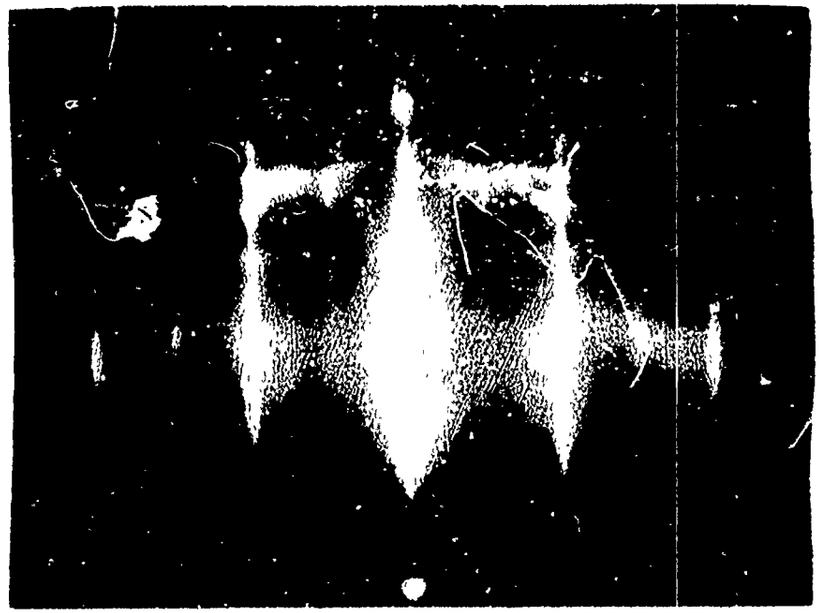

(b)

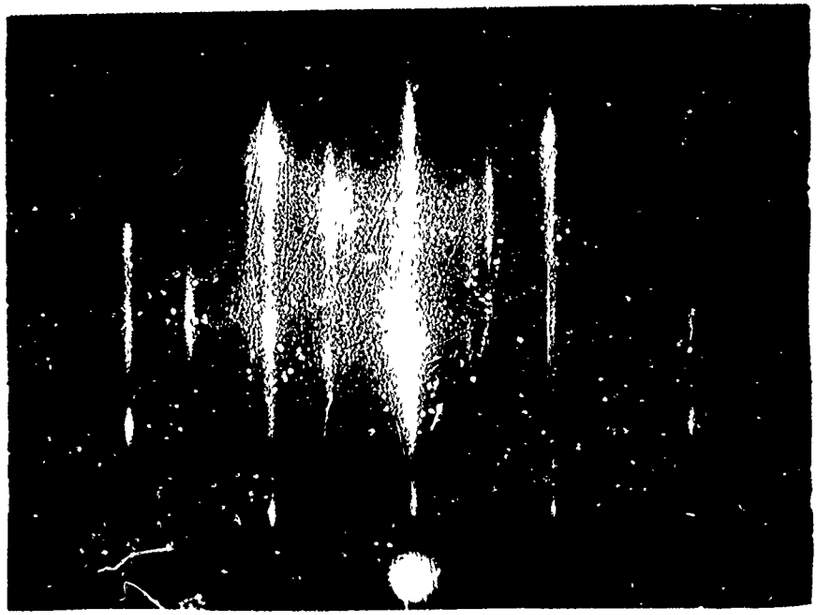

(c)

FIGURE 20

GLANCING ANGLE ELECTRON DIFFRACTION PATTERNS
OF ADSORPTION STRUCTURES ON (100) FACE OF COPPER

(a) (100) $[01\bar{1}]$

(b) (100) [001]

(c) (100) $[01\bar{1}]$

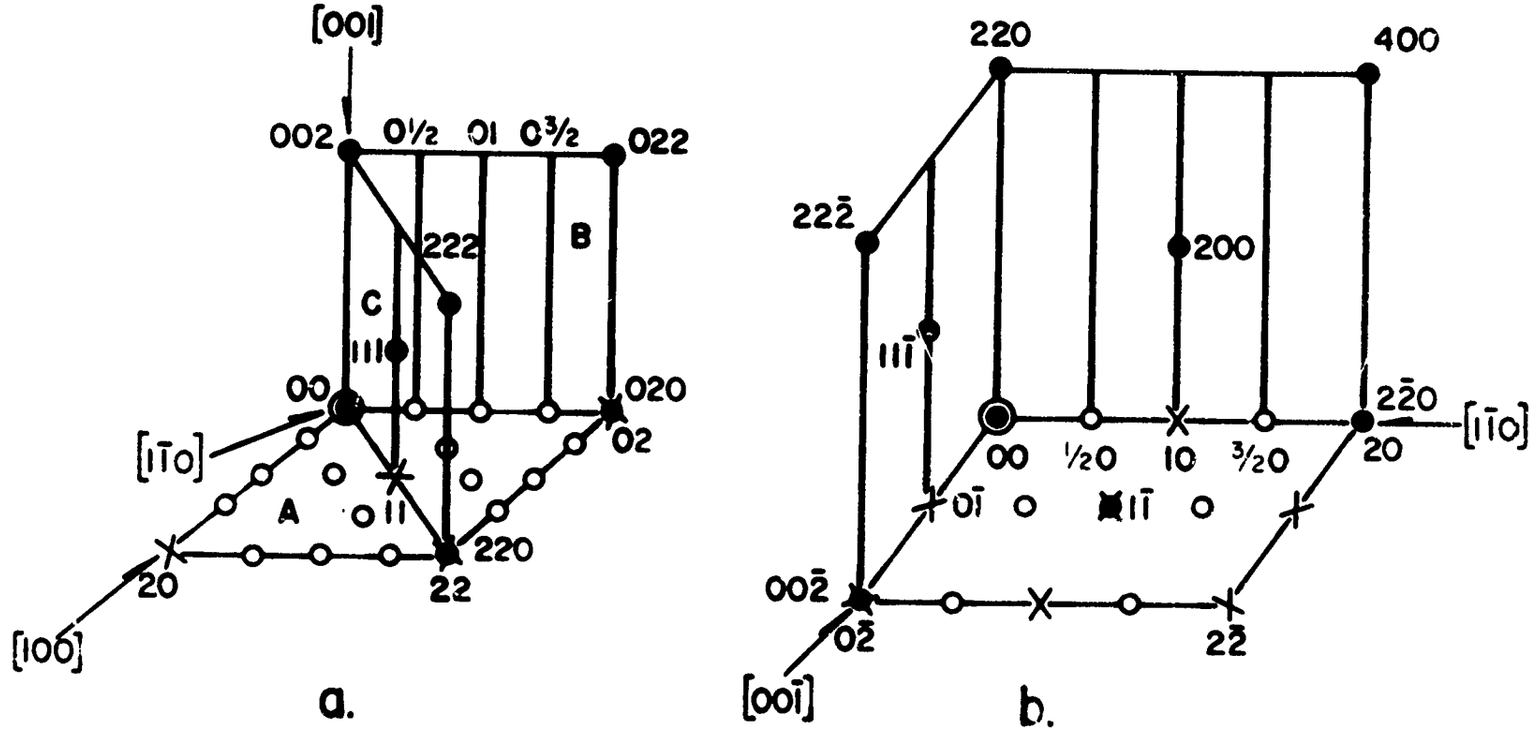

FIGURE 21

RECIPROCAL LATTICE DRAWINGS SHOWING THE RELATIONSHIP BETWEEN SPOTS OBSERVED IN LEED AND STREAKS OBSERVED IN HIGH ENERGY ELECTRON DIFFRACTION.

surface after exposure to oxygen at 700° C and a pressure of 6×10^{-3} torr for 1 minute. This pattern can be explained on the basis of one set of extra lines corresponding to a spacing four thirds that of the normal d_{022} copper spacing. All the other extra lines in the pattern can then be explained as a result of double diffraction. The diffraction pattern taken with the beam in the [001] direction on this surface showed only the normal copper lattice streaks.

b. (110) Face

Figures 22a, 22b, and 22c show electron diffraction patterns from a (110) surface exposed to oxygen at 800° C at a pressure of 2×10^{-4} torr for twelve minutes. No extra lines are present in Fig. 22a, but both Figs. 22b and 22c show two extra lines between each pair of normal lines. These patterns indicate a surface structure with a rectangular lattice having the dimensions of $\underline{a} \times 3 \times \sqrt{2}\ \underline{a}$, i.e. a cell which is equal to the copper spacing in the [001] direction and three times the copper spacing in the $[1\bar{1}0]$ direction.

Figures 23a, 23b, and 23c show patterns from another (110) surface oxidized at 800° C and 2×10^{-4} torr for 1 hour. These patterns can be interpreted on the basis of two surface structures, one with an $\underline{a} \times 2\sqrt{2}\ \underline{a}$ cell and the other with an $\underline{a} \times 3\sqrt{2}\ \underline{a}$ cell. Figure 21b shows the reciprocal lattice drawing relating the $\underline{a} \times 2\sqrt{2}\ \underline{a}$

(a)

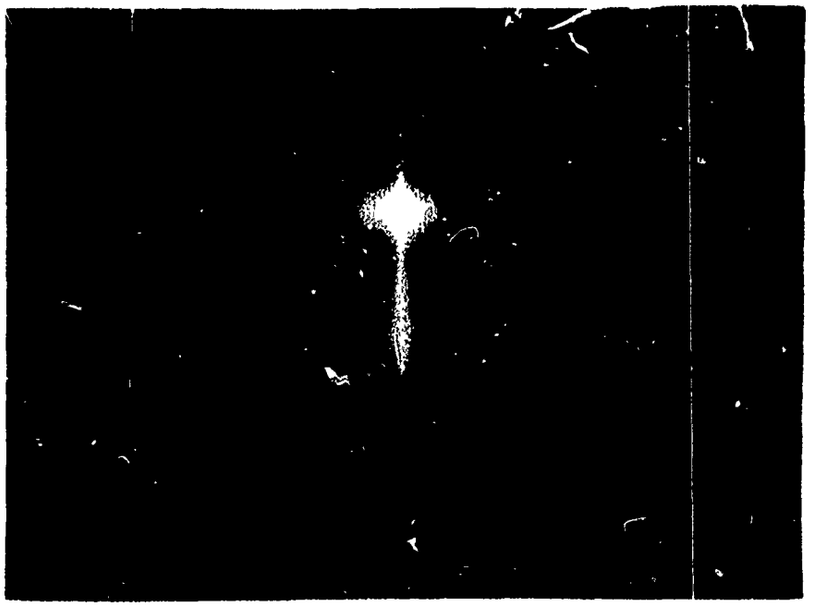

(b)

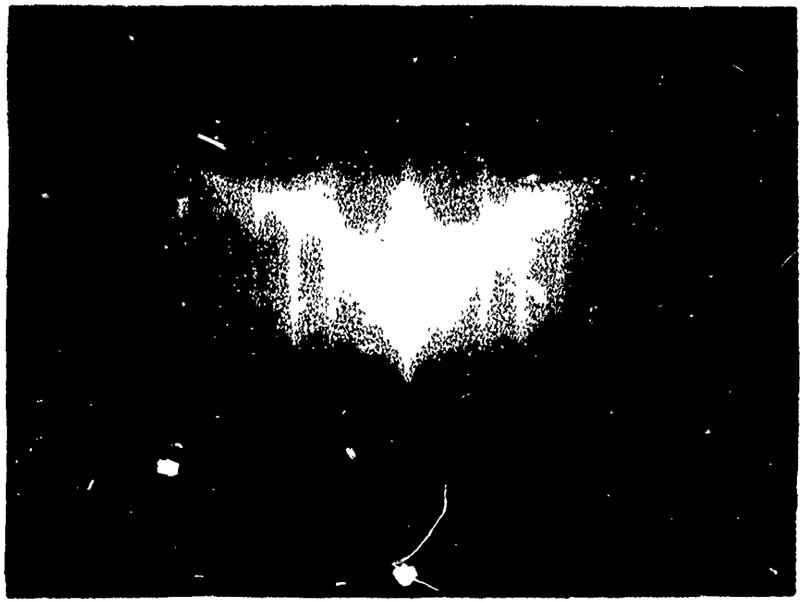

(c)

FIGURE 22

GLANCING ANGLE ELECTRON DIFFRACTION PATTERNS OF ADSORPTION STRUCTURES ON (110) SURFACE

(a) (110) $[1\bar{1}0]$
(b) (110) $[3\bar{3}2]$
(c) (110) [001]

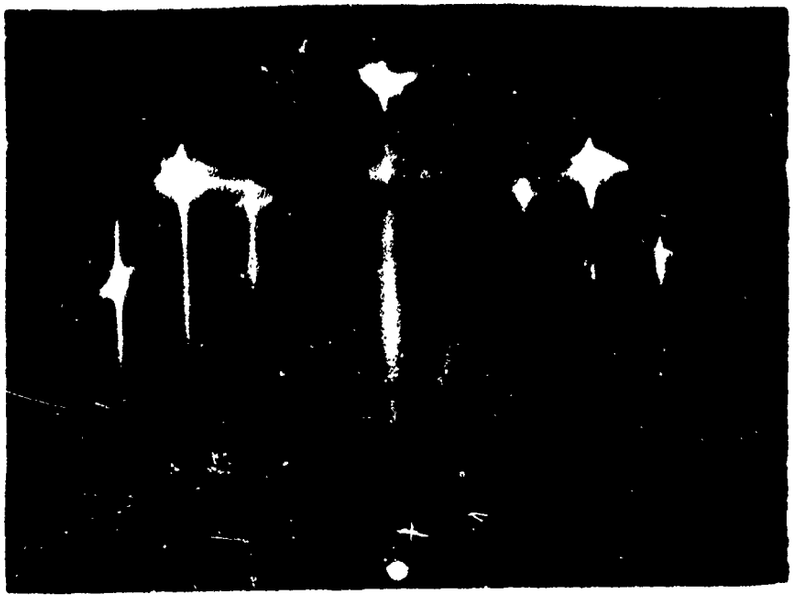

(a)

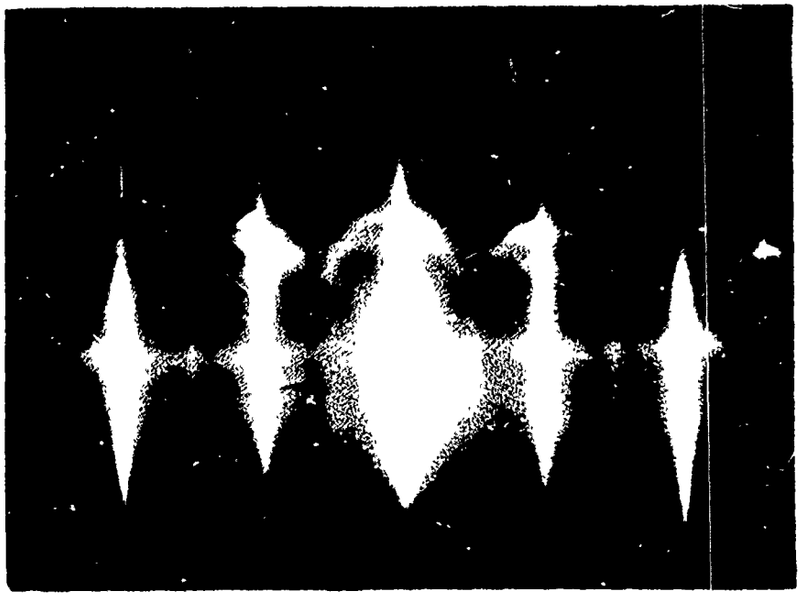

(b)

(c)

FIGURE 23

GLANCING ANGLE ELECTRON DIFFRACTION PATTERNS OF ADSORPTION STRUCTURES ON (110) SURFACE

(a) (110) $[1\bar{1}0]$

(b) (110) $[1\bar{1}2]$

(c) (110) [001]

pattern to the LEED pattern observed by Simmons (14).

c. (311) Face

Figures 24a and 24b show the electron diffraction patterns from a (311) surface which was exposed to oxygen at 800° C at a pressure of 2×10^{-4} torr for 1 hour. Figure 24a, taken in the $[1\bar{4}1]$ direction shows four extra lines between the normal copper lines. Figure 24b, however, taken with the beam in the $[01\bar{1}]$ direction shows no extra lines. A reasonable structure explaining these patterns has not yet been determined.

2. Super-Structures

Electron diffraction patterns from (111) surfaces oxidized at 700° C or higher for periods of time slightly less than necessary to produce oxide nuclei on the surface showed a parallel array of very closely spaced lines or streaks. Figure 25a shows a $(111)[1\bar{1}0]$ pattern from which the complete reciprocal lattice for the structure producing the pattern can be obtained. The lattice spacing in the $[11\bar{2}]$ direction can be determined directly by measurement of the distance between two adjacent lines lying on a Laue zone. Each of the areas showing maximum intensity of the streak pattern corresponds to a Laue ring or zone. These originate in the intersection of the Ewald reflecting sphere with successive reciprocal lattice planes along the direction of the electron beam.

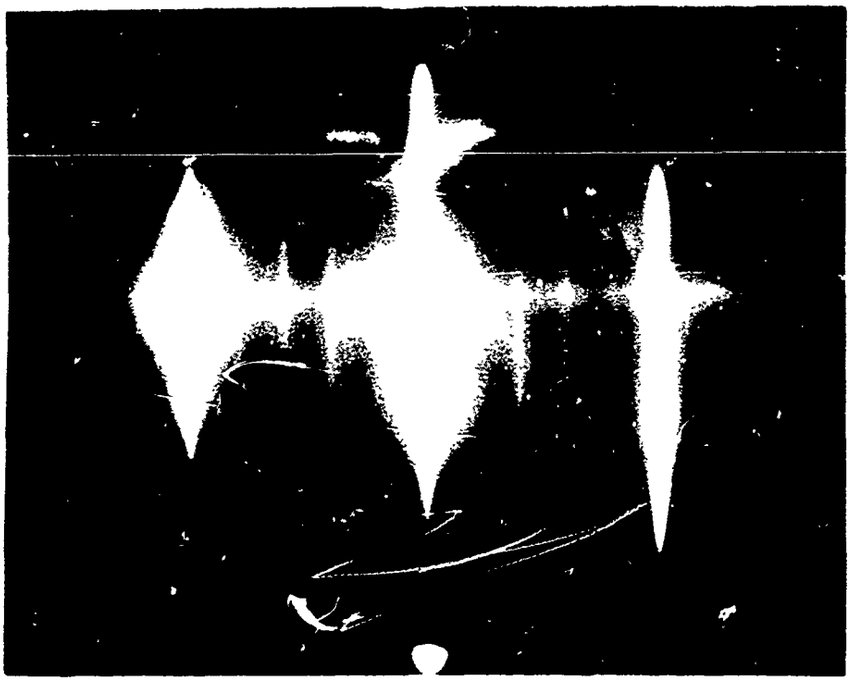

(a)

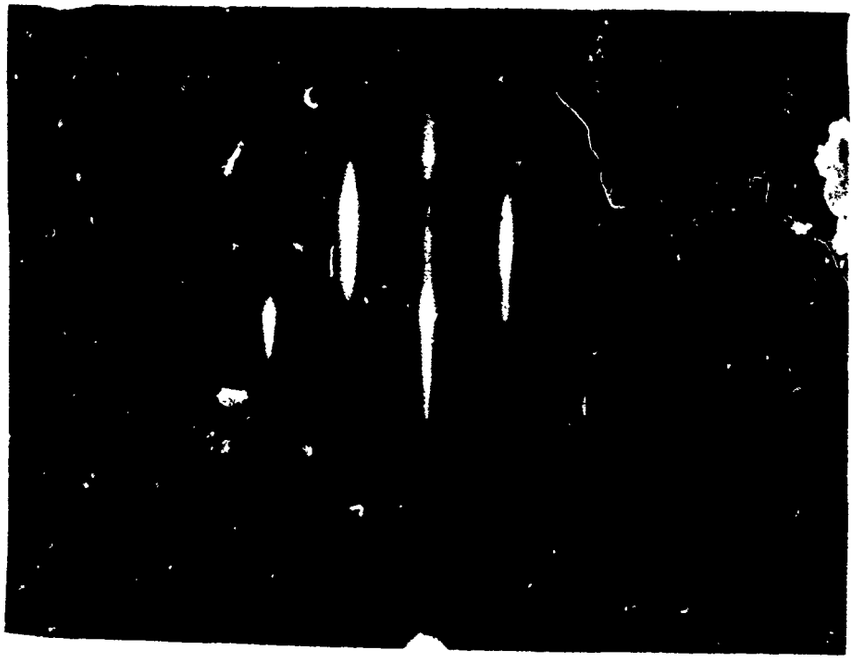

(b)

FIGURE 24

GLANCING ANGLE ELECTRON DIFFRACTION PATTERNS OF ADSORPTION STRUCTURES ON (311) SURFACE

(a) (311) $[1\bar{4}1]$

(b) (311) $[01\bar{1}]$

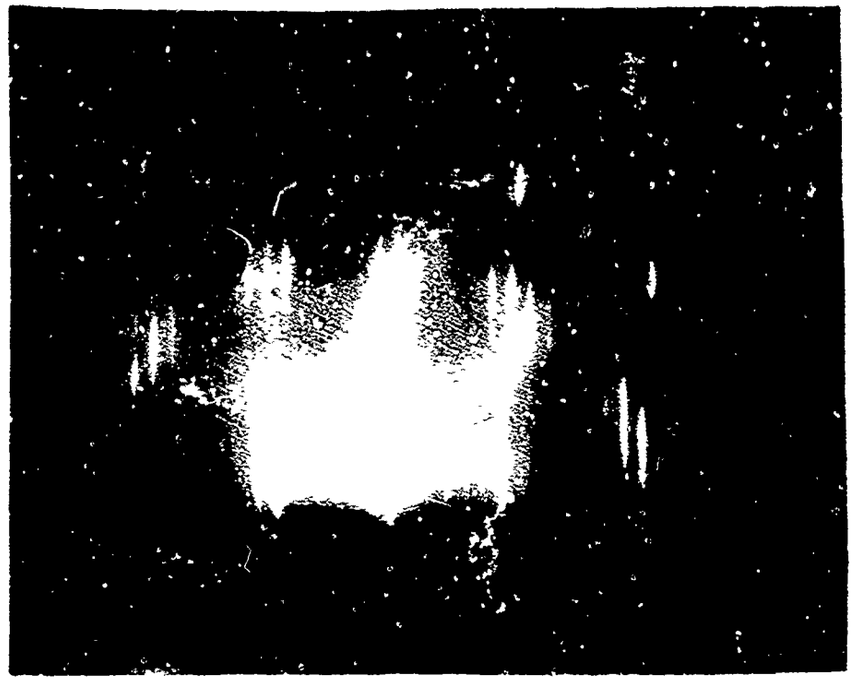

(a)

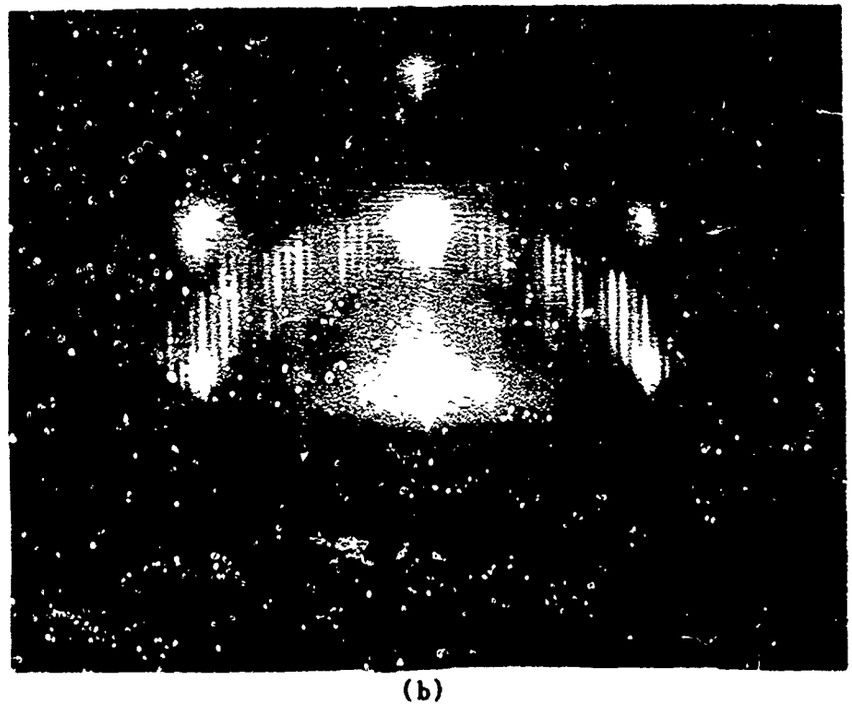

(b)

FIGURE 25

GLANCING ANGLE ELECTRON DIFFRACTION PATTERNS OF (111) SURFACE SHOWING DIFFRACTION LINES CORRESPONDING TO A CELL OF VERY LARGE DIMENSIONS

(a) (111) $[\bar{1}10]$

(b) (111) $[\bar{2}11]$

The measurement of the spacings of the Laue zone rings (33) then permits the determination of the spacing of the reciprocal lattice in the $[1\bar{1}0]$ direction from the formula:

$$s = \frac{2nL^2\lambda}{(R_n)^2 - 2R_oR_n}$$

where (34,35)

s = spacing in direction parallel to beam

n = order of intensity maxima

L = sample to photographic film distance

R_o = radius of zero order maxima

R_n = radius of n order maxima

λ = wave length of electron beam

Tilting of the sample during examination in the electron beam showed clearly that the reciprocal lattice was made up of a regular array of rods normal to the crystal surface. Figure 26 shows a schematic diagram of the appearance of this reciprocal lattice. The real lattice corresponding to this reciprocal lattice is a two dimensional hexagonal array of points in the (111) plane and a diagram of this is also shown in Fig. 26.

Figure 25b is an electron diffraction pattern of the same (111) surface taken with the beam in the $[\bar{1}\bar{1}2]$ direction. This shows quite clearly that the normal copper $[2\bar{2}0]$ distance is divided exactly into 20 1/2 divisions, which corresponds to the 26.2 Å spacing

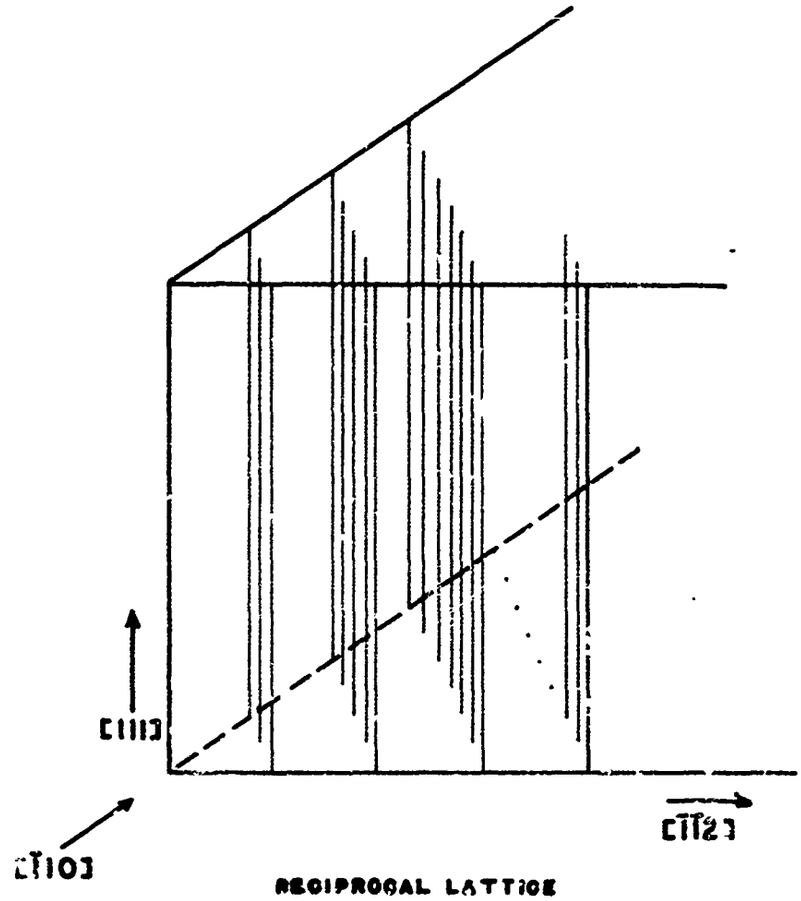

FIGURE 26

RELATIONSHIP BETWEEN RECIPROCAL LATTICE RODS AND TWO DIMENSIONAL REAL LATTICE OF POINTS

determined from measurements of the distance between the Laue rings shown in Fig. 25a.

This structure is also easily seen in Figs. 27a and 27b. In this case a (311) face was oxidized under conditions which produced (111) and (100) facets belonging to the $[01\bar{1}]$ zone. These facets are shown in the electron micrograph, Fig. 27c. Figure 27a, taken with the beam in the $[01\bar{1}]$ direction, thus gives diffraction patterns for both (111) and (100) surfaces. Figure 27b, on the other hand, taken with the beam in the $[\bar{2}33]$ direction (perpendicular to the $[0\bar{1}1]$) gives a view of the reciprocal lattice on the (111) face at an angle of 30° to the direction of the reciprocal lattice rods. The structure derived from these patterns for the (111) facets is identical to that derived for the flat (111) surface. The structure corresponding to the (100) facets has not yet been worked out in detail.

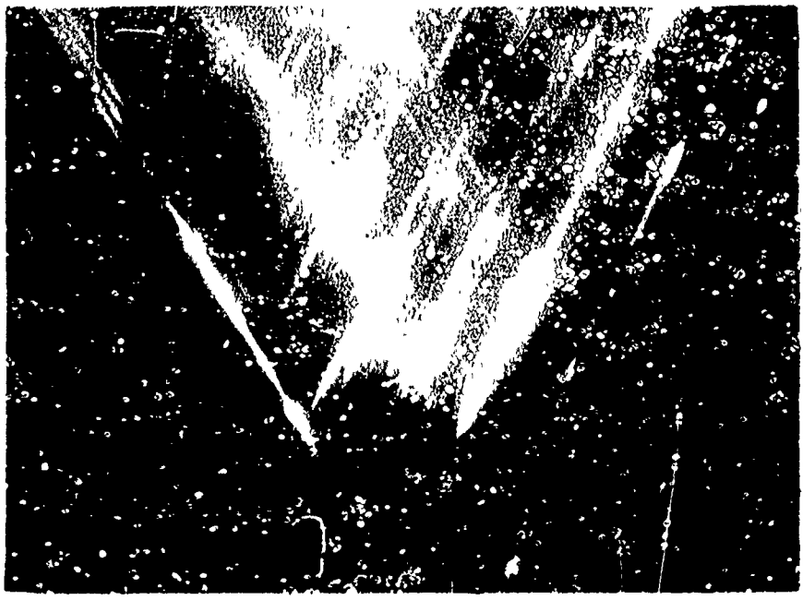

(a)

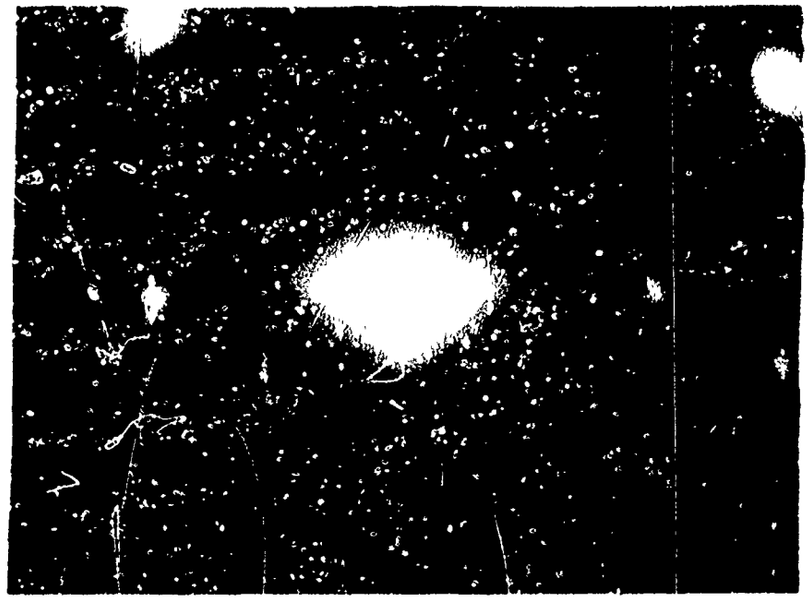

(b)

(c)

FIGURE 27

(311) FACE OXIDIZED AT 800°C, 7 X 10^{-4} TORR FOR 10 MINUTES

(a) Glancing angle diffraction pattern of (311) [01$\bar{1}$]

(b) Glancing angle diffraction pattern of (311) [$\bar{2}$33]

(c) Electron micrograph

J. Kinetics

1. Method of Calculation

For the purpose of measuring the rates of oxidation of the various crystal faces, disc shaped samples were used which were approximately 1.8 cm in diameter and .1 cm thick with a small hole hear the edge, by which the sample could be supported. For these samples, about 10% of the sample area consisted of surfaces with orientations other than that of the two flat surfaces of the disk. The results were calculated on the assumption that all of the sample's surface was of one orientation. (A discussion of the error due to this assumption can be found in Section V-C-1.)

The volume of the system was determined by expansion of oxygen from the reactor system into an evacuated vessel of known volume. The ratio of the pressure in the system before and after the expansion gave the volume of the system by means of the equation

$$V_{system} = V_{known} \cdot \frac{P_{final}}{P_{original} - P_{final}}$$

The Pirani gauge which was an integral part of the system was used for determining $\frac{P_{final}}{P_{original} - P_{final}}$ in the pressure range of 10^{-2} - 10^{-3} torr. The result was not a function of the sensitivity of the Pirani gauge but

was a function of its linearity and was repeatable to .5%. With a knowledge of the volume of the system and a continuous record of the pressure in the system during an oxidation (Fig.4), the quantity of gas taken up by the copper sample could be calculated. From the rate of pressure drop in the system, the volume of the system, the temperature of the gas, and the area of the sample, the sticking coefficient of the sample could be calculated. The following is a sample calculation of these quantities.

a. Definition of Symbols

α = sticking coefficient =

$$\frac{\text{rate molecules are irreversibly adsorbed}}{\text{rate molecules strike the surface}}$$

Q ($g\ O_2/cm^2$) = quantity of oxygen taken up by surface

J ($g\ O_2/cm^2 sec$) = rate of oxidation of surface

$k = 1.74 \times 10^{-3}\ g\ O_2\ torr^{-1}\ liter^{-1}$

P (torr) = oxygen pressure

V (l) = volume of system

A (cm^2) = area of sample

M ($g/cm^2 sec\ torr$) = rate oxygen strikes surface per torr = $.329\ T^{-\frac{1}{2}}$

T_g (°K) = gas temperature

b. Sample calculations

Calculation showing determination of quantity of gas taken up by a square centimeter of sample for a 1 scale division pressure change. (sample area = 5 cm^2)

$$Q = \frac{k \cdot P \cdot V}{A} = \frac{1.74 \times 10^{-3} \text{g } O_2}{\text{torr liter}} \times \frac{1 \text{ torr}}{7.45 \times 10^4 \text{ scale division}} \times$$

$$\frac{1 \text{ scale division}}{1} \times \frac{.91 \text{ liter}}{1} \times \frac{1}{5 \text{ cm}^2} =$$

$$4.25 \times 10^{-9} \text{ g } O_2/\text{cm}^2$$

Calculation showing determination of sticking coefficient corresponding to a pressure decrease of 1% per second. (sample area = 5 cm^2)

$$\alpha = \frac{\text{scale slope}}{\text{scale height}} \times \frac{k \cdot V}{A \cdot M} = \frac{1 \text{ scale division}}{\text{sec}} \times$$

$$\frac{1}{100 \text{ scale divisions}} \times \frac{1.74 \times 10^{-3} \text{g } O_2}{\text{torr liter}} \times \frac{.91 \text{ liter}}{1} \times$$

$$\frac{1}{5 \text{ cm}^2} \times \frac{\text{cm}^2 \text{ sec torr}}{1.26 \times 10^{-2} \text{g } O_2} = 2.5 \times 10^{-4}$$

In some experiments the crystal was heated by an external resistance furnace; for these studies. the gas temperature was taken to be the crystal temperature. In

most experiments, however, the crystal was heated by induction and the walls of the reaction vessel were only slightly warm to the touch. Under these conditions it would not be correct to assume the sample temperature or the wall temperature represented the true gas temperature. A gas temperature of 50° C was considered to be a reasonable approximation and was used for the calculation of the sticking coefficient when using the induction heater, regardless of the sample temperature. The gas temperature influences the calculation of the sticking coefficient as the inverse square root of the absolute temperature; thus, an error of 100° C in the gas temperature would cause a 10% error in the value of the sticking coefficient. When the resistance furnace was used, a minor correction was also made for thermomolecular flow and the quantity of gas in the system.

A few experiments which used the resistance furnace heating method were repeated with the induction heater. The corrected results from the two heating methods were identical within the normal reproducibility of the equipment.

2. Range of Measurement

Oxidation rate measurements were obtained for the (111), (100), (110), (311), (332) crystallographic faces at temperatures from 250° C to 600° C and oxygen pressures from 2×10^{-4} torr to 3×10^{-2} torr. In terms of average

oxide thickness the measurements were made over an oxide range of from a few angstroms to approximately 500 angstroms.

3. Pressure Dependence

In no case in the range of these measurements was a variance of sticking coefficient with oxygen pressure found. In other words, the oxidation rate in $g/cm^2 sec$ was a linear function of the oxygen pressure over the range of measurement. This was true for all crystal faces studied.

4. Temperature Dependence

Each crystallographic plane studied was found to have its own temperature dependence of oxidation rate. Since the sticking coefficient was independent of pressure, it was found most convenient to plot the sticking coefficient (α) at 10^{-6} g O_2/cm^2 average coverage against temperature. An Arrhenius plot of these values gave straight lines from whose slopes activation energies could be obtained. Figure 28 shows graphically the results obtained for each of the faces studied. The frequency factors and activation energies calculated from the curves are also shown in Fig. 21. Table 2 lists the coefficients of the equation for the sticking probability (α) in the form

$$\log \alpha = a + \frac{b}{T_{(abs.)}}$$

for the lines on the graph along with the standard deviation calculated for from seven to twenty independent measurements.

TABLE 2

Coefficients of the equation $\log \alpha = a + b/T$

Face	a	b x 10^3	Remarks
(111), (332)	-1.11	-2.0 ± .1	(332) rate = (111)
(100)	- .76	-3.0 ± .4	
(110)	.17	-3.6 ± .4	above 400° C
(311)	1.19	-4.3 ± 1	
(110)	-3.89	- .9 ± .2	below 400° C

The (332) face which is 10° off the (111) face gave the same results as the (111) face.

5. Time Dependence

The quantity of oxygen taken up by a copper surface was a function of the time of oxidation. In a majority of the experiments, the conditions of oxidation were chosen so as to produce oxide nuclei on the surface after a short induction period. The oxidations were usually continued until the surface was nearly completely covered by the lateral growth of these nuclei. In a few experiments,

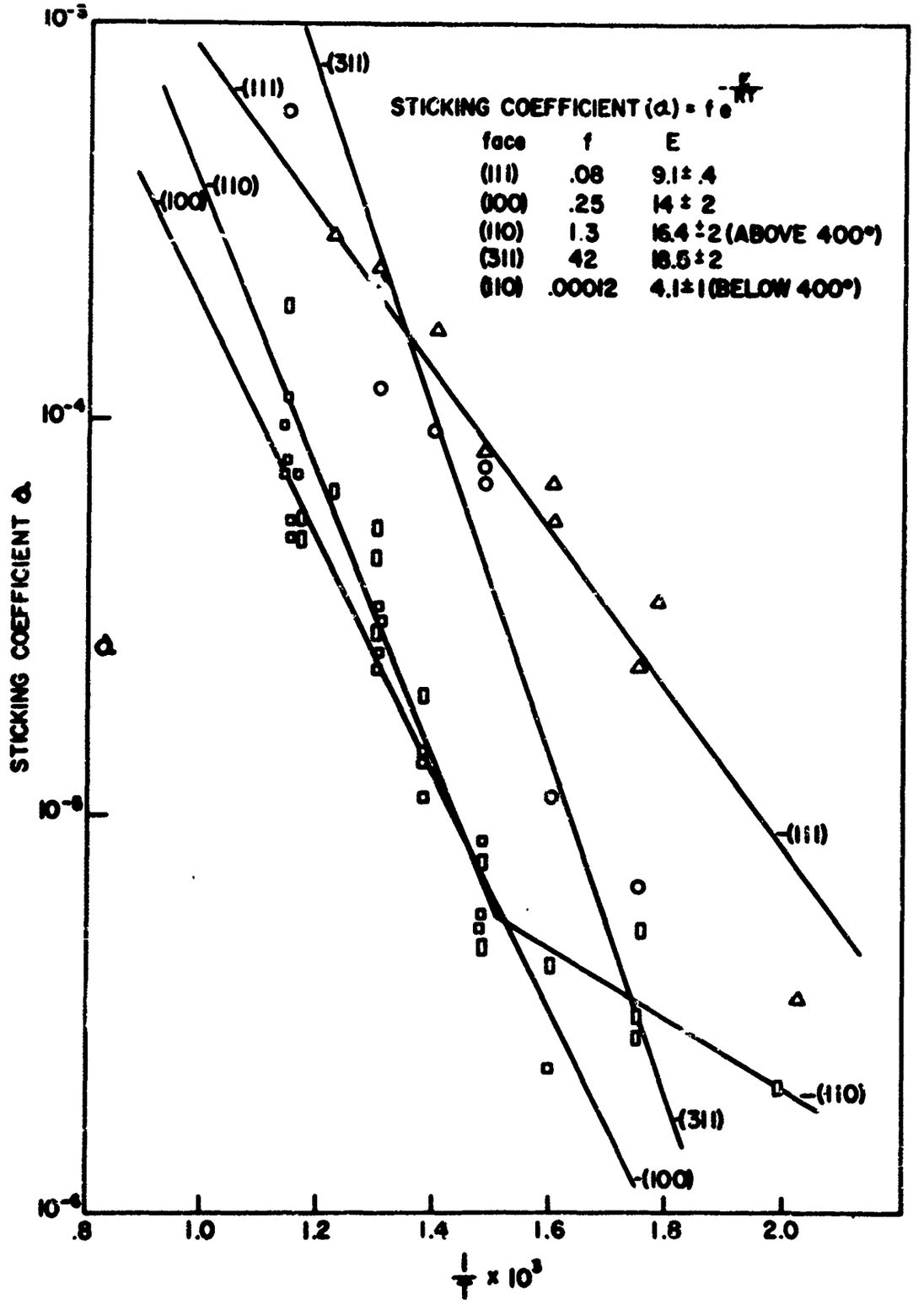

FIGURE 28

STICKING COEFFICIENT OF OXYGEN ON COPPER AS A FUNCTION OF TEMPERATURE.

however, the conditions were such as to yield an induction period of a few hours duration. In three experiments, the conditions were chosen so that a continuous oxide film was formed very quickly and the growth of this film was followed to thicknesses of approximately 1000 Å.

In those experiments in which the induction period was long, a linear growth law $Q = kt$ was obtained, where Q is the mass of oxygen taken up by the surface per unit area and t is the time of oxidation.

Three oxidations at oxygen pressures of 1×10^{-2} torr were carried out on the (110) and (311) faces at temperatures from 300°- 400° C. These conditions were found to produce a continuous oxide film within a minute of the start of the oxidation. Under these conditions a parabolic growth law $Q^2 = kt$ was observed.

During the period of time when oxide nucleation and growth was occurring, a growth law of approximately $Q^{4/3} = kt$ was obtained. This portion of the oxidation curve was often preceded by a linear portion, which corresponded to the induction period. The duration of this first portion of the oxidation was found to be difficult to reproduce. This was apparently a result of the previous history of the sample (see Sec. IV-A). Figure 29 shows a representative plot of Q versus t with the experimental sticking coefficients indicated at various points along the curve.

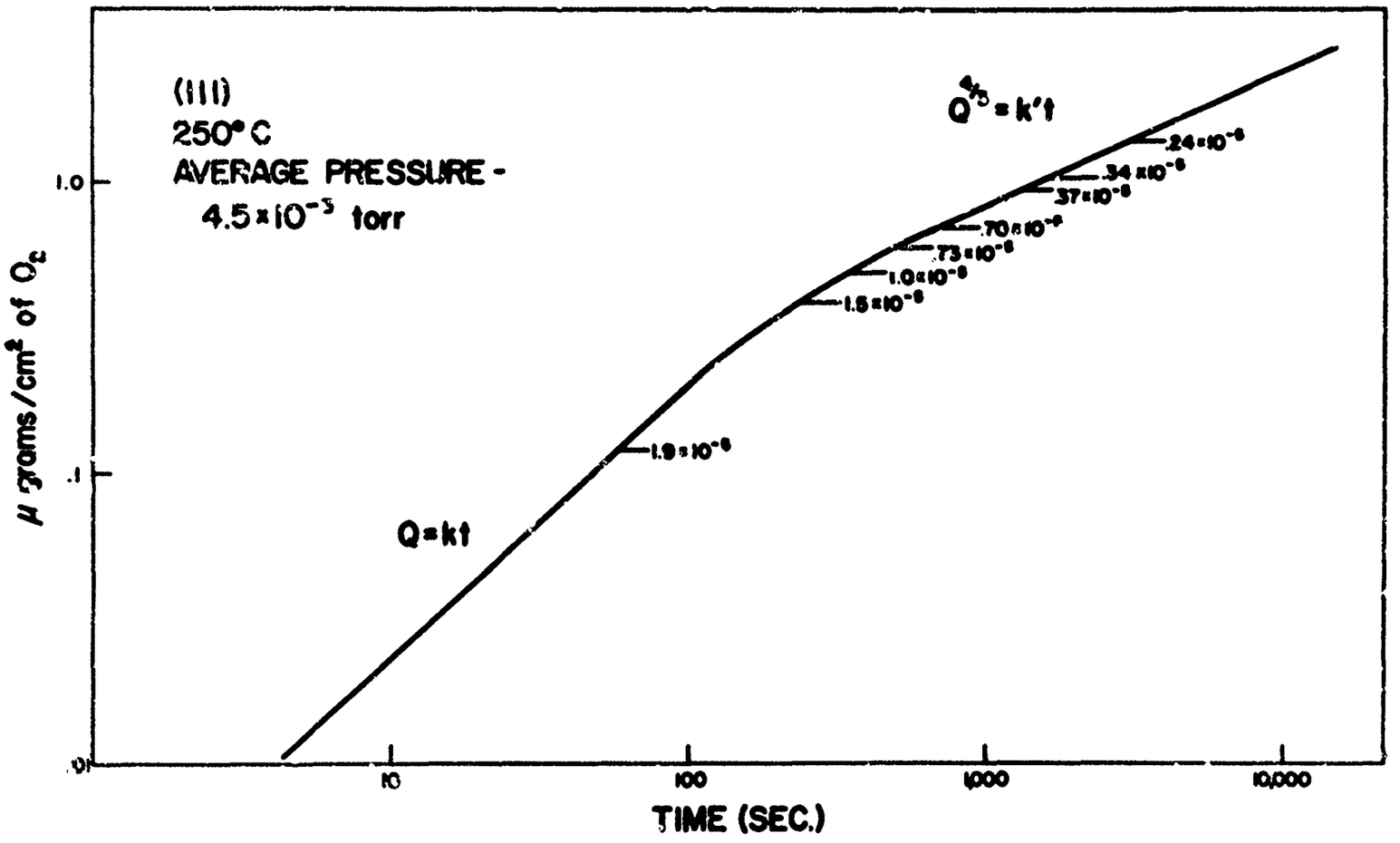

FIGURE 29

TOTAL OXYGEN UPTAKE BY COPPER SAMPLE AS A FUNCTION OF TIME.

K. Electrometric Reduction

Electrometric reduction, utilizing the apparatus described in Sec. III-D, was used to determine the quantity of oxygen present on a crystal surface as oxide. Since the total uptake of oxygen by a crystal was known from the kinetic measurements in system B, the difference between these two amounts of oxygen should be a measure of the amount of oxygen dissolved in the metal lattice. The results of these measurements are shown in Table 5.

It can be seen from the data in the table that only those samples for which the oxidation was terminated below 1 $\mu g/cm^2$ oxygen uptake showed a positive indication of appreciable oxygen solution. Many of the electrometric reductions actually indicated about 5% more oxide on the surface than was determined from oxygen uptake measurements. This discrepancy is thought to be due to less than 100% efficiency of the electrometric reduction system.

TABLE 3

Comparison of Electrometric Reduction Data with Oxygen Uptake

Face	Temperature	Av. Pressure (torr)	Oxygen Uptake $\mu g/cm^2$	Oxygen Reduced $\mu g/cm^2$
(100)	500° C	10^{-3}	.33	.15
(100)	500° C	10^{-3}	.50	.20
(100)	400° C	2×10^{-3}	.55	.20
(100)	500° C	10^{-3}	.47	.22
(100)	500° C	10^{-3}	.68	.25
(311)	400° C	2×10^{-4}	.40	.40
(110)	250° C	10^{-2}	.70	.75
(100)	500° C	10^{-3}	1.21	.93
(311)	450° C	5×10^{-4}	1.15	1.30
(111)	300° C	2×10^{-4}	1.25	1.35
(110)	300° C	10^{-2}	1.73	1.73
(100)	400° C	10^{-3}	1.71	1.85
(100)	600° C	10^{-3}	2.00	1.80
(100)	600° C	10^{-3}	2.5	2.6
(311)	350° C	10^{-2}	2.6	2.6
(110)	500° C	2×10^{-3}	3.1	3.0
(111)	400° C	10^{-3}	3.9	4.3
(110)	500° C	2×10^{-3}	4.9	5.0
(311)	500° C	10^{-3}	8.7	9.0

L. Oxygen Solution

Since only a few of the electrometric reduction experiments showed positive evidence of oxygen solution in the metal, a number of special experiments were carried out in an attempt to confirm that oxygen solution was occurring.

A 5/8 inch sphere was oxidized at 250° C and 1 torr oxygen for five minutes in order to produce a thin continuous film of oxide on the surface. This film was approximately 1000 Å thick on the (100) face and showed interference colors. The sphere was then heated to 750° C in a vacuum of less than 10^{-7} torr for a short period of time. After cooling, there was no indication of oxide on the copper surface. When this experiment was repeated on a 1 mm thick (111) sample, the oxide also disappeared when the sample was heated to 750° C. However, after slow cooling it was found that the surface contained oxide nuclei comparable to those obtained on a sample which had been oxidized at a low oxygen pressure and high temperature. An electron micrograph of this sample is shown in Fig. 30. It is quite clear from the conditions of these experiments that the oxide originally on the surface dissolved in the metal. The reprecipitation of oxide on the surface of the thinner crystal was a result of saturating the metal with oxygen at the elevated temperature so that on cooling the metal became supersaturated and the oxygen then precipitated out as oxide.

FIGURE 30

OXIDE NUCLEI PRECIPITATED ON THE (111) FACE FROM AN OXYGEN SATURATED COPPER SAMPLE DURING COOLING IN VACUUM.

M. Oxidation of Thin Films

Copper single crystal films approximately 1000 Å thick with a (100) orientation, which were prepared by evaporation onto a heated rocksalt substrate, were oxidized in system A. After oxidation, a layer of carbon was evaporated onto the film for support and the oxidized copper film was floated off the rocksalt with distilled water. After a brief second rinse in distalled water, the films were dried and mounted on electron microscope grids for examination in the electron microscope. In the first few experiments, the copper films were stripped from the rocksalt and mounted on electron microscope grids prior to oxidation. This procedure was discontinued because the oxide nuclei became detached from the copper film and were lost if not supported.

Figures 31 and 32 show the appearance of a thin film after oxidation at 550° C at 10^{-2} torr for 7 min. One half of the film was shadowed with platinum and the specimen dissolved in dilute nitric acid so that the surface features could be observed by electron microscopy of the replica while the other half was examined directly by transmission electron microscopy and transmission electron diffraction. There were observed numerous nuclei of two types: 1) approximately square nuclei with the [100] direction normal to the surface, and 2) approximately three armed triangular nuclei with

Replica

Stripped Film

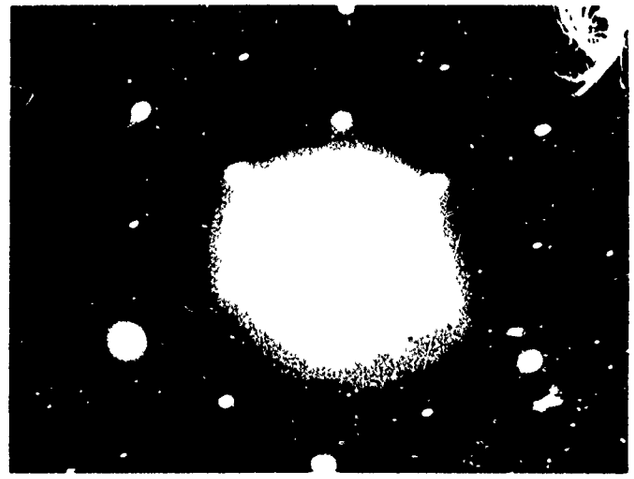

F. D. Pattern

FIGURE 31

CU FILM ON NACL -OXIDIZED: 550°C, - $10\mu 0_2$ - 3 MIN

Replica

Stripped Film

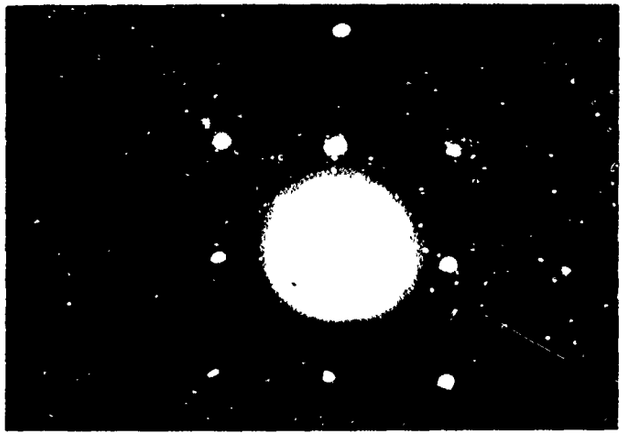

E. D. Pattern

FIGURE 32

CU FILM ON NACL - OXIDIZED: 550°C, - $10\mu O_2$ - 3 MIN

[111] direction normal to the film surface. Both types of nuclei lay in holes in the foil. The copper metal had apparently diffused away from the area adjacent to the nuclei and in most cases left the copper oxide nuclei completely free of the metal film.

Contamination

During this study, some oxidations were inadvertently made on contaminated samples. In only one case was the contaminant identifiable and its source determined. In all other cases the contaminant was unknown and its concentration insufficient to be detectable as a separate phase by glancing angle electron diffraction Electron diffraction was however, a powerful tool for the detection of the presence of a contaminant since the contaminants almost always altered the epitaxial relationships between the copper sample and the oxide. Most often the contaminant resulted in random copper oxide being formed. In other cases, however, it would cause an oxide of a very high degree of orientation to occur but with an epitaxy different from that occurring on clean surfaces.

An equally powerful method of determining the presence of a contaminant was to examine the shape of the oxide nuclei themselves, since these, in the presence of contaminants, grew with strange forms. In most cases these contaminated nuclei would be the same shape over the entire surface, indicating a uniform distribution of the contaminant. In a few cases, isolated groups of unusually shaped nuclei were present indicating a localized contaminant. Figures 33a, b, c, and d show some typical examples of nuclei grown under contaminated conditions. It was possible to distinguish between contaminated and

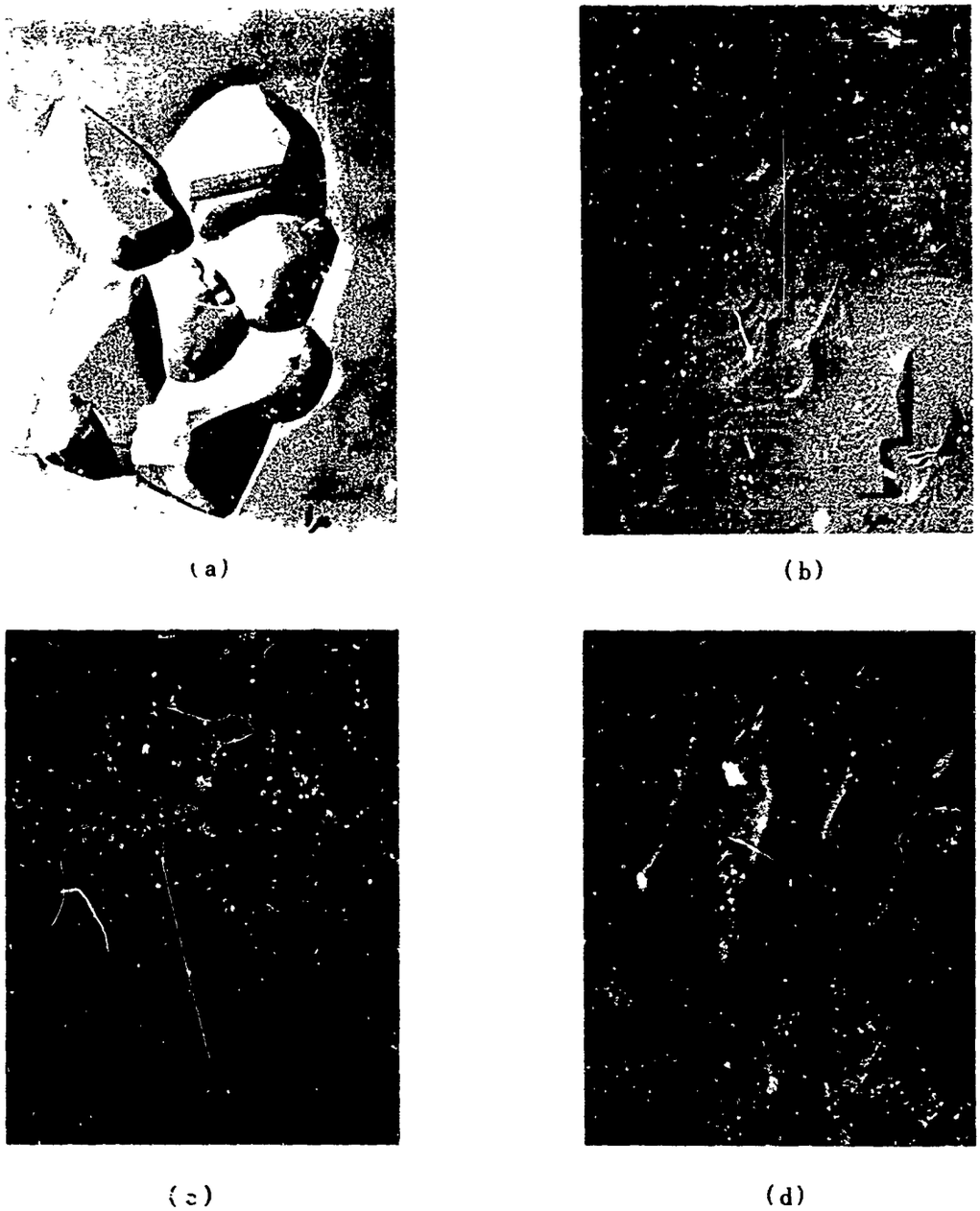

FIGURE 33

ELECTRON MICROGRAPHS OF CONTAMINATED OXIDE NUCLEI

(a) (100) face, 700°C, 3 X 10^{-4} torr, 10 minutes

(b) (100) face, 500°C, 1.7 X 10^{-4} torr, 3 hours

(c) (111) face, 800°C, 10^{-3} torr, 15 minutes

(d) (111) face, 500°C, 1.5 X 10^{-4} torr, 6 hours

and uncontaminated oxidations simply by an examination of the form of the nuclei. It was found that a contaminated sample never produced the same shape nuclei twice, except in the case of the one known contaminant. The reproducibility of the regular shaped nuclei was therefore a good criterion for the lack of contaminant in the system.

Figure 33a is an electron micrograph of a contaminated sample showing small, well formed nuclei but with many different orientations present. The diffraction pattern in Fig. 27b shows the multiplicity of these orientations.

When copper samples were oxidized in system A at temperatures above 600° C for long periods of time in low oxygen pressures, a contaminant appeared on the surface as small rounded particles which pinned the surface steps formed by thermal etching. This material was identified as amorphous SiO_2 by electron diffraction. Figures 34c and 34d show a surface replica of such a contaminated sample and its associated diffraction pattern containing diffuse rings from silica.

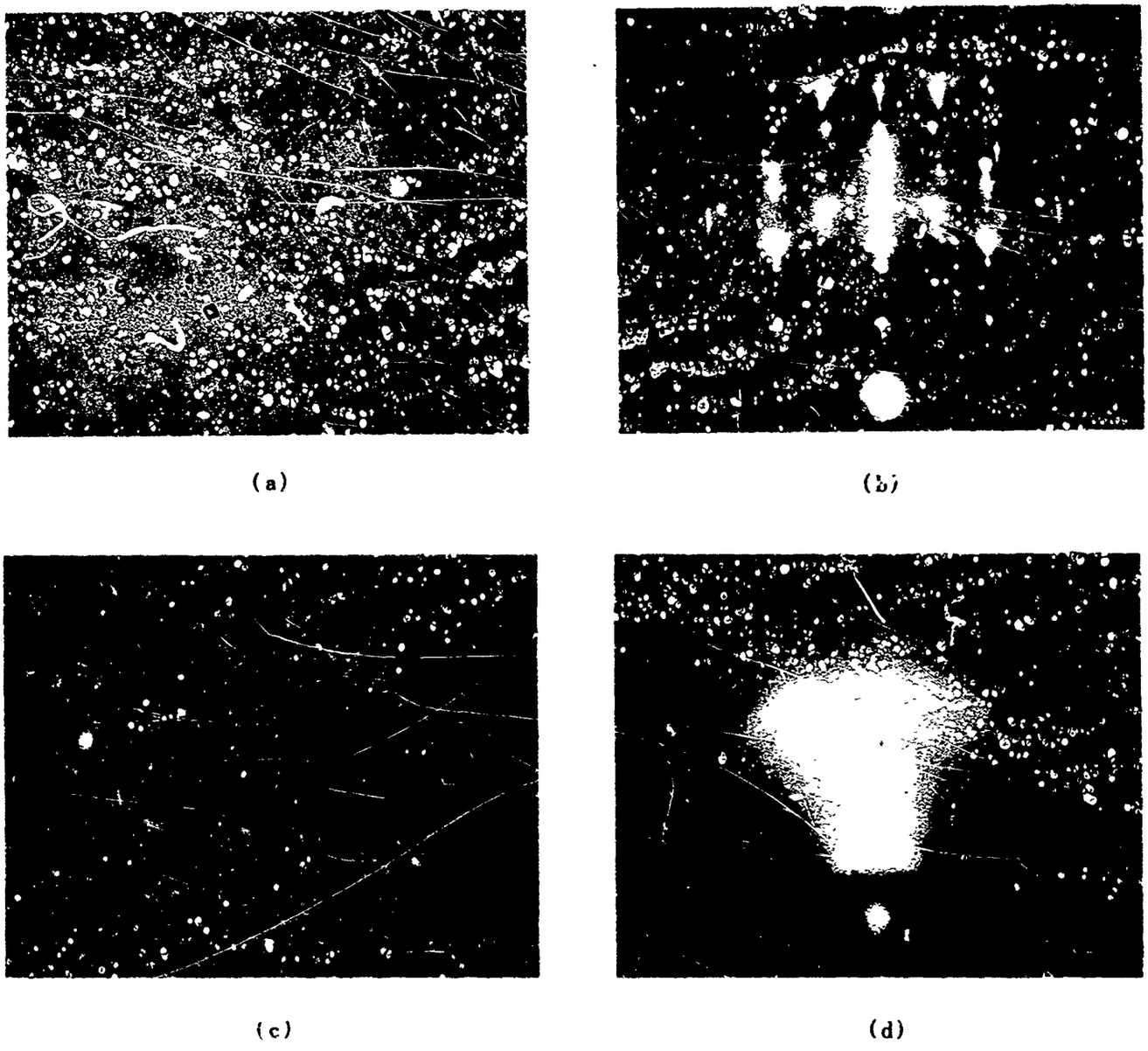

(a) (b)

(c) (d)

FIGURE 34

CONTAMINATED OXIDE NUCLEI:

(a) Electron micrograph of (100) face, 400°C, 10^{-2} torr 5 minutes

(b) Electron diffraction pattern associated with a.

(c) Electron micrograph of (100) face, 800°C, 5×10^{-4} torr, 1 hour

(d) Electron diffraction pattern associated with c.

V. DISCUSSION

A. Topography

It is quite evident from the preceding results that a smooth copper surface does not remain smooth when exposed to a low pressure of oxygen at elevated temperatures. Two types of changes in the topography of the surface occur. First, the metal surface may become roughened on a microscopic scale by the development of facets. This is called thermal faceting or thermal etching. Secondly, the metal surface may become roughened by the development of isolated oxide nuclei. Both of these processes are related in that they are largely the result of the high mobility of copper and oxygen on the metal surface. The surface mobility of copper in vacuum and in hydrogen has been thoroughly investigated by Choi and Shewmon (39), by Hackerman and Simpson (40), and by Gjostein (41). Bradshaw (42) studied the influence of a low pressure of oxygen and found the surface diffusion rate of copper enhanced by a factor of about three over the diffusion rate in vacuum.

1. Thermal Faceting

Copper surfaces exposed to oxygen at all pressures used in this work and at temperatures above 500° C generally showed the development of facets. These facets were primarily of the type $\{100\}$ and $\{111\}$, although

these low index planes were frequently joined by small segments of high index planes. Facets were observed both on samples which showed no surface oxide (i.e. the surface was in the induction period) (Figs. 18b and 27b), and on crystal surfaces which showed oxide nuclei.

These facets develop on most metals so as to minimize the surface free energy of the gross crystal in the presence of an oxygen atmosphere. The mechanism of their formation on various metals is uncertain (46). Hondros and Moore (47) indicate that for silver, evaporation of the metal was essential for the formation of facets. This is apparently not true in the case of copper, since faceting was observed at temperatures far below that at which the evaporation rate of either copper or cuprous oxide is appreciable.

In oxidations at the higher temperatures used in this work, the facets are noticeably influenced by the presence of the oxide nuclei; i.e., the facets are larger and are curved in towards the nuclei, as shown in Figs. 10b and 13c. This enhanced faceting in the immediate vicinity of the oxide nuclei may be due to an increased diffusion rate caused by a strain field set up close to the growing nuclei. There is some evidence that this enhanced faceting develops during the cooling of the sample after removal of the oxygen atmosphere (6, 48).

2. Density of Oxide Nuclei

In Section IV-E, it was shown that the density of oxide nuclei on the copper surface was 1) directly proportional to the oxygen pressure, 2) only slightly dependent on crystal face, 3) an exponential function of the reciprocal of the temperature, and 4) independent of time, after the nuclei had obtained a size of a few microns and until the time when the nuclei began to grow together. These relationships can be explained in terms of a diffusion controlled growth process.

Kahlweit (49) has shown for the case of internal precipitation of oxide particles in dilute metal alloys that, for diffusion controlled growth, the density of precipitated reaction products in a plane is directly proportional to the flux of reactant into the plane. This result is also applicable to the density of nuclei formed on the surface if the flux rate is assumed to be the rate at which the crystal takes up oxygen and the plane of precipitation is taken as the surface. Thus, the direct proportionality between the density of the nuclei and the oxygen pressure is explained since the rate at which the sample takes up oxygen is directly proportional to the oxygen pressure.

The exponential relationship between the density of nuclei (N) and the reciprocal of temperature can also be explained in terms of diffusion controlled growth.

The energy (E), obtained from the experimental slope of an Arrhenius plot of 1/T versus the logarithm of the density of nuclei determined at constant pressure, has been shown by Grönlund (2) to be equal to twice the activation energy for surface diffusion. Table 4 compares the values obtained by Grönlund for various crystal faces with those obtained in this work.

It is the opinion of this author that the density of nuclei as a function of temperature should have been determined at constant flux and not at constant pressure since the density of nuclei is a function of the flux. Using the kinetic data from this work, a corrected set of activation energies was calculated and these are also shown in Table 4.

TABLE 4

Activation Energy (kcal/mole) for Surface Diffusion on Various Crystal Faces as Calculated by the Method of Grönlund (2)

	(111)	(100)	(110)	(311)
Grönlund's values (2)	18	23	10	15
This work (constant pressure)	16	13	12	12
This work (constant flux)	21	20	21	21

The identity of the diffusing species for which the above activation energies are calculated is not known. The corrected activation energy values in Table 4 are

identical, however, to the value of 20 kcal determined by Bradshaw (42) for copper surface diffusion in the presence of 5×10^{-6} torr of oxygen. There are two apparent mechanisms for surface diffusion in which the activation energies for the movement of copper and oxygen would be the same. One possible mechanism would be the joint migration of both the copper and oxygen atoms as a molecular unit, such as Cu_2O. The other possible mechanism is a ring rotation process in which the movement of an oxygen atom in one direction is balanced by the movement of a copper atom in the opposite direction.

A discussion of the mechanism of growth of the oxide nuclei on copper has recently been published by Rhead (7). In this paper, Rhead analyzed the work of Grönlund and arrived at the conclusion that "whatever diffusion mechanism accounts for growth of the particles it may not be very different from surface diffusion of the metal."

The variation of the number of nuclei per unit area with time can not be approached in the mathematical manner of the above discussions. This is due to the lack of sufficient experimental observations of the relationship between time and density of nuclei. A few general remarks, however, can be made. It is expected that after the induction period, oxide nuclei precipitate on the surface due to the surpassing of a "critical concentration"

of oxygen in the surface layer. This "critical concentration" is the minimum oxygen concentration in copper which will precipitate oxide nuclei at that temperature. The surface layer involved in this solution may extend to several microns in depth under certain conditions. At this time the number of nuclei will grow very rapidly to some maximum value and the concentration of oxygen on the surface between nuclei will fall to some lower value, preventing further nucleation. At this point the surface is covered with many small nuclei and Ostwald ripening (7, 49) may occur to some extent. (Ostwald ripening is the growth of larger precipitate particles at the expense of the small particles as a result of the variation of surface energy with particle size.) It was observed in this work that the density of nuclei as determined in the electron microscope when the nuclei were small was greater than that determined in the optical microscope at a later time in the oxidation when the nuclei were larger. The nuclei which remain, however, continue to grow because of further oxidation and are soon too large for Ostwald ripening to be significant and the density remains constant until the nuclei grow together and form a continuous film.

3. Topography of Oxide Nuclei and Surrounding Metal

a. Surface of Oxide

It is clear that if an oxide nucleus were not

growing (i.e. increasing in volume) it would, by diffusion, come into equilibrium with its environment. This equilibrium would be the lowest energy state for the system of oxide on metal, and would be governed by the surface free energies and interfacial energies of the metal and oxide. The oxide nuclei observed in this work are not static but are growing nuclei and their configuration will be governed by the various surface energies involved, the mode of growth, and the diffusion rates of the oxygen and metal atoms.

The faces which might be expected to develop on the surface of an oxide particle, from surface energy considerations alone, would be low index planes. Figure 13a does indeed show the existence of fairly well developed (100) planes on small oxide nuclei formed on the (111) face of copper. However, to continue such growth, the transport of material must take place over greater and greater distances. This is because it seems likely that the majority of the oxide is added to a nucleus at its periphery and must diffuse to the top of the nucleus. It is clear that at some point this transfer can no longer take place sufficiently rapidly and the nuclei become truncated. This rounding off or faceting of the upper surface of the nuclei can be seen in Figs. 12b and 13a, and in many of the other micrographs in this work.

A second type of facet development which often

occurs is seen in Fig. 12a. The oxide nuclei show two low index planes which are connected by a rather poorly developed high index plane that makes a small angle with the substrate surface. This configuration is apparently due to the tendency for lateral growth resulting from the addition of oxide to the nuclei at the periphery. It is not apparent why the (111) oxide plane parallel to the surface is not formed instead of the high index plane since the close packed plane would have a lower surface energy.

An analysis of the shape of the oxide nuclei appearing on the (100) face of copper is more difficult. It would be expected from the epitaxial relationships observed, which show (111) planes of oxide parallel to (100) copper, that nuclei with bases the shape of regular equilateral triangles should occur. In fact, the observed nuclei are triangular, with four different orientations as expected, but in most cases they tend to be 90°, rather than 60° triangles (Fig. 9a). A close examination of the electron micrographs of the nuclei reveals that many of the nuclei show a small section, either on the top of a nucleus or at the tip, with the expected 60° angles (Fig. 9b). This portion of the nucleus also seems to show inclined (100) planes, as in the case the nuclei on the (111) face. The tendency for the basal angles to be greater than 60° is not a result of misorientation of

the copper face, since each of the four equivalent orientations shows the same features. Nuclei of this type were never observed on the (111) face and so the odd shape is apparently a result of the basic symmetry difference of the substrate and the oxide at their interface.

b. Topography of Metal in Vicinity of Nuclei

The topography of the metal in the vicinity of a nucleus is described in Section IV-D for an oxidized (110) face of copper. This topography is equally representative of the other surfaces studied when oxidized at sufficiently high temperatures. The general features of this topography were: 1) the oxide nuclei always appeared to penetrate deeper into the surface at their outside edges, and 2) the nuclei were always surrounded by a mound of copper outside of which there was a shallow broad depression in the surface.

These features are in excellent agreement with the results of Wenzel [illegible] teristics, at first glance, appear to be most strange. However, they are not unreasonable when one considers the probable mechanisms of growth and the volume changes which occur during the oxidation process.

The growth of a small volume of oxide, which was formed initially in the metal surface by a precipitation process, involves an expansion of the unit cell of copper

by 64%. This expansion of the lattice sets up local stresses in the vicinity of the oxide nucleus which can lead to slip, so that as the nucleus grows, excess copper is actually pushed ahead of the oxide in a ridge. The actual amount of copper in this ridge will depend on the detailed mechanism of the growth of the oxide nucleus.

If the growth of the oxide nucleus was the result of either oxygen diffusion to the nucleus from the gas phase, or of interstitial diffusion of oxygen in the metal, it would be expected that the volume of metal displaced by the nucleus would be about 39% of the volume of the oxide formed. This assumes that the oxide nucleus is not expanding above the metal surface. On the other hand, if the growth of the oxide is the result of either a substitutional diffusion of oxygen in the bulk or at the surface, the diffusion process removes a number of metal atoms from the oxide-metal interface equal to the number of oxygen atoms arriving, so that the volume of metal pushed out by the growing nucleus would be only 10% of the volume of the oxide formed.

It is plausible, whatever the mechanism for growth, that "excess" copper will be "pushed" ahead of the growing oxide nuclei by a stress induced creep or slip. In either case the result would be the development of a mound of copper on the metal surface around the oxide nuclei.

The oxide, however, does not contain itself to the original surface and below, but also grows above the surface. This process reduces the quantity of metal which must be "pushed" before the growing nuclei.

The volume of the ridge of "excess" metal observed in high temperature oxidation (Fig. 15) is approximately 30% of the volume of the nucleus below the original surface. It is thus concluded that the major mechanism of growth at high temperatures is not by diffusion of substitutional oxygen. The mechanism of growth therefore involves the arrival of oxygen from the gas, diffusion of oxygen on top of the metal, or interstitial diffusion. The 10% difference between the expected and the observed amount of metal in the ridge ahead of the nuclei is due to part of the nuclei growing above the original surface.

The existence of oxygen in the copper lattice as an interstitial ion is most unlikely because of the large size of the oxygen ion and this possibility is therefore rejected. Growth by arrival of oxygen at the oxide from the gas phase should yield oxidation rates which increase as the amount of oxide surface increases. This is not the observed kinetics and thus, this mechanism is also ruled out. It is therefore concluded that the mechanism of oxide growth at high temperatures is by oxygen diffusion on top of the metal surface, in agreement with Menzel (50).

It is indeed difficult to determine the exact nature of the diffusion species which is controlling the oxide growth. In Section V-A-2, the similarity of activation energies, determined from data on the density of nuclei, and those for surface diffusion of copper, seemed to indicate that copper was the diffusing species. This agreement of numbers, however, could be merely coincidence since other evidence in the literature (50) and from this work suggests that oxygen is the diffusing species. Apparently under these conditions of oxidation, both oxygen and copper atoms are highly mobile on the surface, and in fact, the mobility of both undoubtedly is involved in the overall process.

The slight depression in the surface outside the ridge of metal is thought to form during the cooling of the sample. The phenomenon of surface faceting on cooling a copper sample which has been exposed to oxygen at low pressure and high temperatures has been observed by Menzel (6) and the enhanced development of these facets in the vicinity of oxide nuclei by Bouillon (48).

It is to be expected, as indicated above, that stresses would be set up in the vicinity of the oxide nuclei, and that these stresses could lead to slip occurring in the metal. Figures 14c and 14d show the edge and tip respectively of a nucleus on the (110) surface. Extending out from this nucleus in the $[1\bar{1}0]$

direction are lines which at the tip have the appearance of slip lines. Farther back from the tip of the oxide nucleus, these lines clearly develop into (111) planes, which are the slip planes in copper metal. The amount of slip required to produce facets of the size observed would be, however, much greater than the amount of slip normally observed in pure copper. It is thought that these facets may actually be the result of slip, but that the size of the facets may have been increased by the process of surface diffusion.

B. Structure

1. Adsorption Structures

The two dimensional structures reported in Section IV for the (100) and (110) copper faces are identical with the adsorption structures for chemisorbed oxygen observed on these faces by Lee (13) and Simmons (14) using low energy electron diffraction (LEED). The extreme difference between the conditions used in the LEED work and the conditions used in this work deserves discussion. In the LEED work, minimum oxygen exposures of 10^{-7} torr minutes for the (110) face and 2×10^{-6} torr minutes for the (100) face at room temperature were required to produce the adsorption structure. In the high energy electron diffraction work, exposures of 10^{-2} torr minutes at 800° C were required to produce the observed structure. It is believed that the 10^{4} increase in oxygen exposure at 800° C is necessitated by the rapid solution of oxygen into the metal at this temperature. (See discussion on oxygen solution in Sec. V-C-2.)

Because of the necessity of cooling the sample and exposing it to the atmosphere, in order to transfer it from the reaction vessel to the diffraction unit, it can not be stated unequivocally from the above data that the observed adsorption structure was present on the sample at the end of the oxidation period. It is thought, nevertheless, that a two dimensional adsorption structure

of the type observed above does exist on the copper surface at elevated temperatures in the presence of oxygen. The structures observed by high energy electron diffraction were a function of the reaction conditions. It can be stated that the structure observed was dependent on the oxidation conditions and not on the cooling rate of the sample or the reaction of the sample with air during the transfer from the reaction system to the diffraction apparatus, since the adsorption structure observed varied with the oxidation conditions. The work of Sewell (51) on the reaction of oxygen with nickel provides additional support for the existence of such adsorption structures on metals at elevated temperatures. In this work, the diffraction patterns from a nickel crystal exposed to a low pressure of oxygen in an ultra-high vacuum diffraction unit (52) were studied at high temperatures. This study showed not only the existence of diffraction lines from the metal and from nickel oxide nuclei, but also the presence of lines from a two dimensional adsorption structure.

It should also be pointed out that many of the diffraction patterns showed both diffraction lines from oxide nuclei as well as from an adsorption structure. This demonstrated the presence of an oxygen adsorption structure between the nuclei at the time of observation, and indicated that such a structure probably existed during the reaction.

An interesting question which arises is, why should such a thin surface structure be sufficiently stable to further oxidation that it can be transferred in air from the reaction vessel to the diffraction unit without modification? The answer to this question is not yet available. However, both Lee (13) and Simmons (14) have found that the adsorption structures on copper are remarkably resistant to further oxidation at room temperature.

The diffraction data for the (311) face shown in Figs. 24a and 24b has not yet been interpreted. There is no LEED work available on this face of copper for comparison. It seems apparent, however, that this pattern is also due to a two dimensional adsorption structure on the metal surface.

2. Diffraction Patterns Corresponding to Large Lattice Parameters

The diffraction patterns reported in Section IV-I-2 showed a very small spacing of diffraction lines which indicated a two dimensional centered rectangular cell of dimensions 15.1 Å by 26.2 Å on the (111) face after a short oxidation. A similar pattern has been reported by Krause (53). In Krause's experiments, the diffraction pattern was obtained from a (111) face of a copper sphere which had a thin film of copper evaporated onto its surface at room temperature and was then annealed at

500° C in a rather poor vacuum of 5×10^{-6} torr. Krause also stated that a similar pattern could be obtained after a slight thermal oxidation of this copper sample.

Krause has proposed that the diffraction pattern observed can be explained on the basis of a hexagonal array of screw dislocations at the interface between the substrate and a slightly disoriented evaporated copper film. It seems likely, as shown below, that this is a possible explanation, but it is probably not the correct one.

The diffraction pattern observed in this study corresponds to a reciprocal lattice consisting of a hexagonal array of rods, and the real lattice derived from this is a planar array of points in a hexagonal arrangement. It is not possible to locate the atoms specifically in this structure, but only to say that the structure shows the periodic scattering array indicated by the two dimensional lattice.

There are a number of possible phenomena which could lead to periodic structures giving the required type of reciprocal lattice. The most likely structures are discussed below.

Probably the simplest two dimensional structure which would give the observed reciprocal lattice is a hexagonal array of oxygen atoms adsorbed on the metal surface with the observed cell size. There are two

factors which make this possible structure rather unlikely. First, it is highly unlikely that adsorbed oxygen atoms spaced 15 Å apart on the surface would have sufficient influence on each other to create and hold together the perfectly regular large spaced lattice observed, although possible adsorption sites approximately 15 Å apart do exist on the (111) surface. Secondly, in such an adsorption structure only a small fraction of the surface would consist of oxygen atoms, and with the small electron scattering factor of oxygen the diffracted intensity would be extremely low and probably undetectable.

A possible structure which should be considered is that of a superlattice of oxygen in copper. It is quite clear from the data in the results that oxygen is dissolved in the metal. An ordered array of oxygen atoms in substitutional sites in the copper lattice can be conceived which would give the proper shape for the reciprocal lattice. However, if the structure is based on substitutional oxygen, it is not possible to derive a superlattice with the proper dimensions without changing the copper parameters, and no change in these parameters has been observed. An interstitial location of the oxygen atoms seems unreasonable from the viewpoint of the size of the oxygen atom.

A two dimensional superlattice of oxygen and copper on the surface of the (111) plane of copper is likewise

ruled out on the basis that the repeat distance in the observed structure is not an integral multiple of a normal repeat distance for copper atoms in this plane.

Another possible explanation of the observed diffraction pattern is that there exists a two dimensional hexagonal network of interfacial dislocations between an oxide and the metal surface. An array of screw dislocations resulting from a small rotational disorientation about the [111] axis could lead to a periodic arrangement of atoms at the interface which would give the desired reciprocal lattice. Krause (53) has suggested this explanation for his results, only he has attributed the pattern observed to a rotational disorientation of deposited copper. This is highly unlikely since his diffraction pattern is identical to the patterns observed in this work where the copper crystals were only exposed to oxygen. It is apparent that his pattern is also due to the presence of oxygen from his annealing treatment in a poor vacuum. This still does not rule out the interfacial dislocation explanation, however. The high intensity and the sharpness of the diffraction lines indicate a very high regularity in whatever structure there is which leads to the pattern. So far, no observed networks of interfacial dislocations reported in the literature have shown anywhere near the regularity which would be required (54).

A rotation of the oxide about the [111] axis by about two degrees would be required to give a screw dislocation network of the dimensions required. There is no evidence in this study to indicate rotational disorientations of this order of magnitude on the (111) face.

It is also possible to think of a network formed of an array of edge dislocations resulting from the misfit between the oxide and the copper substrate. However, from the measured differences in lattice parameters of the oxide and metal, the network of dislocations expected would be much smaller than the dimensions required to explain this pattern.

The solution of oxygen in copper might, under suitable conditions lead to a periodic arrangement of thin platelets of precipitated Cu_2O. Such a periodic array has not been observed and it seems unlikely that precipitation of oxide would show the high degree of regularity necessary.

A final possibility, which is purely conjectural, is that in the solid solution of oxygen in copper there is a periodic variation of oxygen concentration. This would lead to oxygen-poor regions with a lattice parameter slightly smaller than that for the uniform solid solution and oxygen-rich regions with a slightly larger lattice parameter. This essentially amounts to a displacement type disorder that could lead to "side-band" type

diffraction patterns (55) similar to those observed in a number of metal solid solutions (56).

3. Epitaxy

The first part of this discussion is on the orientation of oxide nuclei observed on various crystal planes while the latter part is concerned with the lateral compression existing in very thin oxide films as a result of epitaxial forces.

a. Orientation

Cuprous oxide was the only oxide formed on the copper surface under the conditions used in this work. The orientation relationships observed and reported in Section IV-C for the (111), (110), and at low temperatures on the (100) faces of copper are the same as those reported by Lawless (57) and Menzel (58). The high temperature, high pressure, epitaxial relationships observed on the (100) face (Fig. 10b) have not been previously reported in the literature. Lee (13) however, reports an adsorption structure which was formed at room temperature at oxygen exposures of 3×10^{-6} to 3×10^{-5} torr minutes which is strikingly similar. This structure is reported as an oblique cell with sides running in the [051] and [017] directions on the (100) copper surface, with all four of the equivalent orientations present.

The only relationship which can be drawn from the observed epitaxy is that, with the exception of the high temperature form of nuclei on the (100) face, there is always a parallelism of one closest-packed direction in the oxide and metal. Although it is clear that the epitaxy which is obtained must be the one of minimum interfacial energy, it is not clear what factors determine the interfacial energy. It is apparent that the magnitude of the interfacial misfit is not the only factor in determining this energy since it is possible to choose orientations on some planes which would have a smaller misfit.

b. Compression

It was found that a (111) copper surface, which had been oxidized at 500° C or above in an oxygen pressure of 10^{-3} torr or less for a time slightly less than that required to produce oxide nuclei on the surface, showed an oxide phase in glancing angle electron diffraction after cooling. The surface of these samples as seen in the electron micrographs (Fig. 18b) consisted of shallow steps with very smooth planes approximately 5000 Å wide between steps. The diffraction pattern (Fig. 19) indicated that the oxide phase on these surfaces was present as a continuous film on the order of 5 - 15 Å thick. It is thought that this oxide was formed by precipitation of dissolved oxygen as the sample cooled.

On the (111) face this oxide film is compressed 1.1% in the plane of the surface. One possible explanation for this result is that the oxide on the (111) face is strongly bound to the underlying metal and that when the metal cools to room temperature, its thermal contraction being greater than that of the oxide will result in an abnormal compression of the oxide film. The magnitude of the resulting compression for a temperature drop of 750° C is approximately the amount observed. However, this explanation would yield a compression that is a function of the oxidizing temperature and no such dependence was found for oxidations between 500° C and 800° C.

A much more likely explanation of the observed lateral compression of the oxide on the (111) face comes from the theory of Van der Merwe (59). In this theory Van der Merwe determined the interfacial energy as a function of the interfacial misfit between two phases. He then proposed that if one of the phases is present as a thin film, a homogeneous plane strain will occur in the film in such a direction as to reduce the density of interfacial dislocations and thus the energy in the interface. He then calculates that the strain resulting in the minimum energy for the system is given by:

$$\varepsilon_m = \frac{(1-2\sigma)(2-f)(1+f)\,\mu_0\, a}{8\pi^2(1-\sigma)(2+f)f\,\mu_a\, h}\ \beta \ln\left[2\beta(1+\beta^2)^{\frac{1}{2}} - 2\beta^2\right]$$

where,

$$f = \frac{b-a}{a}$$

$$\beta = \frac{8\pi\mu_a\, f}{(1-\sigma)\left(\frac{1+\mu_a}{\mu_b}\right)(2+f)^2\mu_0}$$

μ_a, μ_b, μ_0 = rigidity modulus

$\sigma_a, \sigma_b, \sigma$ = Poisson's ratios

a = lattice parameter of film

b = lattice paramster of substrate

h = film thickness in Å

(subscripts a, b, o refer to film, substrate, and interface respectively)

To obtain a numerical solution of this equation one needs to know the elastic properties of the oxide, the metal, and the interface. These quantities have never been determined for the oxide or the interface. In order to estimate the magnitude of the strain in a thin parallel oriented oxide on the (111) face of copper, assume that

$$\sigma_a = \sigma_b = \sigma = .3 \quad \text{and} \quad \mu_a = \mu_b = \mu_0$$

With f = .15, and a = 2.47 Å, the equation for ε_m reduces to

$$\varepsilon_m = -\frac{2\%}{h}$$

where the minus sign indicates compression. For a film

ten angstroms thick the compression of the film would be .2%. This value is somewhat less than the observed compression but in view of the assumptions necessary to get a numerical solution, the disagreement is not unreasonable.

It should be pointed out that Borie (60) has obtained comparable results for oxide grown on the (110) face of copper. A refined x-ray diffraction technique was used in these studies and it was determined that the oxide lattice planes parallel to the metal surface were expanded in a direction normal to the surface by about 1 - 2%. This is comparable to the lateral compressions observed in the present work.

C. Kinetics of Oxidation

1. Sample Shape

Before a proper interpretation of the kinetics of the oxidation of copper can be given, an analysis of the effect the sample size and shape may be playing on the measurement of total uptake of oxygen by the sample must be made. As stated in the section on sample preparation, the samples were of disc shape, approximately 1 mm thick and 9 mm radius. For this shape approximately 10% of the total surface is composed of crystal faces other than the face under investigation. If the major surface is the (111), an examination of the kinetic data shows that an "average surface" oxidized at approximately one third the rate of the (111) face and thus, the contribution to the total uptake by the edge of the sample would be approximately 3%. An "average surface" is defined as a surface giving an oxidation rate corresponding to a weighted average of the rates of all of the crystal faces. On the other hand, if the major surface is a (100), then the "average surface" will oxidize about 3 times as fast as the (100) face and the edge of the sample will represent 30% of the total uptake by the sample. Calculating the kinetic rates on the basis that all of the sample area is composed of the one crystal face, thus leads to values approximately 7% low for the (111) face and approximately 20% high for the (100) face.

These two calculations represent the range of errors due to the presence of the edge area. For a surface such as a (311) at 300° - 400° C where the oxidation rate is about the same as that of an average surface, there would be no error in assuming that all of the surface is the (311) surface.

2. Induction Period

It has been suggested by various workers (9, 10, 11) that the induction period is due to oxygen solution into the copper lattice. It is thus desirable to investigate first the data in the literature on oxygen solution in copper and then to compare the kinetic data obtained in this work during the induction period in the light of this data. With this information and a knowledge of the nature of the surface during the induction period, speculation as to the mechanism of oxidation and the rate controlling step can be made.

a. Solution of Gas in the Metal

The ability of copper to dissolve oxygen has been known for many years. However, the data available from several investigators on this solubility shows considerable disagreement (Fig. 36) and the diffusion rate of oxygen in copper has not yet been determined experimentally. However, from the work of Van Der Schrick (9, 61) on the oxidation of copper, an approximate value

of the diffusion constant for oxygen in copper can be calculated. This calculation is made by comparing the amount of oxide determined gravimetricly and by electrometric reduction. If the difference in the two results is taken to be the quantity of oxygen dissolved, and if it is assumed that the surface concentration is equal to the solubility limit of oxygen in copper (C_s) at that temperature for all times, then the diffusion coefficient can be calculated from the equation (62):

$$D = \frac{Q^2_{dis}}{4t\pi C_s^2}$$

where,

Q_{dis} = quantity of oxygen dissolved

t = time of experiment

C_s = solubility limit of oxygen in copper as obtained from Fig. 36.

An average of Van Der Schrick's data gives a value of D at 550° C of approximately $10^{-8} cm^2/sec$ if an average of the solubilities shown in Fig. 36 is used for C_s. It is also possible to make approximate calculations of the diffusion rate of oxygen in copper at 900° C from the work of Young (63) on the internal precipitation of oxide nuclei in copper on cooling. In this work it was found that significant oxide was precipitated at a depth of 2 mm after a 6 hour exposure of the sample to

oxygen at 900° C. From the formula (64)

$$C_{(x,t)} = C_s \left(1 - \text{erf} \frac{x}{2\sqrt{Dt}}\right)$$

if $C_{(x,t)}$ is assumed to be at least ½ C_s, then D must be $>10^{-6}$cm^2/sec. This calculation has the advantage that it is independent of C_s, which is in some doubt, but since no information is given on the maximum depth at which oxide was formed, no calculation can be made as to the upper limit of D. Figure 35 gives D as a function of temperature for several diffusion species in copper for comparison with oxygen diffusion as calculated above (dashed line), and for oxygen diffusion in silver and silver self diffusion.

From the fact that the oxidation rate is constant during the induction period, it is apparent that the diffusion of oxygen into the bulk of the sample is not the rate controlling process. Instead, the rate controlling process appears to be a surface step in which O_2 is involved. Using the diffusion data in Fig. 35, the oxidation rate calculated from Fig. 28, and the induction period data from Fig. 5, the oxygen concentration at the surface (C_s) when oxide nuclei are formed can be calculated by the formula (62)

$$C_s = \frac{J}{\sqrt{\frac{D}{\pi t}}}$$

where,

J = oxidation rate

D = diffusion rate

t = induction time.

This formula is valid if D is independent of concentration and the initial oxygen concentration in the metal is zero.

The values of C_s obtained in this manner are a function of oxygen pressure, crystal face, and oxidizing temperature. They are greater the lower the temperature and the higher the oxygen presure, and approximately an order of magnitude larger for the (111) face than any other face under similar conditions. For the (111) face at 10^{-2} torr and 300° C, an oxygen concentration of 1 atom % is required for precipitation while for the (100) face at 700° C at 10^{-3} torr a concentration of only .01 atom % is required for precipitation. These values which indicate the range of concentration are considerably above the solubility limits given in Fig 36. This is to be expected since the solubility limit values in Fig. 36 represent the concentration of oxygen in copper which exists in equilibrium with copper oxide. On the other hand, the critical concentrations determined above represent the oxygen concentration in copper which will cause the precipitation of an oxide phase at a moderately

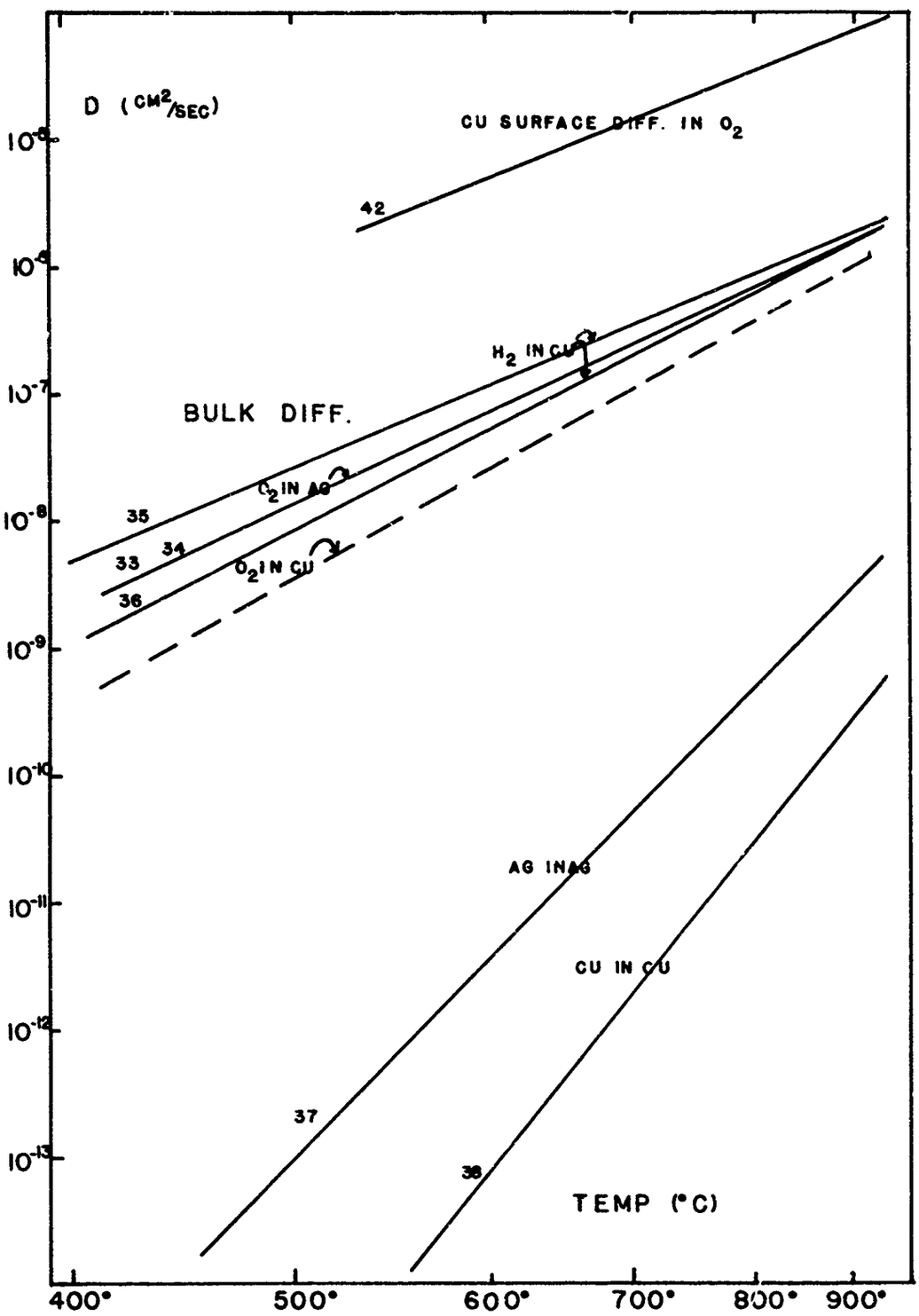

FIGURE 35

DIFFUSION RATES IN COPPER AND SILVER METAL.

rapid rate. This supersaturation of the copper lattice is a necessary requirement for the nucleation of an oxide phase, because there exists an activation energy for nucleating a new phase. In this case, the activation energy not only involves the free energies of the various surfaces but also the hydrostatic strains due to the larger molar volume of the precipitate (65).

A second observation which supports the existence of a large supersaturation of the copper lattice at low temperatures is that once oxide nuclei are formed, essentially all of the oxygen that had been taken up by the sample during the induction period is precipitated on the surface. That is, if one looks at the time series of oxidation on the (111) face at 400° C, which is shown in Fig. 8, the amount of oxide on the surface at 5 minutes is not equivalent to the amount of oxygen taken up by the sample in the interval from the preceding picture. It is equivalent to the total amount of oxygen taken up by the sample since the oxidation began. When oxidations are performed at temperatures above 600° C, the supersaturation which occurs is much smaller and a significant portion of the oxygen taken up by the sample is lost to solution into the bulk and thus does not precipitate on the surface. It is therefore concluded that solution of oxygen in the metal is a reasonable explanation of the induction period.

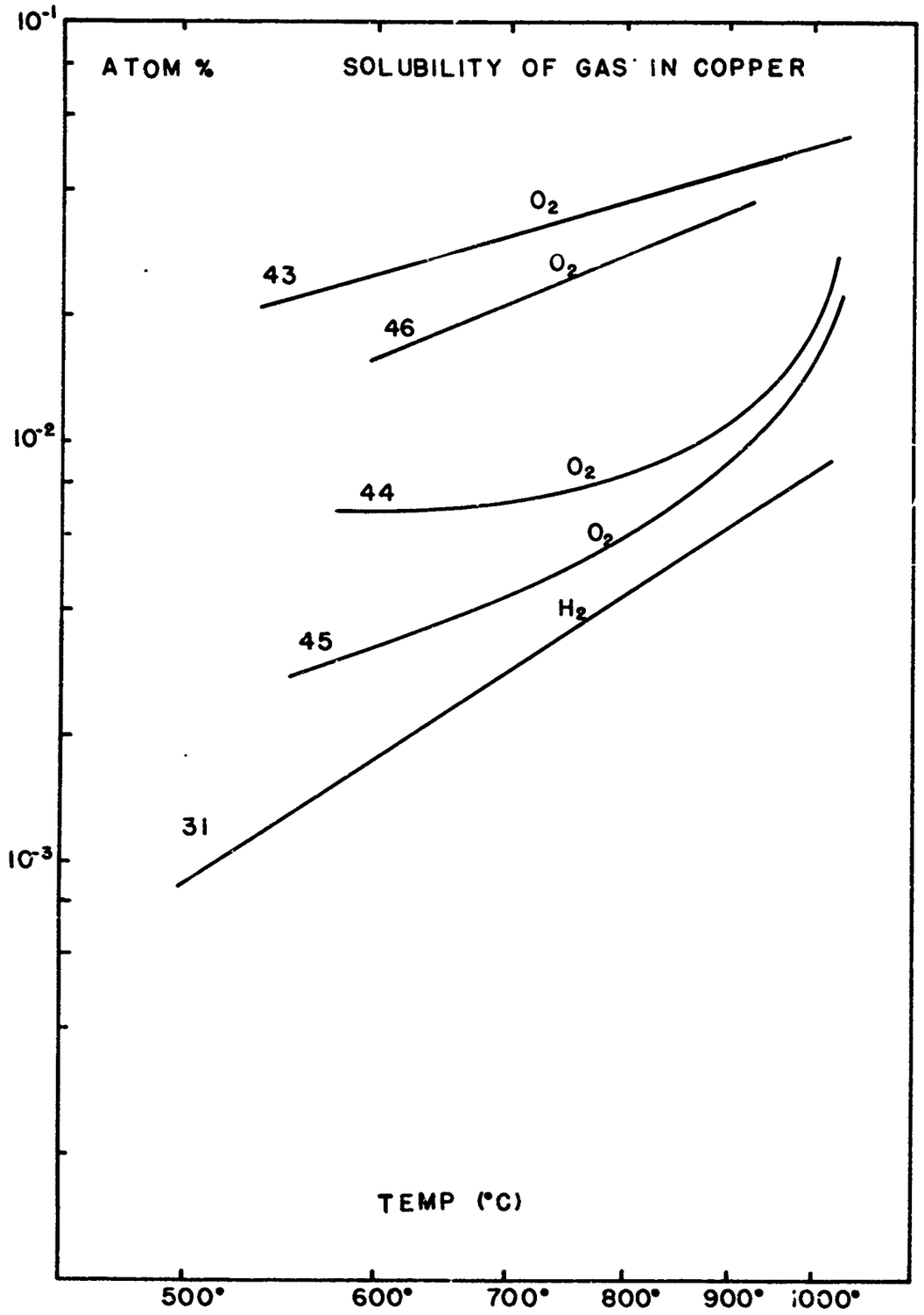

FIGURE 36

SOLUBILITY OF GASES IN COPPER.

The other possible explanations, dissociation of the oxide to metal and oxygen and evaporation of the oxide can be ruled out by the arguments presented by Van Der Schrick (9). The possibility that the induction period is due to reduction of the oxide by residual gases in the vacuum system or by dissolved gases in the sample can also be eliminated. The first because the concentration of residual gases in the system is known to be much too small. The second because variation of outgassing treatments fail to influence the duration of the induction period except in the case when hydrogen is known to be dissolved in the sample.

b. Nature of Surface

The fact that the sticking coefficients obtained in this work for the induction period were on the order of 10^{-5} indicates that the metal surface is covered by a layer of some type. This is based on the fact that low energy electron diffraction (LEED) work indicates that oxygen chemisorption on a clean copper surface is essentially non-activated (66) and thus, for a clean copper surface, a sticking coefficient of approximately one would be expected.

It is suggested, from the discussion in Section V-B-1, that the surface of the metal during the induction period is actually covered with a chemisorbed structure consisting of both oxygen and copper atoms. Such a layer

on the surface would decrease the probability that an arriving oxygen molecule would stick and the low sticking coefficients observed would be expected.

c. Rate Controlling Step

The rate controlling process must take place on or across this surface adsorption structure since it involves the oxygen molecule as shown by the linear dependence of oxidation rate on oxygen pressure. Trapnell (67) suggests that the limiting process may be the transfer of oxygen into the underlying lattice by a place exchange mechanism which requires an O_2 molecule on the surface before it can occur. Another possible limiting mechanism is the transfer of electrons through the chemisorbed structure to the O_2 molecules on the surface. This is similar to the mechanism proposed by Rideal and Jones (68) in 1929 for the rate controlling step in the oxidation of metals such as tungsten in which the oxides produced are volatile.

It would appear that the magnitude of the activation energy, the frequency factor and their variation with crystal face could be used to determine if one of these models is correct. However, too little is known at this time to make such an evaluation.

3. Nucleation and Growth Period:

At the end of the induction period there was no

abrupt change in the oxidation rate. Instead, the rate slowly decreased from the J = k law to a law closely approximated by $J = kt^{-1/3}$. It is suggested that this decrease in the oxidation rate is due to the covering up of the metal surface by the oxide nuclei.

If the probability of an oxygen molecule striking an oxide nucleus and being permanently retained by the surface is much less than the probability of retention for oxygen striking the surface in between the nuclei, then the rate of oxidation J per unit area will be the rate per unit area of metal (j_m) times the fraction of the surface which is metal $\left(\frac{A_m}{A_T}\right)$. That is,

$$J\ (g\ cm^{-2}sec^{-1}) = j_m\ (g\ cm^{-2}sec^{-1}) \times \frac{A_m}{A_T} \qquad \text{(equation 1)}$$

where A_T is the total surface area.

The rate J is equal to $\frac{dQ}{dt}$, the rate of change of the total quantity of oxygen taken up by the sample. Also, the fraction of surface which is metal $\left(\frac{A_m}{A_T}\right)$ plus the fraction which is oxide $\left(\frac{A_o}{A_T}\right)$ must be equal to 1. Making these two substitutions in equation 1, one obtains

$$\frac{dQ}{dt} = j_m \left(1 - \frac{A_o}{A_T}\right) \qquad \text{(equation 2)}$$

However, $\left(\frac{A_o}{A_T}\right)$ is a function of Q in the following manner: $Q \propto NV_n$. That is, the amount of oxide on the surface per square centimeter is proportional to the volume of the individual nuclei (V_n) times their density on the surface in numbers per square centimeter (N). If it is assumed that the nuclei are in the form of circular cones, then, the volume of a nucleus is equal to $\frac{1}{3}\pi r^2 h$, where r is the radius of a nucleus, and h is the height of a nucleus. If the height of a nucleus is proportional to some power x of the radius, then from equation 2, the amount of oxide on a surface is related to the radius of the nuclei by

$$Q \propto V_n \propto r^{(2+x)} \qquad \text{(equation 3)}$$

The area covered by oxide is, however,

$$A_o = N\pi r^2 \quad \text{and thus}$$

$$A_o \sim Q^{\frac{2}{2+x}} \qquad \text{(equation 4)}$$

Substituting equation 4 into equation 2 and rearranging, one obtains

$$\frac{dQ}{1 - kQ^{\frac{2}{2+x}}} \sim dt \qquad \text{(equation 5)}$$

Since $kQ^{\frac{2}{2+x}} < 1$, this equation can be expanded into a power series of the form

$$\left[1 + kQ^{\frac{2}{2+x}} + \left(kQ^{\frac{2}{2+x}}\right)^2 + \left(kQ^{\frac{2}{2+x}}\right)^3 + \cdots\right] dQ \sim dt \quad \text{(equation 6)}$$

which on integration yields (if at t = 0, Q = 0)

$$Q + \frac{2+x}{4+x} kQ^{\frac{4+x}{2+x}} + \frac{2+x}{6+x} k^2 Q^{\frac{6+x}{2+x}} + \frac{2+x}{8+x} k^3 Q^{\frac{8+x}{2+x}} + \cdots = k' t$$

(equation 7)

which within the experimental accuracy can be represented by

$Q^{\frac{4}{3}} = k'' t$ or, in terms of the rate of oxidation, by

$$J = k''' t^{-1/3} \quad \text{if} \quad 1/2 \leq x \leq 1/3.$$

4. Continuous oxide film

When sufficient metal surface has been covered by the oxide nuclei, the contribution to the total rate of oxidation by oxidation occurring on the surface of the oxide becomes significant and the $J = kt^{-1/3}$ law no longer holds. At this point the rate controlling process becomes transport through the oxide and a parabolic rate law is obtained.

VI. CONCLUSIONS

The early stages of the thermal oxidation of clean copper surfaces in low pressures of oxygen between 150° C and 900° C have been studied. Topographic features of the surfaces were determined by means of optical and electron microscope observations. Structural features were ascertained from high energy electron diffraction studies. Kinetic data were obtained from continuous measurements of the oxygen pressure decrease in a closed reactor vessel.

The general features of the reaction of oxygen with copper were as follows:

1) For a short period of time after admitting oxygen to the copper surface, no oxide formed. The time before oxide appeared on the surface is referred to as the induction period and was found to be a function of crystal face, temperature, and oxygen pressure.

2) This induction period was followed by the sudden appearance of isolated oxide nuclei. The number of nuclei/cm^2 grew rapidly to some maximum value and then decreased slightly, after which the number remained constant until the nuclei began to grow together to produce a continuous oxide film.

A reasonable mechanism for this oxidation process can be proposed, based primarily on the data obtained in this study.

The first process involved in the interaction of oxygen with clean copper surfaces is chemisorption. This process is essentially non-activated and the sticking coefficient is high. Thus, at a pressure in the range of 10^{-4} to 10^{-2} torr a complete adsorption layer would be formed in less than a second. This chemisorbed layer is rapidly converted to an ordered adsorption structure by a process of diffusion of both copper and oxygen atoms. Evidence for the formation and existence of such a structure comes both from LEED studies and from high energy electron diffraction data. This adsorbed layer is remarkably protective and the sticking coefficient falls to values of about 10^{-5}.

Oxygen adsorption on this structure is associated with the solution of oxygen into the metal lattice. Electron diffraction and electron microscope data give no indication of the formation of an oxide phase during this induction period. The kinetic data obtained during this solution process reveal that the rate of oxygen uptake by the sample is directly proportional to the oxygen pressure and the rate is constant with respect to time. This indicates that the adsorption layer on the metal is essentially unchanged during this process and that the rate controlling step involves the oxygen molecule.

When sufficient oxygen has dissolved into the

metal to produce a critical concentration of oxygen in the copper lattice, cuprous oxide is precipitated. This critical concentration is probably closely related to the stresses created in the lattice as a result of the oxygen solution. This precipitation of oxide produces nuclei distributed randomly over the surface. The initial growth of these oxide nuclei reduces the oxygen concentration in their vicinity and further nucleation of oxide can no longer occur. At this time there exist many nuclei on the surface, the smaller of which are incorporated into the larger nuclei by a process of Ostwald ripening. The final number of nuclei/cm^2 is directly proportional to the oxygen flux as would be expected if the mechanism of precipitation were diffusion controlled.

The oxide nuclei grow predominantly laterally on the surface of the metal with only a slight increase in thickness with time. The kinetic data during this growth period indicate that the rate controlling process is the same as in the induction period. Electron diffraction data show that an adsorption structure is present on the surface between the oxide nuclei. The oxygen uptake follows a $Q^{4/3} = kt$ law. This results from the fact that the oxidation rate is proportional to the fraction of the metal surface which is not covered by oxide nuclei. The mechanism of the growth of the oxide nuclei probably involves the surface diffusion of both copper and oxygen atoms on the adsorption structure between the nuclei.

With continued growth, the oxide nuclei begin to grow together to form a continuous oxide film. The mechanism of growth now becomes one of bulk diffusion through the oxide and a parabolic rate law is obtained.

VII. BIBLIOGRAPHY

1. J. Bardolle and J. Benard, Compt. rend., 232, 231 (1951).
2. F. Grönlund, Publications Scientifiques et Techniques, N° N.T., 88 (1960).
3. W. W. Harris, F. R. Ball, and A. T. Gwathmey, Acta Met., 5, 574 (1957).
4. F. Grönlund and J. Benard, Compt. rend., 240, 624 (1955).
5. J. Benard, "L'Oxydation des Metaux" (Gauthier-Villars, 1962), ed C^{ie}, page 82.
6. E. Menzel, Z. Physik, 132, 508 (1952).
7. G. E. Rhead, Trans. Faraday Soc., 61, 797 (1965).
8. A. Rönnquist, J. Inst. Metals, 91, 89-94 (1962-63).
9. G. Van Der Schrick, Ph. D. Thesis, University Libre de Bruxelles, 1960.
10. C. Kaechenbeeck-Van Der Schrick, Ph. D. Thesis, University Libre de Bruxelles, 1962.
11. E. Menzel and W. Stossel, Naturwissenschaften, 41, 302 (1954).
12. E. Menzel and K. Niederauer, Acta Met., 10, 561 (1962).
13. R. N. Lee, Ph. D. Thesis, Brown University, 1965.
14. G. Simmons, Private communication.

15. H. E. Farnsworth and H. Madden, "Solid Surfaces and the Gas-Solid Interface", Advances in Chemistry Series No. 33 (American Chemical Society, 1961), pages 33, 114.

16. W. H. Orr, Ph. D. Thesis, Cornell University, 1962.

17. E. A. Gulbransen, W. R. Mc Millan, and K. F. Andrew, J. Inst. Metals, 6, 1027 (1954).

18. U. M. Martius, Can J. Phys., 33, 466 (1955).

19. E. Menzel and C. Menzel-Kopp, Z. Naturforsch, 13a, 985 (1958).

20. W. Boggs, P. Trozzo, and G. Pellissier, J. Electrochem. Soc., 108, 13-24 (1961).

21. F. Bouillon, Y. Bouillon-Nyssen and J. Stev[illegible] "Proceedings, Fifth International Conferenc[illegible]r Electron Microscopy", Vol. 1, edited by S. Breese, Jr., 1962, pages 66-67.

22. F. Bouillon and M. Jardinier-Offergeld, Compt. rend., 252, 1470 (1961).

23. F. Bouillon and M. Jardinier-Offergeld, Acta Met., 9, 1041 (1961).

24. S. Leistikow and J. Oudar, Journal De Microscopie, 2, 373 (1963).

25. J. Oudar and J. Benard, Acta Met., 7, 295 (1959).

26. R. Y. Meelheim, Dissertation, University of Virginia, 1958.

27. F. W. Young, Jr., and T. Wilson, Rev. Sci. Instr., 32, 559 (1961).

28. P. Jacquet, Bull, Soc. Chim. France, 3, 705 (1936).

29. H. Miley, J. Am. Chem. Soc., 59 2626 (1937).

30. J. A. Allen, Trans. Faraday Soc., 48, 273 (1952).

31. A. F. Beck and M. J. Pryor, J. Electrochem. Soc., 108, 417 (1961).

32. D. P. Smith, "Hydrogen in Metals", (University of Chicago Press, 1948), pages 75-77.

33. F. M. G. Johnson and D. Larose, J. Am Chem. Soc., 46, 1377 (1924); 49, 3[illegible] (1927).

34. L. Spencer, J. Chem. Soc., 123, 2124 (1923).

35. C. J. Smithells and C. E. Ransley, Proc. Roy. Soc., A 153, 172 (1935).

36. E. Braaten and G. Clark, Proc. Roy. Soc., A 153, 504 (1936).

37. W. A. Johnson, Trans. AIME, 224, 509 (1962).

38. J. Steigman, W. Shockley, and F. Nix, Phys. Rev., 56, 13 (1939).

39. J. V. Choi and P. G. Shewman, Trans. AIME, 224, 509 (1962).

40. N. Hackerman and N. Simpson, Trans. Faraday Soc., 52, 628 (1956).

41. N. Gjostein, Trans. AIME, 221, 1039 (1961).

42. F. J. Bradshaw, R. H. Brandon, and C. Wheeler, Acta Met., 12, 1057 (1964).

43. F. N. Rhines and C. H. Mathewson, Trans. AIME, 111, 337 (1934).

44. A. Phillips and E. N. Skinner, Trans. AIME, 143, . (19 .).

45. W. A. B er, see (44).

46. N. A. G stein, Acta Met., 11, 969 (1963).

47. E. D. Hendres and A. J. . Moore, Acta Met., 8, 647 (19).

48. F. Bouillon, G. Van Der Schrick, and C. Kaeckenbeeck-Van Der Schrick, Acta Met., 10, 647 (1962).

49. G. Bohm and M. Kahlweit, Acta Met., 12, 641 (1964).

50. E. Menzel and Chr. Menzel-Kopp, "Solid Surfaces", (North Holland Publishing Company, 1964), pages 376-380.

51. P. B. Sewell, Private communication.

52. P. B. Sewell and M. Cohen, Appl. Phys. Letters, 7, 32 (1965).

53. G. Krause, Chr. Menzel-Kopp, and E. Menzel, Phys. Stat. Sol., 6, 121 (1964).

54. J. W. Matthews, "Single Crystal Films, edited by M. H. Francombe and H. Sato, (Mac Millan Co., 1964), page 165.

55. A. Guinier, "Solid State Physics", edited by F. Seitz and D. Turnbull, (Academic Press, 1959) Vol. 9, page 294.

56. M. E. Hargreaves, Acta Cryst., 4, 301 (1951).

57. A. T. Gwathmey and K. R. Lawless, "Semiconductors", edited by Gatos, (John Wiley and Sons Inc., 1960), page 483.

58. E. Menzel, W. Stossel, and Chr. Menzel-Kopp, Z. Naturforsch., 12a, 404 (1957).

59. J. H. Van der Merwe, "Single Crystal Films", edited by M. H. Francombe and H. Sato, (Mac Millan Co., 1964), page 139.

60. B. Borie, C. J. Sparks, Jr., and J. V. Cathcart, Acta Met., 10, 691 (1962).

61. F. Bouillon, G. Van Der Schrick, and C. Kaeckenbeeck-Van Der Schrick, Acta Met., 10, 647 (1962).

62. J. Crank, "Mathematics of Diffusion", (Oxford University Press, 1956), page 30.

63. F. W. Young, Jr. "Direct Observations of Imperfections in Crystals", edited by J. B. Newkirk and J. H. Wirnick, (John Wiley and Sons, 1962), page 103.

64. P. G. Shewmon, "Diffusion in Solids", (Mc Graw-Hill Book Co., 1963), page 14.

65. J. Hillard, "Symposium on Nucleation Phenomenon", A. C. S. Division of Industrial and Engineering Chemistry, Dr. A. Michaels, Chairman, 1965, page 151.

66. A. Mac Rae, Surface Sci., 1, 319 (1964).

67. M. Lanyon and B. Trapnell, Proc. Roy. Soc., A 227, 387 (1955).

68. E. Rideal and O. Jones, Proc. Roy. Soc., A 123, 202 (1929).